Potential hazard map for snow disaster prevention using GIS and remote sensing techniques: a case study in northern Xinjiang, China

2015年08月

千葉大学大学院理学研究科

地球生命圏科学専攻　地球科学コース

Gulijianati　Abake

ACKNOWLEDGEMENTS

My deepest and most sincere gratitude go to my supervisor Prof. Ryutaro Tateishi for unparalleled guidance, advices and encouragement throughout the tenure of this work. I extremely appreciate Prof. Takeuchi Nozomu for his valuable guidance, kind advices, and teaching. I would like to acknowledge my dissertation committee, Prof. Ryutaro Tateishi, Prof. Akihiko Kondoh, Prof. Takeuchi Nozomu, and Pro. Josaphat Tetuko Sri Sumantyo for their guidance and advice in improving the manuscript. I am very appreciate the suggestions and contribution of the committee members.

I also gratefully acknowledge Chiba University for providing the facilities during the course of this study. I am grateful to all the faculty members of Chiba University, with whom I had interaction at various stages of research.

Special thanks to go to my former and present colleagues, Dr.Ahmad Al-hanbali, Dr.Toshiyuki Kobayashi, Dr. Nguyen Thanh Hoan, Dr. Bayan A.M.Alsaaideh, Dr. Gegentana, Mrs. Kalb Al-Nur Yishamiding, Mr. Ghayrat Ghalip, Mr. Akber Mamatniyaz, during my research tenure at Chiba University. In addition, I also owe my thanks to friend and well-wishers, Mrs. Aynur Abliz, Mrs. Nurbiya Najeeb, Mrs. Aysultan Mamatniyaz, and Miss. Zinnat Ghalip.

Last, but most of all, my appreciate go to my father Abak S. Mahmud, my father- in-law, my mother, my mother-in-law, my husband Almas A. Ahmad, my brother, and my sister, enough words cannot be found to express their assistance and suggestions towards my progress in life, their warm love, their endless hours of patience, their understanding and their constant encouragement and strength during this study.

This thesis dedicated to my parents and my family for their cherished wishes and dreams.

ABSTRACT

Due to winter circulation of Siberian high and south mountain blockage, north part of Xinjiang Uyghur Autonomy region (hereafter called north Xinjiang) became one of the reach seasonal snow source area, in China. Almost every year, there are snow avalanche (hereafter called avalanche) disasters in north Xinjiang, caused by accumulated heavy snow in winter season. Avalanches are significant natural hazard that have considerable influence on human activities. It affect important lifelines, causing considerable economic loss, and seriously threatening people's lives. Therefore, monitoring hazard areas threated by potential avalanching becomes of the important research issue in north Xinjiang.

This study aims to map potential hazard area to prevent a future avalanche hazard and to provide accurate information for decision makers to mitigate avalanche hazards and related risk. Based on comprehensive analysis over current research status in China and abroad and previous studies, remote sensing (RS) and geographical information system (GIS) techniques, and information system construction technologies etc. are being qualitatively and quantitatively putting into the research on the mapping of potential hazard area. This potential avalanche hazard map is an important tool for land-use planning and safety assessment. It has proven to be the one of the most efficient and the most cost effective hazard mitigation measures.

Based on avalanche definition, which is a mass of snow under motion, sliding and rushing down a steep mountain slope, this study creates potential hazard map at 500m resolution, using snow mass and slope data, which are prerequisite for an avalanche occurrence. Snow mass was calculated from snow volume and average snow density an assumed. Snow volume was generated from existing Canadian Meteorological Centre (CMC) snow depth data and new cloud-free snow cover data. This cloud-free snow cover data was produced from relatively high spatial resolution

optical (MODIS) snow data and cloud-penetration passive microwave (AMSR-E) snow product. AMSR-E data was used to compensate deficiency of MODIS data, which contains cloud area.

Avalanche hazard maps at 500m spatial resolution from 2008 to 2010 were created using GIS-based weighted linear combination method. The dangerous degree of avalanche hazard maps were expressed by a score from 0.5 to 10. Based on the dangerous degree of historical avalanche accident sites, the area of dangerous degree more than 5.0 were decided as the high dangerous area, and those areas were suggested that might endanger villages or human activities. To prevent for a future avalanche hazard, potential hazard map was produced from three-year avalanche hazard maps by taking their averages.

Road accessibility is strategically important not only for the maintenance of economic activities, but also for the emergency services. In mountains area, avalanches are a strong threat, in addition to the victims and direct damage, because they cause a loss of accessibility in roads. To see the risk to traffic roads caused by avalanches, highway network system were analyzed. Finally, for each year, highway network system was classified by dangerous degree and the length of highway sections with high dangerous degree was investigate.

The originalities of this study are: (1) Snow volume product at 500m spatial resolution were generated; it is the first snow volume product in this study area. (2) Potential hazard map at 500m spatial resolution were created by new technique, in the meaning of forecasting potential avalanching. (3) Dangerous degree of highway sections were evaluated to know potential loss of road accessibility.

This study should be useful for the local government and native people in the future to prevent snow related disasters. In future work, more advanced data acquisition techniques should be introduced into potential hazard monitoring model, and new avalanche hazard map will be created, based on the trigger condition of each avalanche type.

TABLE OF CONTENTS

List of Table

List of Figure

Chapter 1 Introduction

1.1 Motivation

Potential hazard refers to the hazard associated with specific environmental factors, such as those induced by geographical condition, which contribute to the hazard associated with different natural disaster. Potential hazard is a position that brings level of threat to life, property, or environment. Most of hazards are inactive or potential, with only a theoretical risk of harm; however, once a hazard becomes "active", it can bring an emergency.

Snow avalanche (hereafter called avalanche) hazard mapping is a set of procedures used by land planning authorities as a tool to prevent settlements, roads and railways being constructed in areas that are endangered by avalanches (Chrustek, P., et al., 2013). It has proven to be one of the most economic effective hazard mitigation measures. The aim of avalanche hazard mapping is to estimate areas endanger to the avalanche hazard and related risk.

Due to winter circulation of Siberian high and south mountain blockage, north part of Xinjiang Uyghur Autonomy region (hereafter called north Xinjiang) became one of the reach seasonal snow source area, in China. Generally, snow days are most common in the period from November through March (Wang, X., et al., 2007). The mean duration of snow cover is about 130 days per year. Almost every year, there are snow avalanches accidents caused by accumulated heavy snow. Avalanches are a significant natural hazard that has considerable influence on human activities, especially, in mountainous area. It will seriously threatening people lives and their productivity, impact transportation lines, communications facilities and vehicles, and so on.

During the winter season of 2008/2009 and 2009/2010, avalanche accidents struck the area near the mountains in the north Xijiang. (1) An avalanche occurred to the tunnel in the Kazak Autonomous Prefecture of Ili on March 14, 2008. Altogether 12 workers were buried, four of

whom have been confirmed dead. More than 50m deep was blocking the entrance of the tunnel construction site. Fig.1.1 shows the mountainous section where a tunnel under construction and grabs clear the snow. (2) Three heavy snowfalls March 16 hit the Guozigou area in the Kazak autonomous prefecture of Yili, undermining conditions at a gas pipeline construction site where the tragedy took place. The tunnel is about 500 km from Urumqi, capital of Xinjiang. Fig.1.2 shows that rescue team consists of armed forces and the police dogs head for the tunnel construction site, try hard to look for the workers in the tunnel construction site.

Fig.1.1 The mountainous section where a tunnel are under construction (left) and grabs clear the snow (right) (from www.chinaview.cn).

(3) February 25, 2010. Ili prefecture in north Xinjiang has experienced the worst snow avalanches in decades this winter. Local weather station has warned that due to the increasing accumulated snow cause severe avalanches in this region. A rescue helicopter arrived a coalmine, where more than 100 workers were trapped. However, it could not locate a landing spot, and left, after dropping some food and a satellite phone. The seven people found dead in the avalanches.

Avalanches in Hejing County have killed at least one, leaving another missing and nearly 500 trapped. Fig.1.3 shows that helicopters were dispatched to rescue people trapped by avalanches. (4) Jan 27, 2010, Yili prefecture in north Xinjiang has endured an unusually harsh winter and heavy snow from a series of Siberian blizzards. They reported death from a fierce cold snap at least 27. Thousands have been left homeless after the heavy snows led houses to collapse while thousands of livestock have died from exposure or starvation after grazing fields were buried in snow.

Fig.1.2 Rescue team try hard to look for the workers in the tunnel construction site (from www.chinaview.cn).

Fig.1.3 Helicopters were dispatched to rescue people trapped by avalanches (from www.chinaview.cn).

(5) Feb.28, 2010, 130 people trapped here by heavy snow avalanches, in Nilka County of Kazak Autonomous Prefecture of Ili. Air rescue provide 3 tons of living goods and 300 kilograms of vegetables and medicines. Fig.1.4 shows rescuers arrange rescue works at a site.

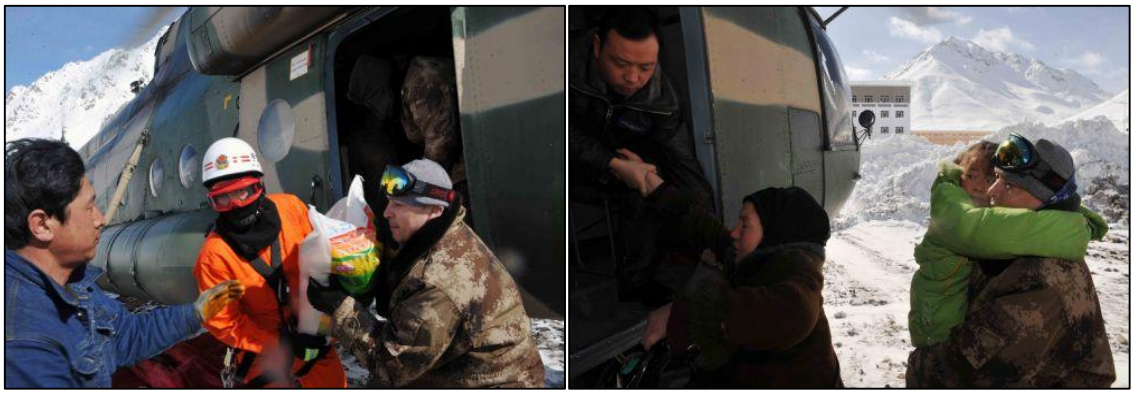

Fig.1.4 Rescuers arrange rescue works at a site (from www.chinaview.cn).

(6) Guozigou mountainous suffered heavy snowfall, on the February 24th, 2010. The accumulated snowfall freeway results thickness up to 70 cm. Guozigou Road Branch organized several days of overnight snow removal machinery and personnel road. Due to continuous snowfall, in the highway, avalanche occurred at four times, resulting in half-buried driveway. Fig.1.5 shows that the Guozigou Road Branch cleaning by snow removal machinery cleaning. (7) January, 8, 2010, avalanches hitting north Xinjiang's Tacheng and Altay region. A total of 261,800 people in 12 counties or cities were affected, 1 dead, over 5,000 evacuated by the avalanches. Fig.1.6 shows that the people cleaning the snow.

Fig.1.5 Snow removal machinery was cleaning Guozigou Road Branch (from www.chinaview.cn).

Fig.1.6 People cleaning snow (from www.chinaview.cn).

These avalanche accidents show that mapping avalanche hazard area will significantly contributed to reducing of the loss of life and damage to towns and farms despite large increase in population and infrastructure in mountains areas. Therefore, to reduce damage from future avalanches, mapping potential hazardous area is very crucial for north Xinjiang area. Effectively conduct the investigation on north Xinjiang area having such condition:

(1) Very wide area with a total land area of 39,845,600 ha;

(2) Areas greatly different in elevation from 1000m to 6300;

(3) Serve climate conditions depending on the season to reject human access for field survey.

Because of the difficulties in field investigation, the avalanche dangerous area must be estimate

by considering other methods. The satellite remote sensing and Geographical information system (GIS) are the sole technical seed. The final target of this study can sufficiently met by taking advantages of their characteristics. The feature of satellite remote sensing are (1) a wide area can instantly observed, (2) it is possible to grasp the outline of a site not allowed by human survey, and (3) periodic recording is possible. GIS is a system that designing to control, store, manage, analyze, and present all types of geographical data. It have capability to model, analyze, map avalanche terrain, and to create maps visualizing terrain features. In addition, it will help to build recognition and education for backcountry users about avalanche hazard area. Using RS and GIS can largely improve the effectiveness and efficiency of avalanche monitoring and early-warning techniques in this study area.

The emphasis of this thesis on using RS techniques and GIS approach to scientifically mapping potential hazard area, visualize the results, and discussing related risks of potential hazard. This thesis aims to contribute new findings to the existing body of knowledge, by applying a GIS-based algorithm to map avalanche hazard, and, proposes the ideas and methods in constructing avalanche hazard mapping over the area of north Xinjiang. It lies in forecasting of potential avalanching.

1.2 Previous study

In the past, not much knowledge existed about this natural phenomenon and people simply tried to avoid building villages in dangerous places. Today, better knowledge exists about avalanche events, but the problem still remains. Because, avalanches are described as unexpectedly, quick movement, and large destructiveness, and, demographic changes and expansion through tourism have led to many people living or spending free time in mountain areas.

Avalanches have been studied by physical geographers since the late 19th century (Eckerstorfer, M., 2012). In these early days of avalanche science, snow was regarded as sediment that accumulates in layers and the geology and geomorphology of snow was of special interest. But these Geographers from the Alps also noted the hazardous nature of avalanches (Fig.1.7).

Fig.1.7 Engraving by D. Herrliberger after D. Duerringer, Topographie der Eidgenossenschaft, 1754. The artwork shows one of the first known graphical representations of an avalanche, threatening a mountain village in the Alps (adapted from Eckerstorfer, M., 2012).

As the number of avalanche fatalities lies nowadays at around 250 persons per year worldwide,

the study of their release mechanisms and dynamics are crucial for a better understanding of the processes involved. Some research has its focus on avalanches as a type of mass movement on hill slopes. Avalanches are widely regarded as sediment erosion, transportation and deposition agents, thus being of geomorphologic significance. Especially in favorable climatic and litho-logical settings, avalanches are an efficient sediment transport mode from high to low relief. Avalanches also contribute to the mass balance of glaciers and provide rock sediment and snow to rock glaciers. However, the importance of avalanches as geomorphologic agents in the alpine cascade is often underrated. Avalanches were considered as subsidiary sediment transport agents, rather than the dominant one. Historically, the interest in avalanche in Arctic regions was more a geomorphologic one.

There are a number of avalanche studies in north Xinjiang. Ma, W. et al. (1990) were studied the relationship between the developments of depth hoar and avalanche release in the Tian Shan mountains. They said that in spring and winter, there is a considerable amount of solid precipitation in the western part of the Tian Shan Mountains. Avalanches frequently occur here, and often endanger national economic construction and human life. Their observation shows that the avalanche occurrences are closely related to the physical characteristics of the snow, especially to the development of depth hoar in the snow cover. The conditions for the development of depth hoar are determined by thickness of the snow cover, air temperature, ground-temperature regime, and the duration of negative temperatures. The results of this study have revealed that the optimum depth of snow cover for the development of depth hoar is about 80 cm in the Tian Shan Mountains, and the mean maximum depth of the snow cover in this region is 78 cm. Therefore, depth hoar develops extraordinarily well. They also mentioned the thickness of depth hoar can reach more than 80% of the total snow-cover depth. That is one of the main reasons why avalanches still occur frequently under the conditions of a limited snow-cover depth

in the western part of the Tian Shan Mountains.

Qiu et al. (1997), their investigated avalanche internal dynamics structures in the Tien Shan Mountains, Xinjiang, with a join project. A medium-size avalanche path has been instrumented with six pressure transducers and two load cells to measure avalanche velocities and impact pressure in the interior of avalanche. During the 1995-1996 winters, the data were recorded of an artificially released avalanche passing by the instruments. The impact velocities were measured to be 6.9m/s by image analysis and 7.1 m/s by the lag time of a pair of first impact waves. They also found that the avalanche velocity almost reached a terminal velocity, and the shape of dense flow declined towards downstream.

Li et al. (1997) studied about preventing avalanches at Guozigou (located in the west part of Xinjiang) in Xinjiang. They said the risks of snow disaster are very serious in this region, and accidents which cost lives often occur. Vehicles are damaged and traffic is cut. Twenty-five people have lost their lives in snow disasters since 1968. After many investigation and studies, they are introducing the reason, the hazard and on-going of snow disaster prevention methods at Guozigou region. Xiong et al. (1999) studied the characteristics and vertical zone spectrum of natural disasters in the Tian Shan Mountains, Xinjiang. They said there are 12 types of disasters in Tian Shan Mountains, they can be divided three zones: first zone is base zone (torrential rain-collapse zone): the various disasters of this zone are caused by sudden precipitation in the low-middle mountain of the arid area. And, the disasters occur mainly from May to August. Second zone is middle zone (snowmelt water-icing zone): most disasters, which happen in the middle-high mountain area, have close relation with variation of temperature. The kinds of disasters include destruction of thawing snow water, icing damage, glacial debris flow, glacial lake burst, thawing sinking, snow drift of Middle Mountain and middle mountain avalanche. Third zone is upper zone (snow drift-avalanche zone): the movement of snow creates disaster in this zone. And,

there are snow drifts of High Mountain above the wooded-line in mountain and the avalanches of High Mountain, which is above 3500 meters and mainly form in summer.

Tao et al. (2007) are studied snow hazard potential evolution along G217 national highway in Tian Shan Mountains using remote sensing and GIS techniques. They mentioned that most places of the actual avalanche accidents are consistent with the places with the high snow hazard potential.

There are, also, sample existing studies related to potential hazard mapping with risk assessment or early warming information. Tachiiri et al. (2008) are used the normalized Difference Vegetation Index (NDVI) and the Snow Water Equivalent (SWE) as predictor variables of snow disaster to assess snow disaster risk in Mongolian. Semakova et al. (2009) are used topographic maps, snow covered map, and snow depth data from meteorological station to map snow avalanches hazard areas in Uzbekistan. In this study, he used geomorphologic parameters, such as slope, aspect, elevation, curvature of terrain and roughness as input data to address the snow avalanche risk management, surviving and monitoring. Covasnianu et al. (2011) are used land cover map and digital elevation model to mapping snow avalanche risk in Ceahlau national park of Romania. Wang et al. (2013) are used terrain factors (slope and aspect), number of snow covered days, and depth of snow from meteorological stations to study in early warming of snow-caused disasters in pastoral areas on the Tibetan Plateau. Liu, et al. (2014) has been adopted two factors, which are the average maximum snow depth in a year and the average number of days with surface snow cover per year, as the most important potential disaster factor to analysis the potential risk snow disaster in the pastoral areas of the Qinghai-Tibet Plateau.

Liang et al. (2009) are used latitude, sunlit and shadowy, wind, and slope as nature factors to assess snow-drifting hazard along railway in north Xinjiang. Liu et al. (2009) are used snow depth, slope, and vegetation as evaluation parameters of snow avalanche along Tianshan highway in

north Xinjiang. Wei et al. (2011) are used meteorological datasets from 1949 to 2000 and digital elevation model to study spatial distribution of snow disaster and establish the regularity of snow disaster in China. Fig.1.8 shows the frequency of snow disaster in China. The area displayed with dark blue color shows the snow disaster area of high frequency. Sun, et al. (2013) is examined spatial distribution characteristics of extreme snow disaster events in Xinjiang, using district data from 1901 to 2010. Fig.1.9 shows the spatial distribution of snow disaster events in Xinjiang from 1901 to 2010. It shows snow hazards mainly distributed in the wide northern areas, especially the Altay Mountains and Hamilton Basin.

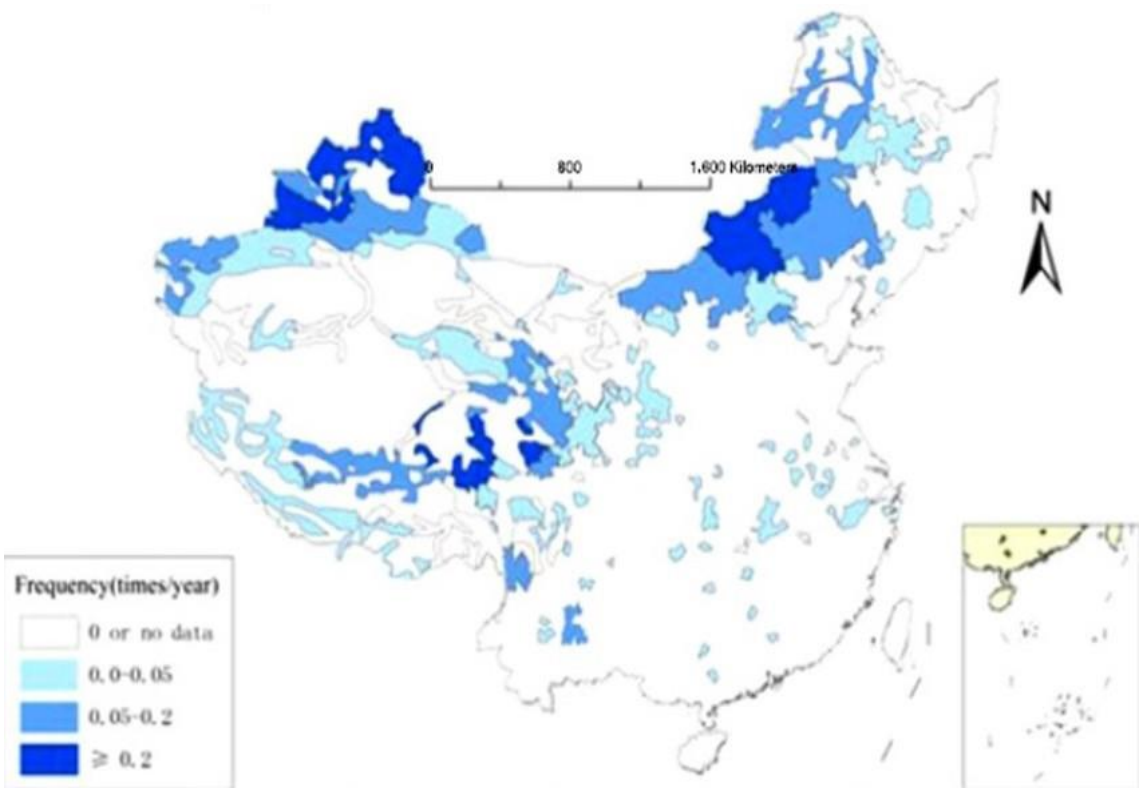

Fig.1.8 The frequency of snow disaster in China (1949-2000) (adapted from Wei et al., 2011)

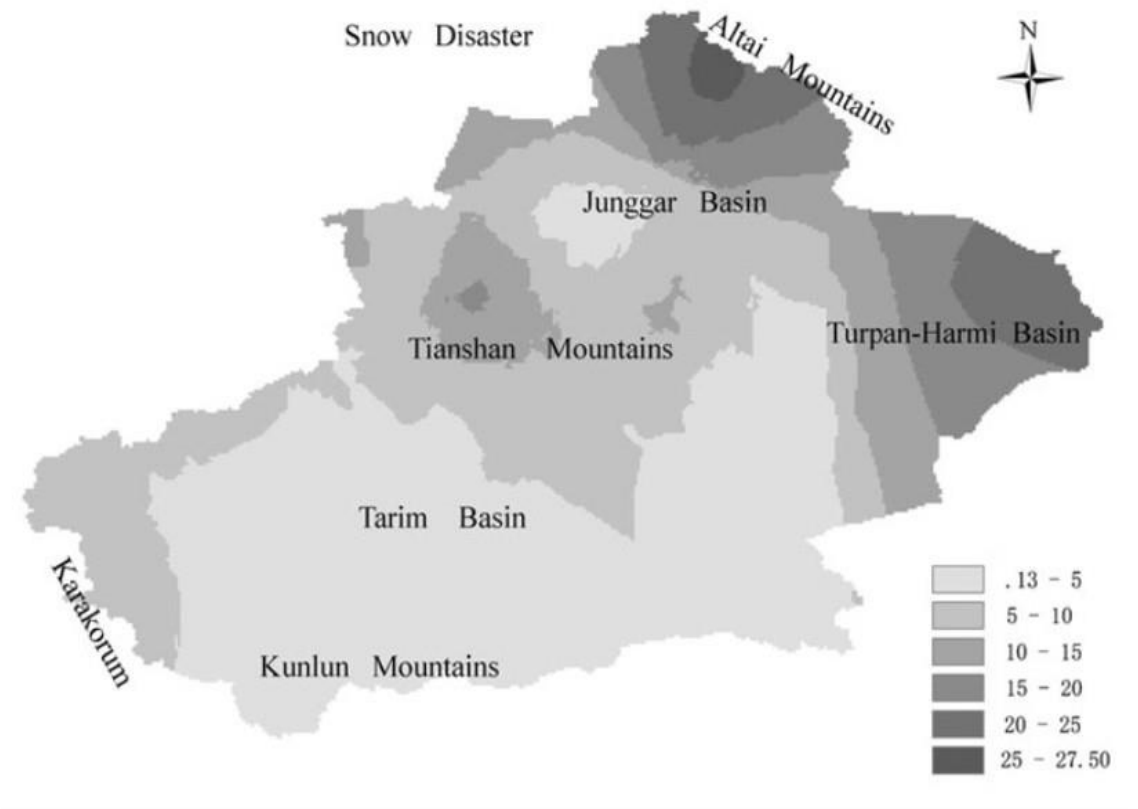

Fig.1.9 The spatial distribution of snow disaster events in Xinjiang from 1901 to 2010 (adapted from Sun, G. et al., 2013).

However, previous studies related to avalanche hazard mainly concentrate on Tian Shan Mountains regions. North Xinjiang, its land area, consists of two large mountain ranges (Tian Shan Mountains and Altay Mountains) with the basin in between. The problem of living with this natural hazard is known and must be addressed. Moreover, it requires a more detailed description of hazard area for forecasting potential avalanching. Even some researchers' studies whole Xinjiang area, but they focus on snow disaster, in generally, not specifically focus on avalanche. So, current research aims to study avalanche disaster in whole north Xinjiang area, including Tian Shan Mountains and Altay Mountains.

1.3 Objective

Accordingly, to help to mitigate the avalanche hazard and related risk, mapping potential hazard area was the main objective of this study. Another main objective is to aid the public in understanding avalanche risk in the mountains. To get the final target of this study, RS techniques and GIS-based algorithm were applied. In order to outline the purpose of this study, specific contents of this research can be summarize into the three points below:

(1) To generate cloud-free snow cover product;

(2) To estimate snow volume from cloud-free snow cover product and snow depth data, and analyse its dynamics;

(3) To calculate snow mass from snow volume and snow density data, and analyse its changes;

(4) To create potential hazard area covering the oases and the mountain district portion behind them, depending on snow mass and steep topography;

The originalities of this study are, firstly, snow volume products at 500m spatial resolution are generated; it will be first snow volume product in this study area. Secondly, potential hazard map at 500m spatial resolution was created by new technique, in the meaning of forecasting potential avalanching. Thirdly, Dangerous degree of highway sections were investigated, in the meaning of prevent road accessibility.

Potential avalanche hazard map from current study would be useful for decision makers to mitigate hazards from potential avalanche. It is not only providing information in prevention of future avalanche, but also has meaning in prevention of risks from global warming. This study should be useful for the local government and native people in the future and hopes play a role to prevention of snow related disasters.

Structure of this thesis organized as following six chapters:

- Chapter 2 introduces the reader theoretical background into avalanche information, such as description and types of avalanche, their formation, and briefly explains the meaning of hazard and risk.
- Chapter 3 describes the case study area with its features; provide available historical avalanche accidents records; and talk about Tianshan snow cover and avalanche research station.
- Chapter 4 presents datasets used in this research and their characteristics.
- Chapter 5 explains the methodology of estimating snow mass and creating potential hazard map.
- Chapter 6 presents outputs of this study and discussion about them.
- Chapter 7 talk about road accessibility and highway dangerous degree situation.
- Chapter 8 summarizes this study with conclusion and future works.
-

Chapter 2 Avalanche theory

Since avalanches are rare events, their study is as exciting as it is challenging. Due to their complexity, avalanche research has a remarkable interdisciplinary nature, crossing several boundaries within the field of physical geography, including natural hazards, meteorology, and geomorphology, as well as in the fields of geophysics and engineering. Avalanche research related to hazard is of most importance, as an improved process understanding of how, when and where avalanches release is crucial for avalanche warning and forecasting.

To understand avalanche phenomena, a review of avalanche fundamentals is necessary, particularly with regards to defining, describing and classifying avalanches. In order to outline the purpose of this study, current section provides a literature review on the fundamentals of avalanches, types of avalanches, and concepts of hazard and risk in related to avalanches monitoring. Experts have built a rich background of knowledge about avalanches. This background information helps to know the complexities in avalanche activity and contribute to present avalanches by using the related nomenclature that is relevant to this thesis. This chapter will aid in outlining the objectives and goals of this thesis.

2.1 **Avalanches**

Avalanches are rapid mass movements occurring in snow covered mountain areas all over the world (Eckerstorfer, M., 2012). It is are the mass wasting of the snow pack and are a particular natural hazard. The physical behavior of avalanches is not entirely known yet, but much theoretical and experimental research has been carried out to understand it (Maggioni, M., 2004).

Increased human activities in mountain regions, mainly due to tourism, in combination with a reduced acceptance of risk from those living in areas exposed to snow avalanches have caused a

growing need for protection against avalanches. The first attempt to formulate a general theory of avalanche motion was made by Voellmy [1955], and this theory is still widely used (Maggioni, M., 2004). Since the 1950s, several other studies have been carried out to elaborate empirical and physical models that are able to give information about run-out distance and impact pressure of avalanches, important variables for avalanche hazard assessment. However, no universal model has so far been developed. A detailed description of all the models developed until 1998 is presented in Harbitz [1998] (Maggioni, M., 2004). In order to perform an avalanche simulation, all the models of dynamics require the definition of the initial conditions in term of release area, fracture depth and friction coefficients; their correct definition is a difficult task, subject to uncertainties. For the purpose of this work, this description is thought to be sufficient.

The avalanche is a mass of snow under motion, sliding and rushing down a steep mountain slope. Under natural conditions, they arise due to disruption of the snow stability on a slope which has been affected by metrological phenomena. Among the permanent factors of avalanche formation are relative altitude, inclination, slope exposure, surface roughness, etc. variable factors are snow fall, types of snow falling, its duration, the air temperature and its changes, solar radiation, the state of older snow and its thickness, etc.

A large mass of snow and sufficiently steep slopes are prerequisite for an avalanche occurrence. Slope is one of the most important geo-morphometric parameters of terrain surface, representing an important role in determining the geomorphologic processes that affect a certain area (Covasnianu, A. et al., 2011). It represents the quantitative measure of maximal change of elevation values, ranging from 0 degree to 90 degree. The most dangerous condition is a snow cover on slopes with a gradient from 30 to 45 degree.

2.2 **Types of avalanches**

A complex process, combining gravity, topographical and meteorological conditions, and

mechanical properties of snow must take place for an avalanche to release (Eckerstorfer, M., 2012). Two general avalanche types are distinguished, loose and slab avalanches, occurring both in dry and wet snow. Dry slab avalanches release starts with a failure in a thin weak layer, or at an interface, underlying a cohesive slab layer. Slab avalanches are distinguishable by characteristic crowns, from where the avalanche bulk detaches (Fig.2.1 a).

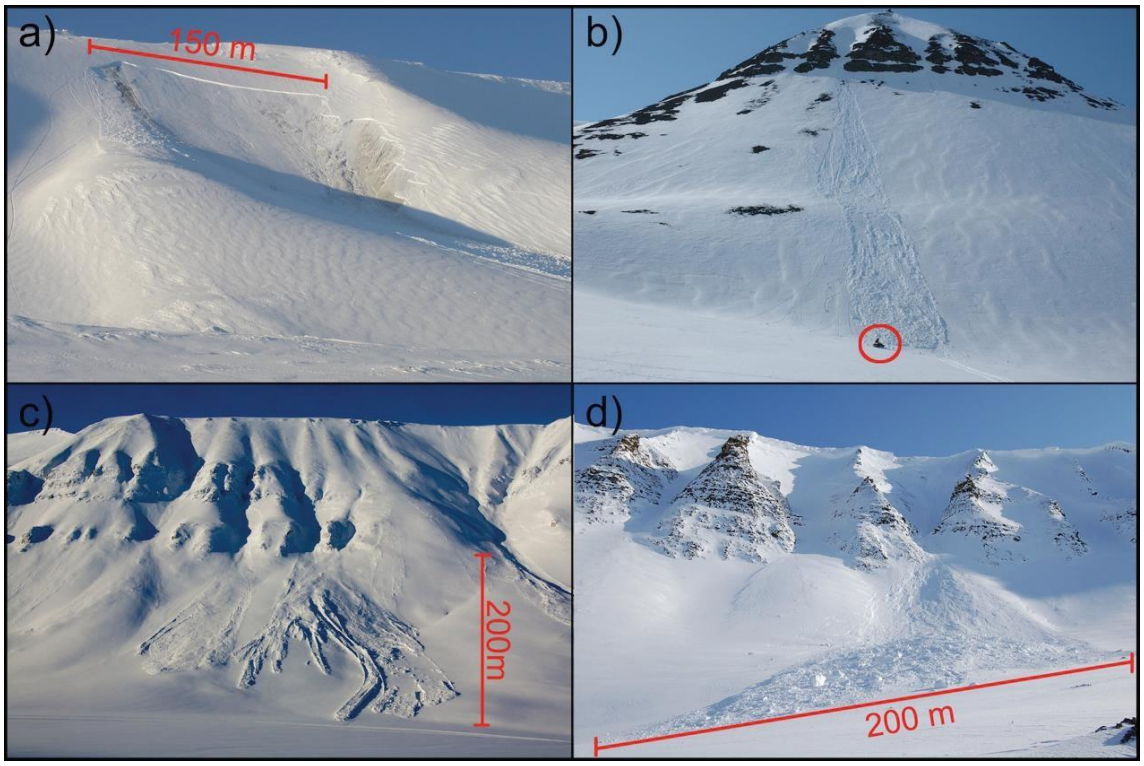

Fig.2.1: Types of avalanches. a) Slab avalanche. b) Loose snow avalanche. Snowmobile in red circle for scale. c) Slush avalanche. d) Cornice fall avalanche (Adapted from Eckerstorfer, M., 2012).

Slab avalanches cause most human fatalities. In over 90 % of all avalanche accidents, the victims trigger the avalanche themselves. Therefore slab avalanche mechanics are of special interest in hazard related avalanche science. For a dry slab avalanche to release, a weak layer must fail in compression and shear. The potential energy gained through this weak layer collapse then

drives the development of a fracture, communicated by the overlying slab. Loose snow avalanches start at a point with a cohesion-less layer and entrain snow in a spreading triangular pattern (Fig.2.1 b). Topography largely controls where avalanches start and how far they run. The most important factor is slope inclination and the majority of slab avalanches releases between 35-45 ° (Eckerstorfer, M., 2012). Meteorological factors, favorable for slab avalanche release are wind velocity and direction, precipitation and air temperature, as well as direct solar radiation over various time scales, all dynamically interacting with the terrain (Eckerstorfer, M., 2012).

Avalanches are also distinguished by their triggering mode, classified into natural and artificial releases. Natural avalanches are of special interest for avalanche forecasting, as natural causes such as a certain amount of precipitation or wind loading lead to overcoming the strength of a weak layer, which eventually fractures and induces a slab avalanche. Cornice fall avalanches are regarded as natural releases, triggered by a collapsing cornice (Fig.2.1d). Cornices are wedge-like snowdrifts that form on lee sides of ridges and slope inflections. Fundamental work on cornices was carried out in the European Alps, due to their particular shape and their ability to trigger avalanches when collapsing. John Montagne, working in the Bridger Range, Montana, did extensive cornice studies, focusing on deformation processes inside the cornice mass, and attributed snow creep and glide to the opening of tension fractures between the cornice mass and the ridgeline, which seemed to be a requirement for entire cornice collapses. Avalanches are also classified into dry and wet avalanches. One type of wet snow avalanche is a slush avalanche (Fig.2.1c). Slush avalanches were first observed in the Arctic, as water-saturated snow flowing along stream channels due to intense spring thawing. Slush avalanches release due to a hydraulic gradient developing from an increasingly inclined melt water table within the snowpack, so that friction at a bed surface can be overcome. This happens due to either intensive spring melting of snow or rain on snow events.

2.3 Understanding risk and hazard

Concise definitions are required to clarify the meaning of certain terms with regards to risk, hazard and danger in avalanche terrain; these terms are often combined or used interchangeably. A complete understanding of the fundamental concepts of risk, hazard, and danger should become basic requirements for anyone undertaking avalanche prediction and risk control (Grant, S., 2008). Each of these concepts has a specific meaning, in related to avalanche activity. These concepts are important when discussing the type of map. Is it a risk map or hazard map**?** The following discussion will attempt to clarify these terms and their relationships with respect to a description of avalanche activity or avalanche terrain.

Risk is a measure of the probability and severity of an adverse effect that can include a potential injury including death, loss of money or loss of possessions (Grant, S., 2008). Any kind of out-of-door activity may cause some kind of risk. These actions bring a risking involved danger to the human; they may lose something that is of important to them. In other words, it must be realized that risk contribute a chance for a human being to experience something that is highly valuable to them. It, thus, gives an opportunity for increase with the effect of a possibility for loss. Risk management is a process for managing or optimizing risks and hazards (Delpare, D.M. 2008). In order to mitigate risk, risk management strategies can be carrying out.

Whereas risk is the likelihood or chance that potential harm occurs, hazard describes the source of potential harm, damage or adverse effects (Grant, S., 2008). A working group in Canada gives a description to avalanche risk and avalanche hazard, through following two equations. Avalanche risk (RA) decided by the physical exposure (EA) of a human or thing to avalanche hazard (HA) (Eq.1.2). Avalanche hazard (HA) is a function of the possibility of avalanches (PA) and the severity of the avalanche (SA) (Eq.1.3). The difference between them is that risk includes exposure, while hazard describe the potential to affect human being.

$$RA = f(HA, EA) \quad \text{(Eq. 1.2)}$$

$$HA = f(PA, SA) \quad \text{(Eq. 1.3)}$$

A hazard rating scale would describe the potential harm from an avalanche for individuals, infrastructure and the environment in the path of an avalanche, particularly in terms of high, moderate and low.

Chapter 3 A case study area

In this chapter, the study area was described where the research illustrated and discussed in the following chapters was conducted. For the case study general information, such as morphology, climate, and meteorology, and historical avalanche accidents dates were provide.

A case study area, which is Xinjiang is located on northwest part of China. Xinjiang Uyghur Autonomic Region, its land divided into two parts by the Tien Shan Mountains (تەڭرى تاغ *Tengri Tagh*), with the south region termed the south Xinjiang and the north region termed the north Xinjiang. North Xinjiang extends from 42° to 50° N and from 79° to 92° E, with a total area of 0.39 million km^2. It is adjacent to Inner Mongolia to the east, and to the former Soviet Union to the northwest. Mountains, plains and desserts are the three major geomorphologic units. North Xinjiang consists of two large mountain ranges, the Tien Shan Mountains to the south and the Altai Mountains to the north, with the Dzungarian Basin (desert) in between. The Tian Shan mountain range marks the Xinjiang-Kyrgyzstan border at the Torugart Pass. The height of Tien Shan mountain peak is 7435m and height of snow line about 3600-4400m. The Altai Mountains in the north shared with Mongolia. The height of Altay mountain peak is 4374m and height of snow line about 3000-3200m (according to Xinjiang statistical book). Fig.3.1 shows the topography and major city location of a case study area.

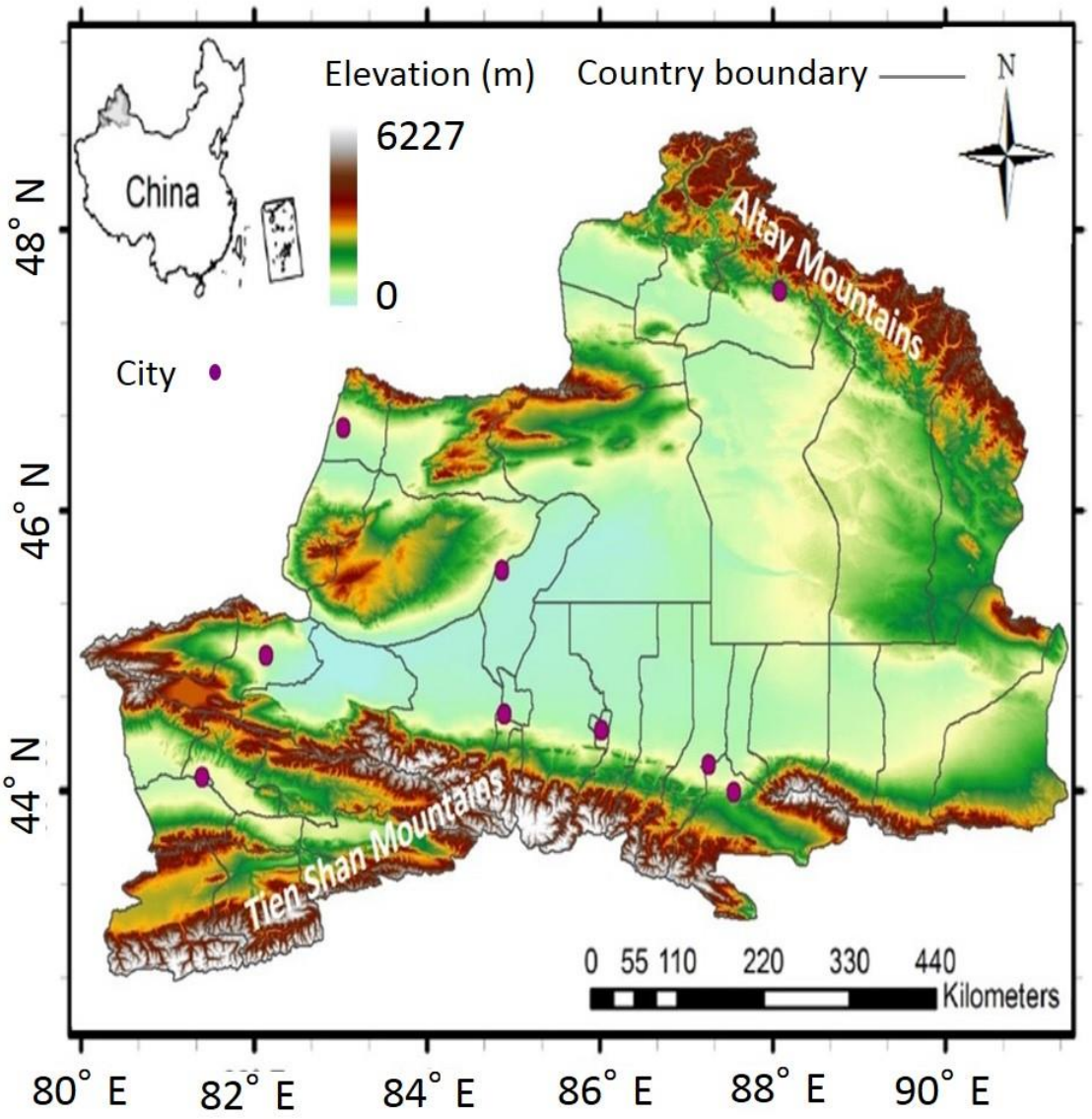

Fig.3.1 Topography and major city location of study area

3.1 Climate and meteorology

In summer it is arid and hot with little rainfall; in winter it is cold and the area receives considerable snow. The extreme minimum temperature may reach −40 °C and the mean duration of snow cover is about 130 days per year, generally from the middle of November through March. Fig.3.2 and Fi.3.7 shows the situation of monthly average temperature and monthly average

precipitation in eight major cities of north Xinjiang, from 208 to 2010. This meteorological records were collected from Xinjiang Statistical Yearbook, which published by China Statistics Press.

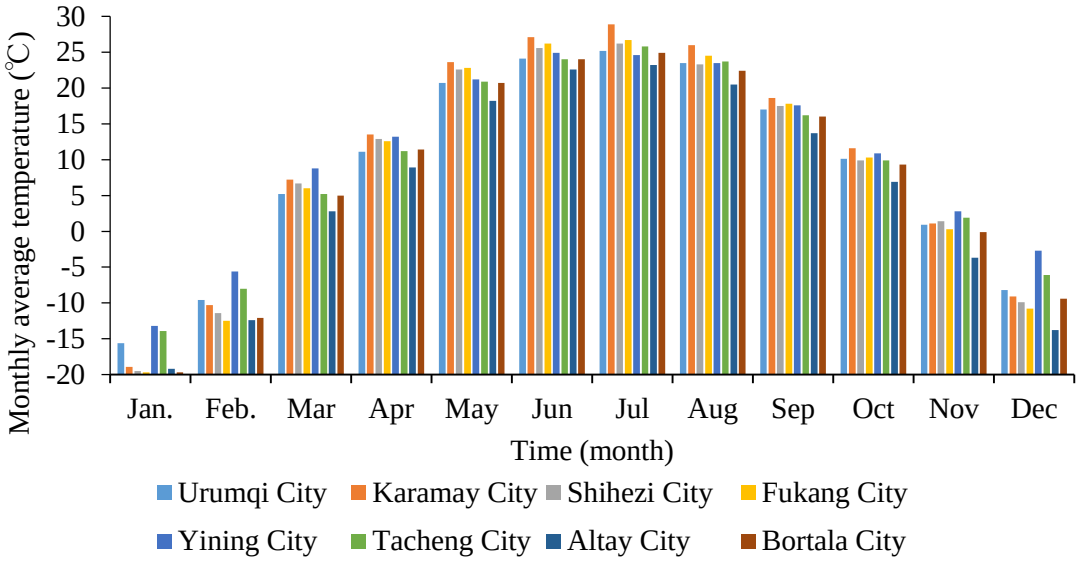

Fig.3.2 Monthly average temperature of major n north Xinjiang (2008)

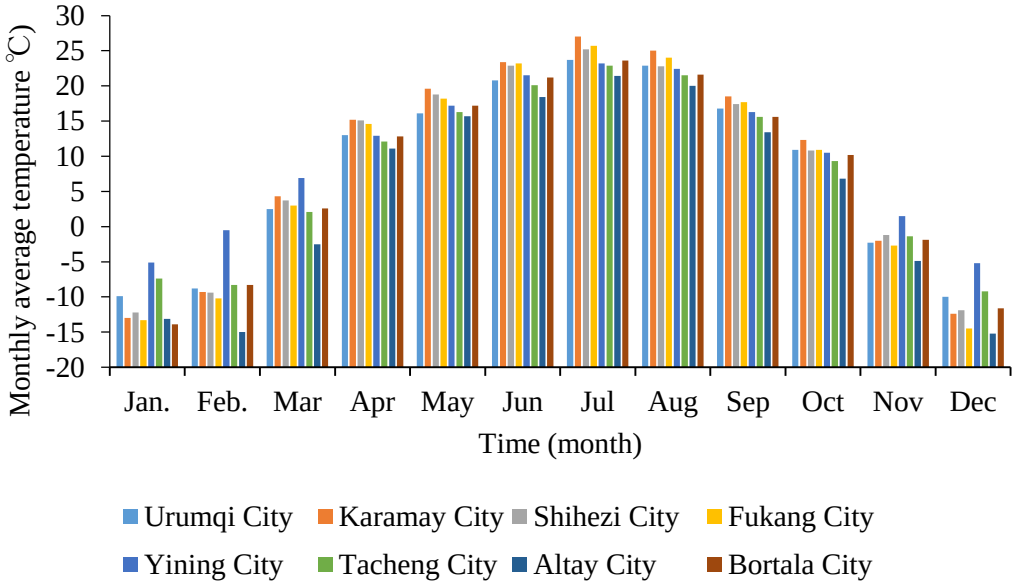

Fig.3.3 Monthly average temperature of eight cities in north Xinjiang (2009)

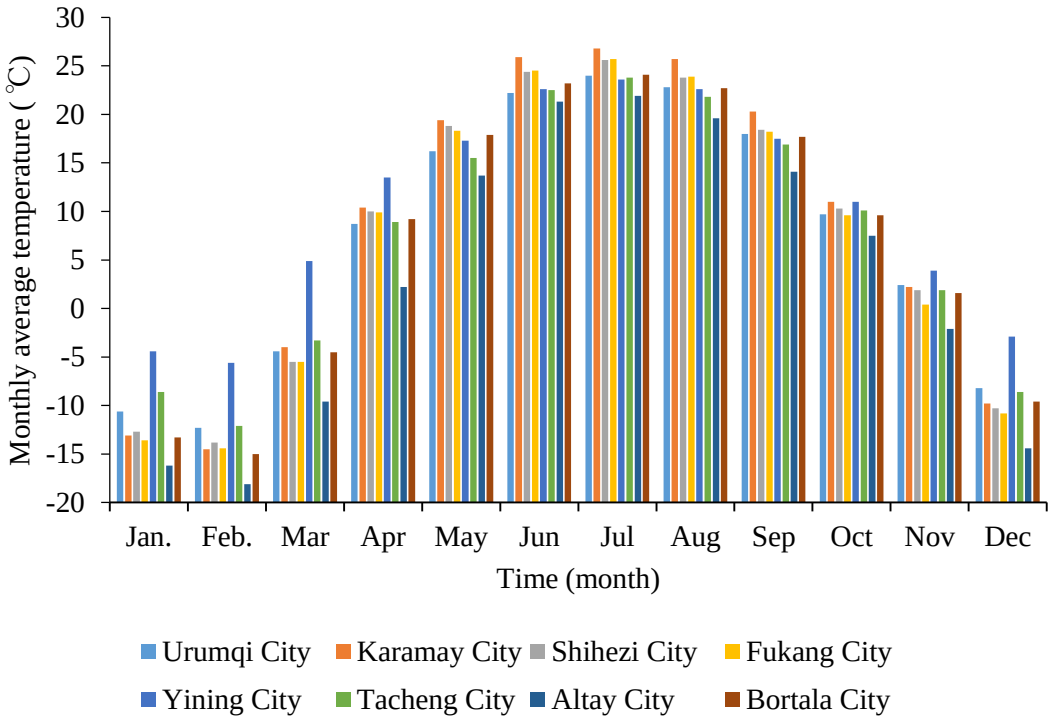

Fig.3.4 Monthly average temperature of eight cities in north Xinjiang (2010)

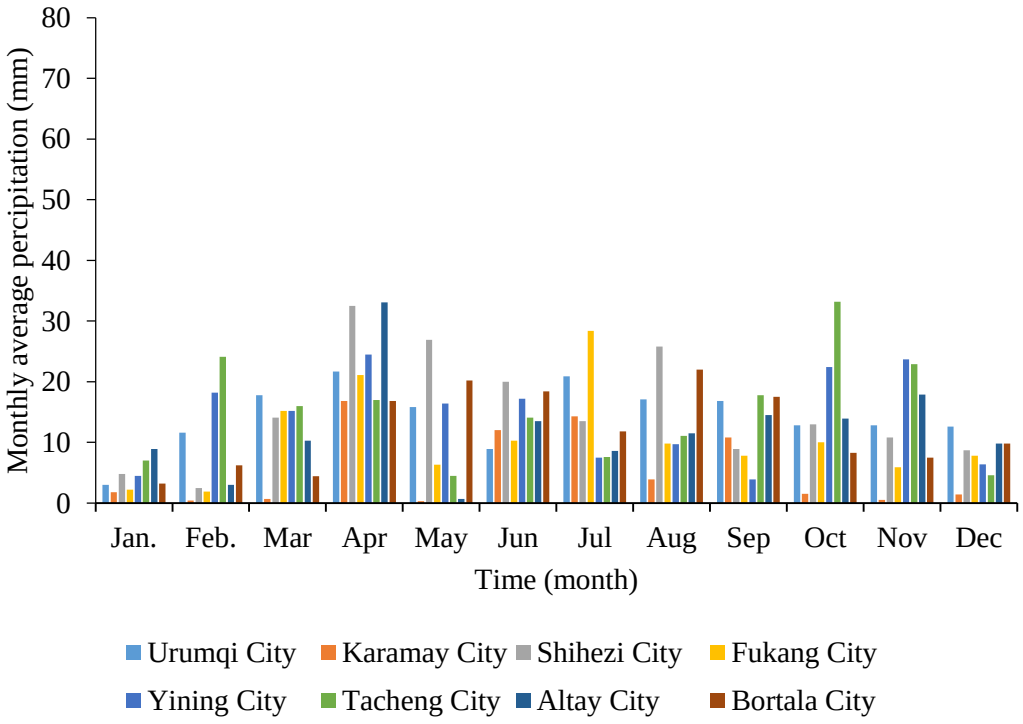

Fig.3.5 Monthly average precipitation of eight cities in north Xinjiang (2008)

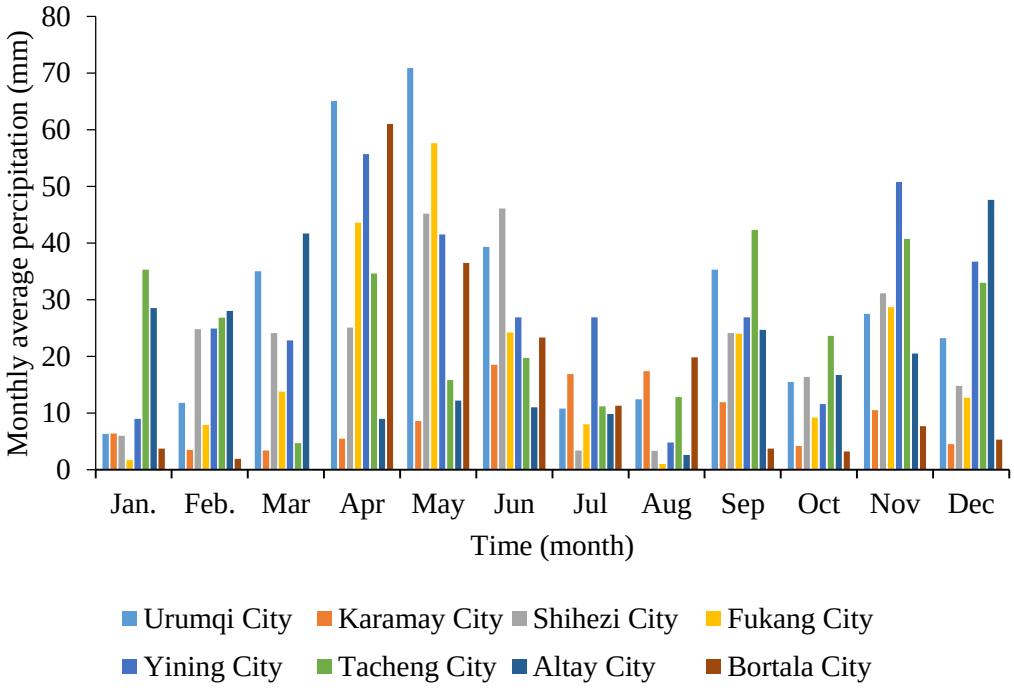

Fig.3.6 Monthly average precipitation of eight cities in north Xinjiang (2009)

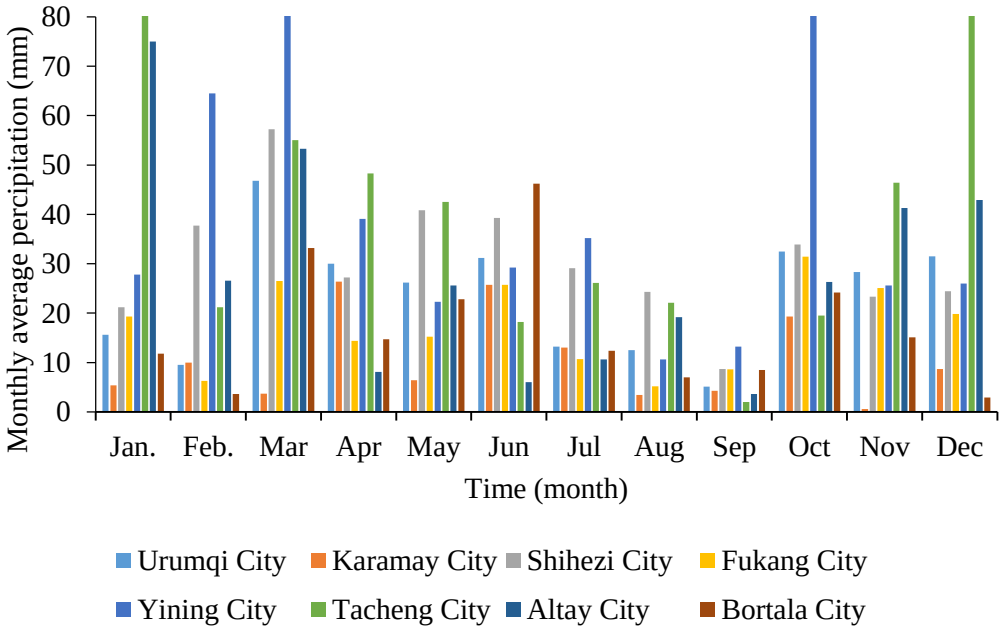

Fig.3.7 Monthly average precipitation of eight cities in north Xinjiang (2010)

3.2 Historical avalanche records in north Xinjiang

Table 3.1 shows the location name of historical avalanche accidents in north Xinjiang, the time of avalanche accidents happen, the human and livestock's losses from avalanche accidents, snow mass of avalanche accident sites at that time, average hazard score of avalanche accident site, and hazard score of avalanche accident sites in that avalanche happen year. The locations of avalanche accidents were showed Fig.3.8.

Table 3.1. Historical avalanches accident records

	Location name	*year*	*Human loss*	*Livestock's loss*
1	Nilka	2010.2.25	Killed 9 people, Trapped more than 400	
2	Nilka	2010.3.2.	Killed 2 people, Missed 2 people, Trapped 27	
3	Ili	2008.3.14	12 missing, 5 people died	
4	Nilka	2010.2.28	130 people trapped	
5	Tekas	2010.1.27	14 people died, thousands of livestock have died	1000 heads died
6	Tacheng	2010.1.10	97,000 people have so far been evacuated	
7	Altay	2010.1.7	620,000 people have been affected	9,234 heads killed

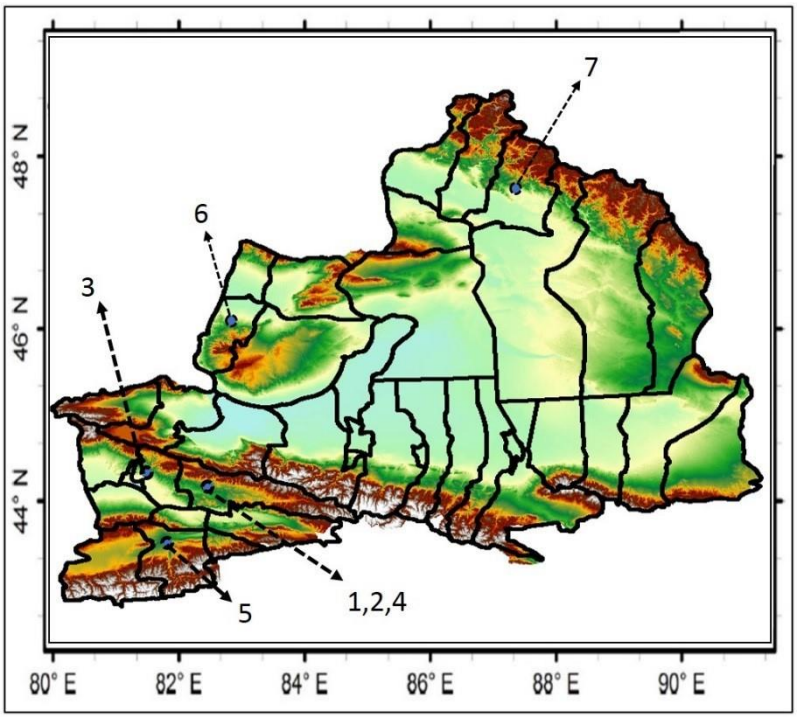

Fig.3.8. Location of historical avalanche accidents in north Xinjiang

3.3 Tianshan snow-cover & avalanche research station

Established in 1967, the Tianshan snow-cover & avalanche research station, Chinese Academy of Science (CAS) is located in the territory of Kunse Town of Xinyuan County beside the upstream section of the Kunse River in the Yili River valley. It lies in the western section of the Tianshan Mountains at 43º16´N and 84º24´E and at an altitude of 1,776 m above sea level. Annual average precipitation and temperature around the Station are 830.2 mm and 1.3ºC, respectively. The Station is 1,000 km from Urumqi, 120 km from Xinyuan and 35 km from Nalati town.

The Station was established originally to develop methods for protecting mountain roads against blowing snow and avalanches. Currently it is the only research base in China focusing on fundamental studies of snow phenomena, i.e. snow dynamics, snow resources, snow hydrology, and exchanges of surroundings with snow cover and blowing snow. It has a total land area of 16 hm^2 with the facilities for recording and measuring meteorological and hydrological parameters,

including air and soil temperature, snowfall and rainfall, wind, solar radiation, snow physics, and surface water runoff and interflow through soil. Fig.3.9 shows avalanche testing system in this station. Research fields includes: (1) Patterns of snow cover under complex topography and non-linear interactions with atmospheric and terrestrial systems; (2) Snow-cover dynamics and global climate change impacts; (3) Snowmelt runoff and hydrologic processes in the mountain area; (4) Disasters and risks related to snow-cover.

Fig.3.9 Avalanche testing system (adapted from Tianshan Snow-cover & Avalanche Research Station, CAS home page)

Conventional station observation can hardly meet practical demands because of unevenly distribution and lack in number of stations. Therefore, estimating potential avalanche hazard area in this study region has a great significance to general public and for avalanche disaster prevention.

Chapter 4 Data used

Available remote sensing products exist at a wide variety of spatial and temporal resolutions. In this chapter introduce data sets used in this study and provide related information. In the Table 4.1, the main characteristics of data sets used in this research were summarized with categories of dataset name, their spatial resolution, number of tiles used present study, the source of data coming, and brief reason for data usage.

Table 4.1. The main characteristics of datasets used in this study.

Data	Spatial resolution	Tile	Number of tiles	Source	Reason for use
MODIS snow cover data	500m	H23v04, h24v04	184	NSIDC	To improve spatial resolution
AMSR-E SWE data	25km		36	NSIDC	To remove cloud coverage
CMC snow depth data	25km		36	NSIDC	To generate snow volume
ASTER GDEM data	30m	N30E70 - N50E90	240	USGS	To estimate potential hazard area
Reference data	Xinjiang statistical yearbook				To analyze hazard area

4.1 MODIS and its snow cover 8-day level 3 global 500m grid data

the Moderate Resolution Imaging Spectra radiometer (MODIS) instrument is a multi-spectral instrument with 36 bands and nominal spatial resolution of 250 m in two bands, 500 m in five bands, and 1 km in another twenty nine bands (Gao et al., 2010). It is operational on two Earth Observation System (EOS) space-crafts, Terra (launched December 1999, over passing the equator about 10:30 am) and Aqua (launched May 2002, over passing the equator about 1:30 pm).

Based on MODIS imagery, a suite of snow and ice products have been provided through the Distributed Active Archive Centre (DAAC) of the National Snow and Ice Data Centre (NSIDC) since September 2000. The MODIS snow cover data is based on a snow mapping algorithm that utilizes a Normalized Difference Snow Index (NDSI) (NDSI = (R green – R_{SWIR}) / (R green + R_{SWIR}). For the MODIS data, NDSI = (R4-R6) / (R4+R6)) and two additional criteria tests (the thresholds of Band 2 and Band 4). The NSDI together with the NDVI were used to map snow in dense forests (http://nsidc.org/data/modis/data_summaries/index.html). The MODIS snow cover 8-day L3 global 500m grid data is data fields of maximum snow cover extent of an 8-day compositing period. The intent of the process for the MODIS 8-day snow cover product is to maximize the number of snow pixels while minimizing the number of cloud pixels (Gao, Y., et.al. 2010). The data consists of 1200 km by 1200 km tiles, in the projection of sinusoidal map at 500 m spatial resolution. The image was coded with integer value as following: sensor data missing as 0; no decision as 1; darkness, terminator or polar as 11; land (no snow detected) as 25; inland water as 37; ocean as 39; clouds as 50, lake ice as 100; snow as 200; saturated sensor detector as 254; and fill-no data expected for pixel as 255. Fig.4.1 shows sample image from MODIS snow covered data.

The reason of selecting MODIS snow cover data is that it has high spatial resolution and time series characteristics, and the data published with quality assessment. In this study, two tiles

(h23v04 and h24v04) of the MODIS 8-day snow cover products from January 1 to December 31 of year 2008–2010 were obtained from NSIDC Distributed Data Archive. Total 184 eight-day MODIS snow cover products were used.

The existing MODIS snow cover data was ideal to use. However, in practice, it was difficult to find a MODIS image that was no cloud contamination for the Xinjiang area (Liang et al., 2008). Clear-sky condition is rare, especially in winter season. (Dietz et al, 2013). Fig. 4.2 displays the monthly cloud-cover percentage for three selected years from MODIS snow cover data in northern Xinjiang.

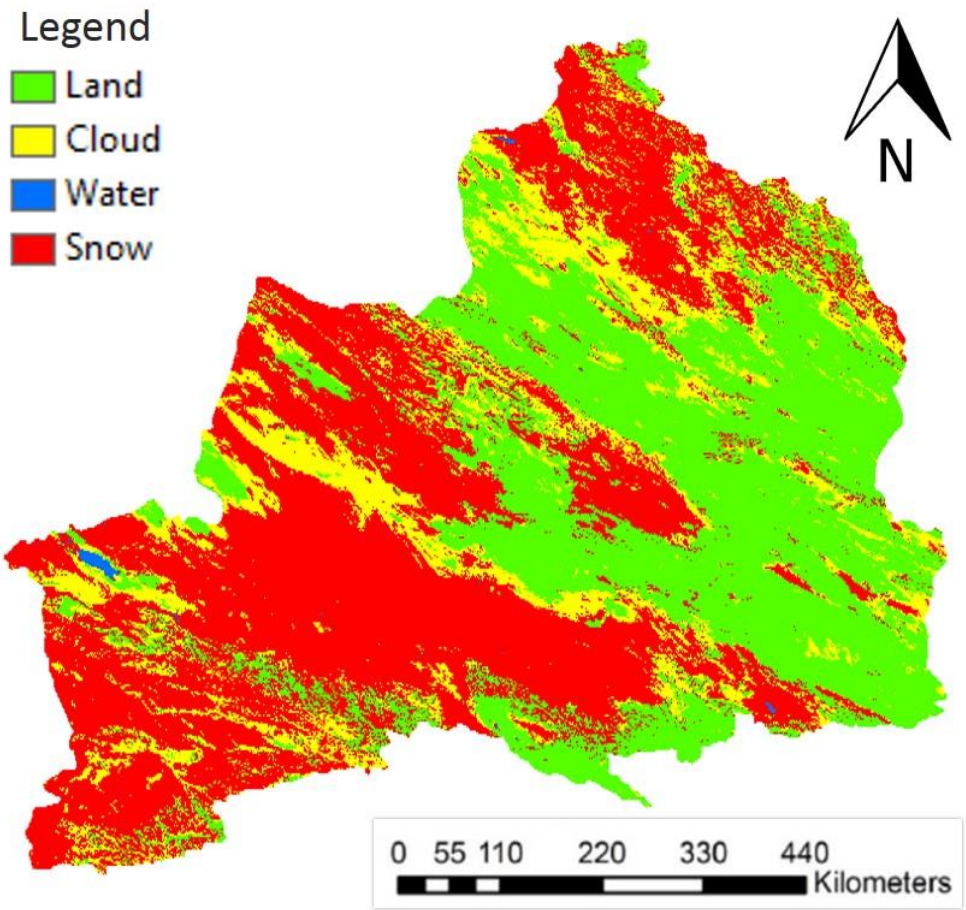

Fig.4.1 The image from MODIS snow covered data (January, 2008).

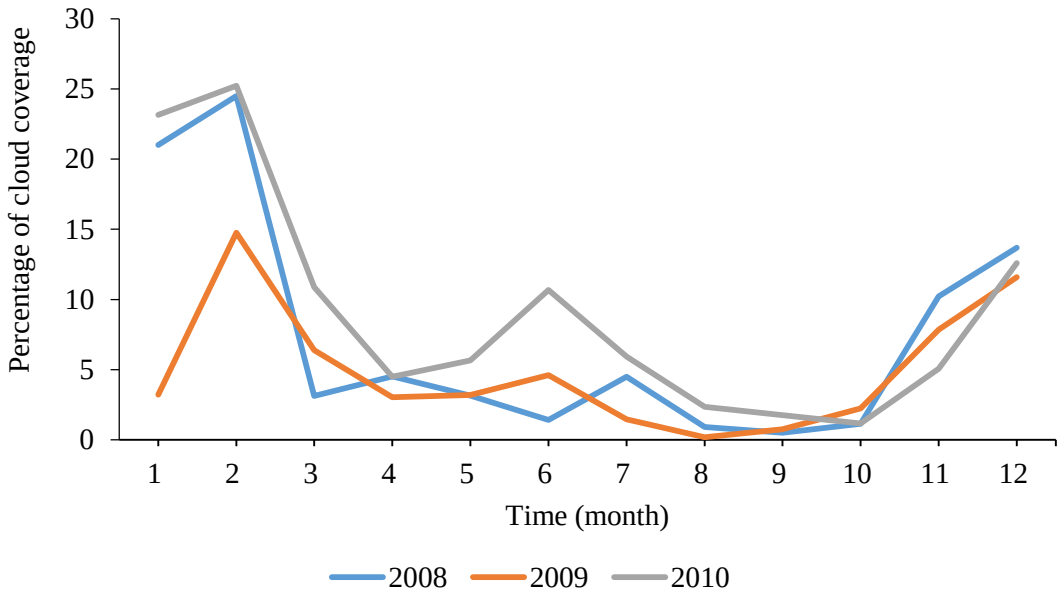

Fig.4.2 the state of cloud coverage from 2008 to 2011

The percentage of cloud coverage is mainly concentrated during winter season. The overall mean cloud-cover percentage in winter months varies from 20% for 2008, down to 10% for 2009, and, increase to 20% for 2010. It is significantly limiting the ability to map the exact of snow-covered area. A shown, cloud coverage became the biggest problem in utilization of MODIS snow cover data. It is often case that a perfect remote sensing product does not exist. Accordingly, a cloud-free time series snow covered product became a major prerequisite, when aiming at estimate accurate snow volume over time.

4.2 AMSR-E and its monthly L3 global Snow Water Equivalent (SWE) product

The Advanced Microwave Scanning Radiometer - Earth Observing System (AMSR-E) instrument is a 12-channel, 6-frequency, conically scanning, passive-microwave radiometer system, which launched on May 2002 on the Aqua satellite. (Gao, Y. et. al., 2010). The AMSR-E measures brightness temperatures ranging from 6.9 GHz to 89 GHz using horizontal and

vertical polarized microwave radiation. The mean spatial resolutions ranges varies from 5.4 km at 89 GHz to 56 km at 6.9 GHz.

The original algorithm of SWE is based on the methods in Chang et al. (1987) and Chang et al. (1997). The AMSR-E L3 SWE product created from AMSR-E/Aqua L2A Global Swath Spatially-Resampled Brightness Temperatures data. More information about the L2A brightness temperature can be seen at http//arcs.colorado.edu/data/ae_12a.html. For each low frequency (<89 GHz), snow depth retrieval is executed using brightness temperatures, and then calibrated and projected to the 25 km Equal-Area Scalable Earth Grids (EASE-Grids) projection. The snow depth is finally converted to SWE storing in HDF-EOS format. Files contain core metadata, product specific attributes, and 721 rows _ 721 columns. Fig.4.3 shows sample image from AMSR-E SWE data.

The value of SWE pixels value are 0 to 240 shows SWE values (mm), 248 shows off-earth, 252 shows land or snow impossible, 253 shows ice sheet, 254 shows water body, and 255 shows data missing. Because original values of SWE were scaled down by a factor 2 for storing in the HDF-EOS file, so, for the application, the data must be scaled up by multiplying by 2 (Gao, Y. et. al., 2010).

Although AMSR-E data has coarse spatial resolution, however, its cloud transparency and time series characteristics were become the reason of select AMSR-E SWE data as one of the data source. The data also published with quality assessment.

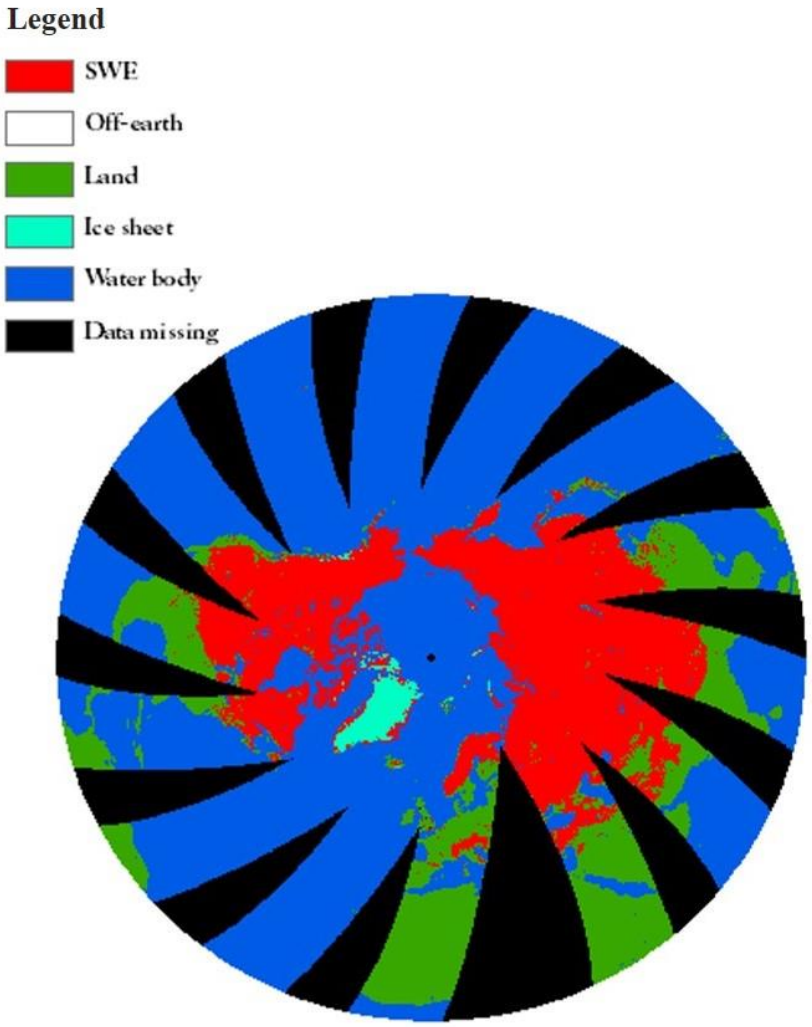

Fig.4.3 The image from AMSR-E SWE data (January, 2008)

4.3 Canadian Meteorological Centre (CMC) global snow depth analysis data

The CMC global snow depth data has been produced in a more-or-less consistent fashion since March 1998 and will be updated annually. The data were obtained from surface synoptic observations (synops), meteorological aviation reports (metars), and special aviation reports (SAs), they were acquired from the World Meteorological Organization (WMO) information system for use in the CMC analyses. It is updated every 6 hours using the method of optimum interpolation following Brasnett (1999) (Brown et al., 2011). The Fig.4.4 shows the flowchart of

CMC snow depth analysis process.

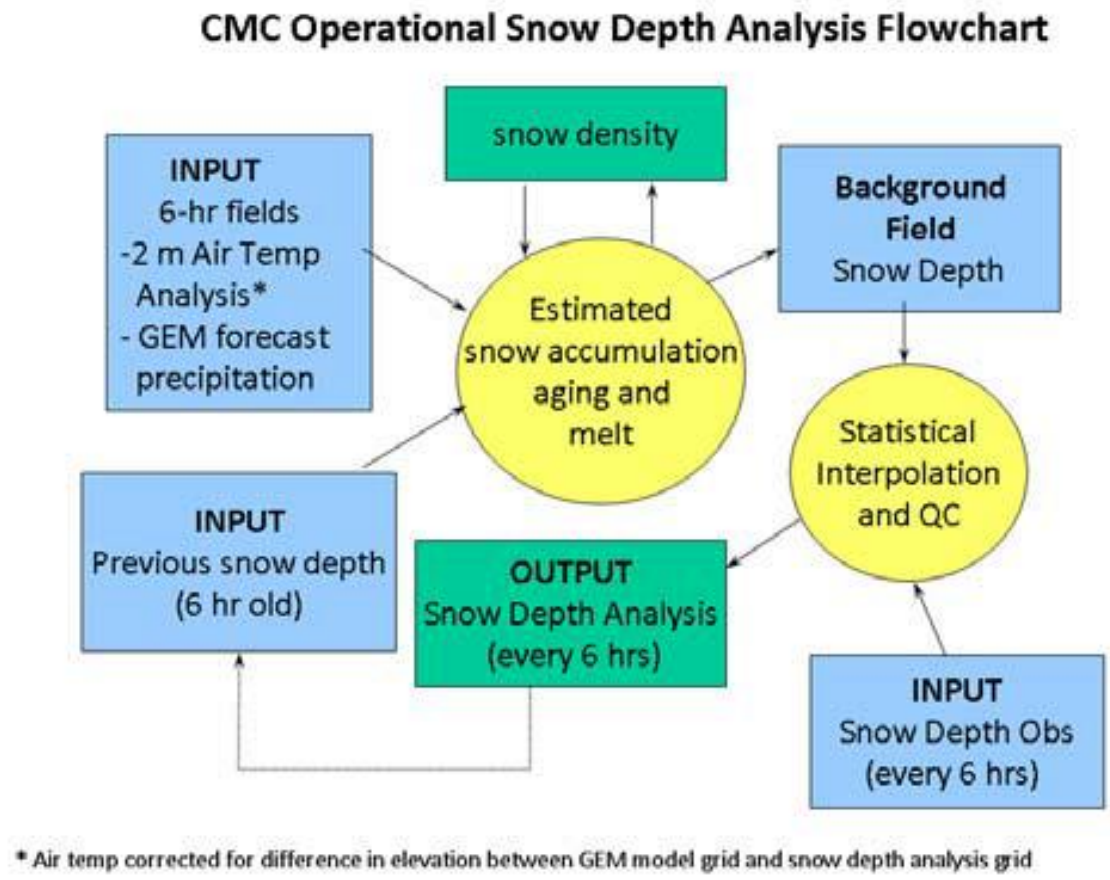

Fig.4.4. Flowchart of CMC operational snow depth analysis process

(Adapted from Brown et al., 2011).

A simple snow accumulation and melt model were provided the beginning hypothesis. The model using analysed air temperatures and GEM forecast precipitation (6 hour). If the analysed screen-level temperature is lower than 0°C, the precipitation is assumed to be snow. In analysis, horizontally 120km and vertically 800m e-folding correlation used for the error correlations; and the vertical correlation is considered the interpolation of screen-temperatures to the 1/3º grid. The analysis also contains an estimation of the snow density. The density of new snow is taken to be

100 kg/m^3 and the density of snow gradually increases as it ages. In thin regions of data, background field used to generate the snow depth. The analysis is not taken into account reliable in some areas, such as Greenland and some locations in the Rocky Mountains (Brown et al., 2011). Fig.4.5 shows the image of CMC snow depth data.

Fig.4.5. The image of CMC snow depth data.

The historical archive of CMC snow depth data has been used in a number of applications. including a global analysis of snow depth for numerical weather prediction (Brasnett, B., 1999); Northern Hemisphere snow cover variability and change from 1915 to 1997 (Brown, R. D., 2000); Gridded North America monthly snow depth and snow water equivalent for GCM evaluation (Brown, R. D. et. al., 2003); a multi-data set analysis of variability and change in Arctic spring snow cover extent (Brown, R.D. et al., 2010); Northern Hemisphere spring snow cover variability and change over 1922–2010 including an assessment of uncertainty (Brown, R.D. and Robinson, D.A., 2011); verification of satellite-derived snow cover products (e.g. Luojus et al., 2010); and the Canadian meteorological centre global daily snow depth analysis, overview, experience and applications (Brown, R.D. et al., 2011).

Bransnett, B. (1999) was present the snow depth operational analysis at the Canadian Meteorological Centre. The analysis takes use of precipitation forecasts and screen-level temperature analyses to estimate snowfall and snowmelt for a global scale. In addition, if snow depth observations are available, these are integrated using the statistical interpolation method. Brown, R.D. et al. (2003) were evaluate GCM snow cover simulations, by developing monthly snow depth and SWE information for North America, using the scheme of the snow depth analysis, which is developed by Brasnett, B. (1999), and CMC snow depth data. Brown, R.D and Mote, P.W. (2009) used CMC snow depth data, as one of the dataset, to evaluate climate model in Northern Hemisphere (Fig.4.6).

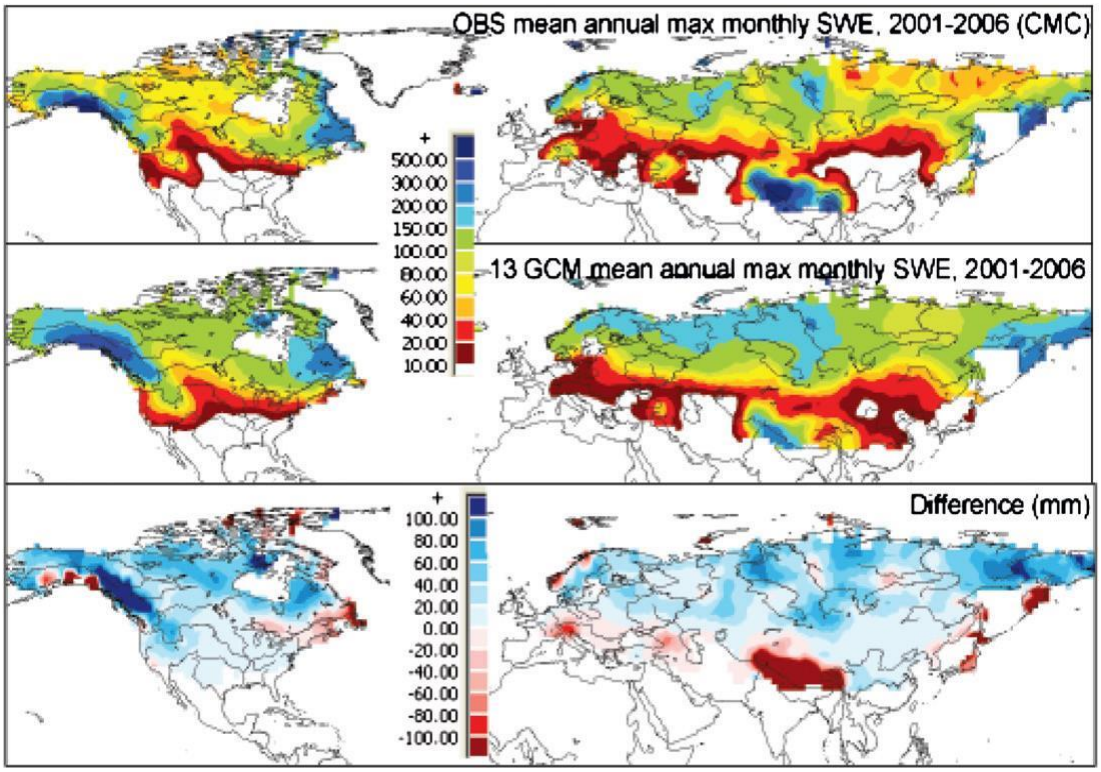

Fig.4.6. Example of CMC snow depth data used for evaluating model output (Upper part: estimated SWE_{max} from CMC snow depth, middle part: thirteen mean SWE_{max} from GCM, lower aprt: the mean model diefferance) (Adapted from Brown, R.D. and Mote, P.W., 2009).

Fig.4.6 shows an example, Global Climate Model (GCM) output evaluated by the CMC snow depth data, from this study. Thirteen mean SWE_{max} from GCM (middle part) and estimated SWE_{max} from CMC snow depth (upper part) from 2001 to 2006 were compared. The mean difference of model is shown in lower part.

Because of unavailability of ground truth data of snow depth for whole study area, CMC snow depth was selected. To validate reliability of CMC snow depth data, field work records from Ye, et.al. (2012) were used. Fig.4.7 shows the 32 snow sampling site in field survey in this study area. Table 4.2 shows sampling site information. Fig.4.8 shows the comparison of snow depth data from field survey and CMC.

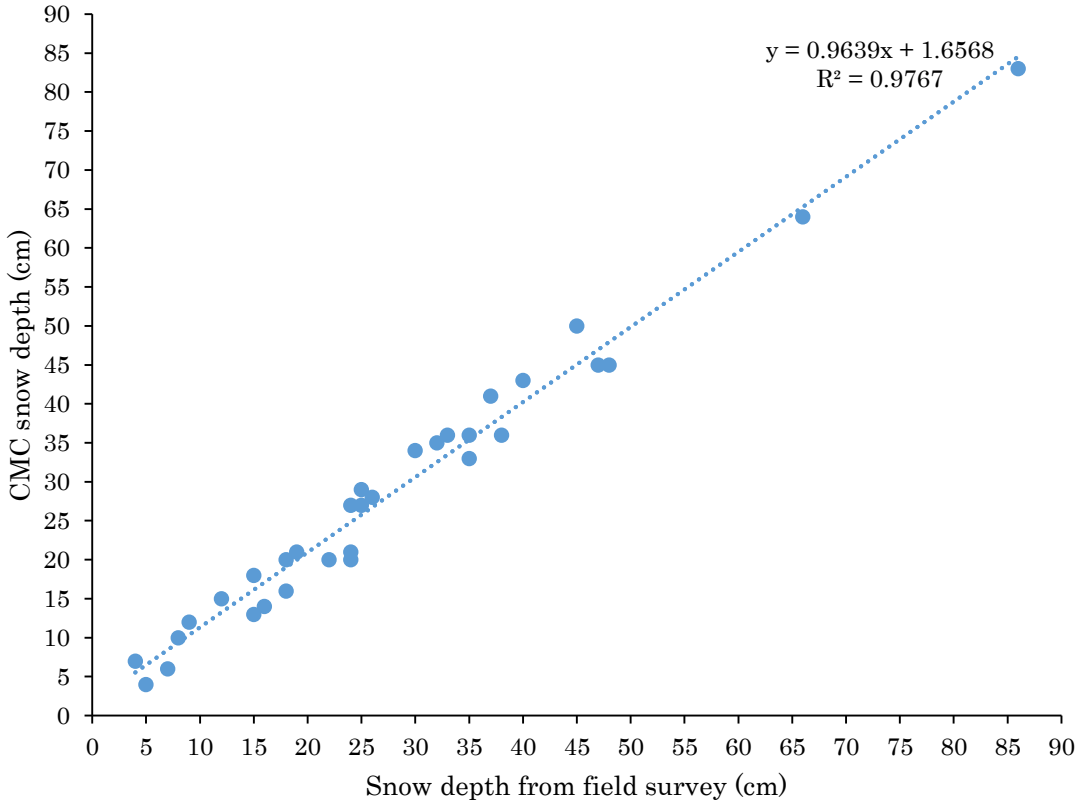

Fig.4.7 Comparison of snow depth data from field survey and CMC (RMSE=7.59).

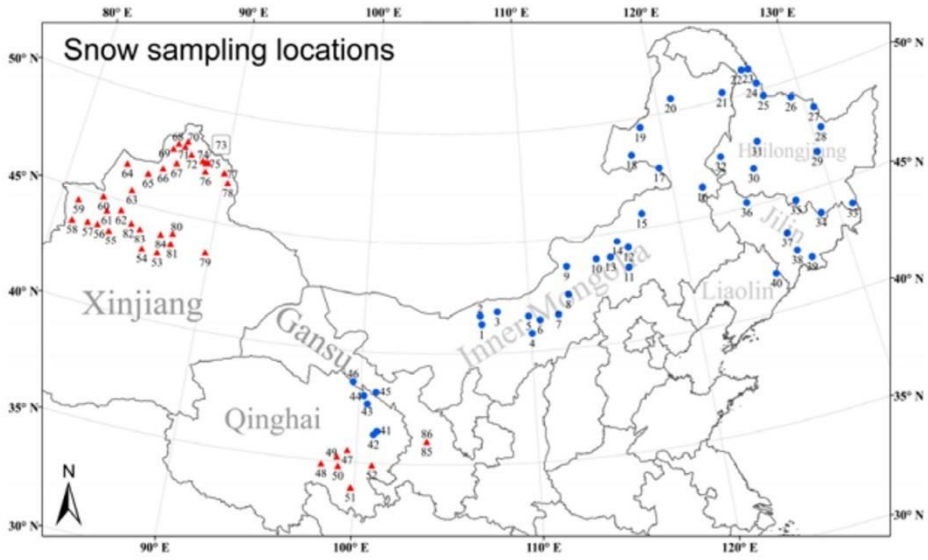

Fig.4.8 The 32 snow sampling locations in the field campaign. The sites are numbered in chronological order (adapted from Ye, et.al.,2012)

Table 4.2 The sampling site information (adapted from Ye, et.al. 2012)

Site	Sampling date	Lat. N (deg)	Lon. E (deg)	Altitude (m)	Snow depth (cm)	Total sampling depth (cm)	Sampling layers	Top layer depth (cm)	Surface BC concentration (ng g^{-1})	Depth-integrated BC concentration (ng g^{-1})	Ratio range of left to right
53	Jan. 31	43.072	86.805	3526	33	26	3	8	179	147	0.74–1.13
54	Feb. 1	43.080	85.821	3131	24	17	3	2	15	30	0.68–1.84
55	Feb. 2	43.506	83.541	988	24	8	2	4	118	107	0.68–1.32
56	Feb. 2	43.661	82.750	1327	22	12	3	4	58	177	0.73–1.38
57	Feb. 2	43.643	82.114	831	18	13	3	4	111	174	0.80–1.33
58	Feb. 3	43.525	81.133	1505	37	30	6	4	28	54	0.41–1.07
59	Feb. 4	44.495	81.152	2127	86	36	6	5	56	80	0.72–1.19
60	Feb. 4	44.956	82.629	237	8	5	2	2	587	567	1.24–1.37
61	Feb. 5	44.380	83.086	1250	24	19	4	3	112	122	0.87–1.21
62	Feb. 8	44.565	83.957	240	9	4	2	1	77	85	0.84–1.06
63	Feb. 9	45.579	84.285	1150	16	1	1	1	91	91	1.06
64	Feb. 9	46.679	83.544	674	25	15	4	2	161	173	0.71–1.29
65	Feb. 10	46.493	85.040	1033	5	2	1	2	89	89	0.99
66	Feb. 10	46.880	85.916	1461	15	10	2	5	31	56	0.86–1.02
67	Feb. 11	47.256	86.714	750	32	16	3	4	253	191	0.71–1.50
68	Feb. 11	48.147	86.557	693	30	20	4	5	121	62	0.77–1.27
69	Feb. 11	47.863	86.285	438	4	4	2	1	227	159	0.96–1.08
70	Feb. 12	48.333	87.128	1606	66	40	8	3	17	17	0.92–1.50
71	Feb. 12	48.072	87.026	934	40	30	5	5	73	55	0.86–1.52
72	Feb. 14	47.793	87.557	560	19	12	3	3	208	124	1.30–1.96
73	Feb. 14	47.553	88.612	1103	38	32	6	4	71	60	0.54–1.17
74	Feb. 14	47.627	88.396	818	35	25	5	4	125	77	0.59–1.56
75	Feb. 17	47.583	88.776	919	48	45	8	5	35	32	0.73–1.89
76	Feb. 18	47.167	88.704	717	26	16	4	2	171	135	1.01–1.22
77	Feb. 19	47.274	89.973	1362	45	45	9	4	36	15	0.80–1.27
78	Feb. 20	46.854	90.319	1438	35	27	6	2	57	20	0.80–1.05
79	Feb. 21	43.534	89.739	2185	47	40	7	6	37	51	0.87–1.15
80	Feb. 23	44.096	87.490	474	18	7	2	3	70	50	1.23–1.32
81	Feb. 23	43.596	87.506	1264	7	6	2	3	62	64	1.01–1.24
82	Feb. 24	44.093	84.802	1864	15	9	2	5	22	20	1.10–1.28
83	Feb. 24	43.934	85.413	1239	12	12	3	3	54	281	1.03–1.10
84	Feb. 25	43.932	86.763	1055	25	6	2	2	373	154	0.86–0.87

4.4 The ASTER Global Digital Elevation Model (ASTER GDEM)

ASTER GDEM is an easy-to-use, highly accurate DEM covering all the land on earth, and available to all users regardless of size or location of their target areas (http://asterweb.jpl.nasa.gov/gdem.asp). In this study, for extract slope feature of study region, the ASTER GDEM was utilized. Fig.4.9 shows the slope data, which is extracted from ASTER GDEM.

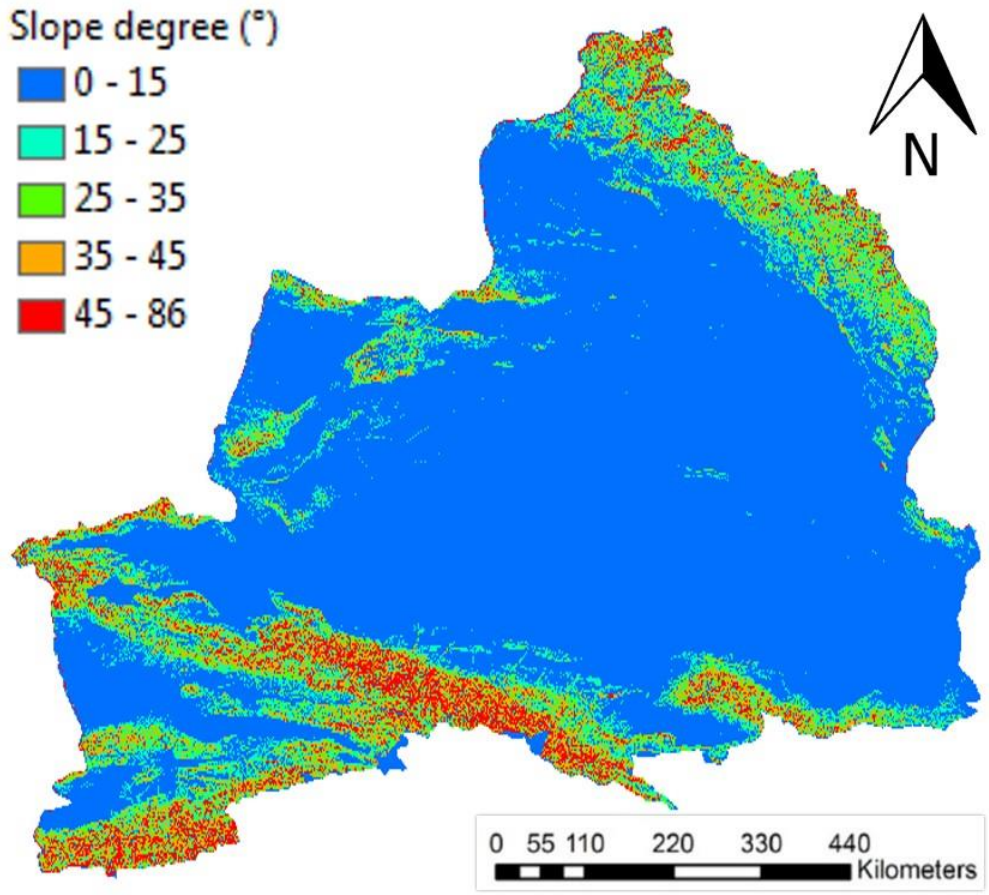

Fig.4.9 Slope data, which is extracted from ASTER GDEM.

The ASTER GDEM is a joint product developed by the United States National Aeronautics and Space Administration (NASA) and the Ministry of Economy, Trade, and Industry (METI) of

Japan. This data produced from the data that is collected from the Advanced Space-borne Thermal Emission and Reflection Radiometer (ASTER), which is a space-borne earth observing optical instrument. It is the only DEM, which covers the Earth entire land at high resolution.

From June 29, 2009, the version 1 of the ASTER GDEM became available for public, and it has been widely used by many users. It has greatly contributed to the community of global earth observing. The version 2 of the ASTER GDEM is developed by using an advanced algorithm, which is makes improvements on the resolution of GDEM and elevation accuracy, and reprocessing a total number of 1.5 million scene data. Accuracy of this version 2 product was validated by the collaborate effort of the United States and Japan. (http://www.jspacesystems.or.jp/ersdac/GDEM/E/4_1.html). The ASTER GDEM Version 2 formally released as an upgrade to Version 1 on October 17, 2011.

4.5 Reference data

For analysis climate futures of the study area, meteorological data set, such as monthly average temperature and monthly average precipitation were used. Those meteorological records between 2008 and 2010 were collected from Xinjiang statistical yearbook, which published by China statistics press. Fig.4.10and Fig.4.11 shows the monthly average temperature variation and the monthly average precipitation variation in north Xinjiang from 2008 to 2010.

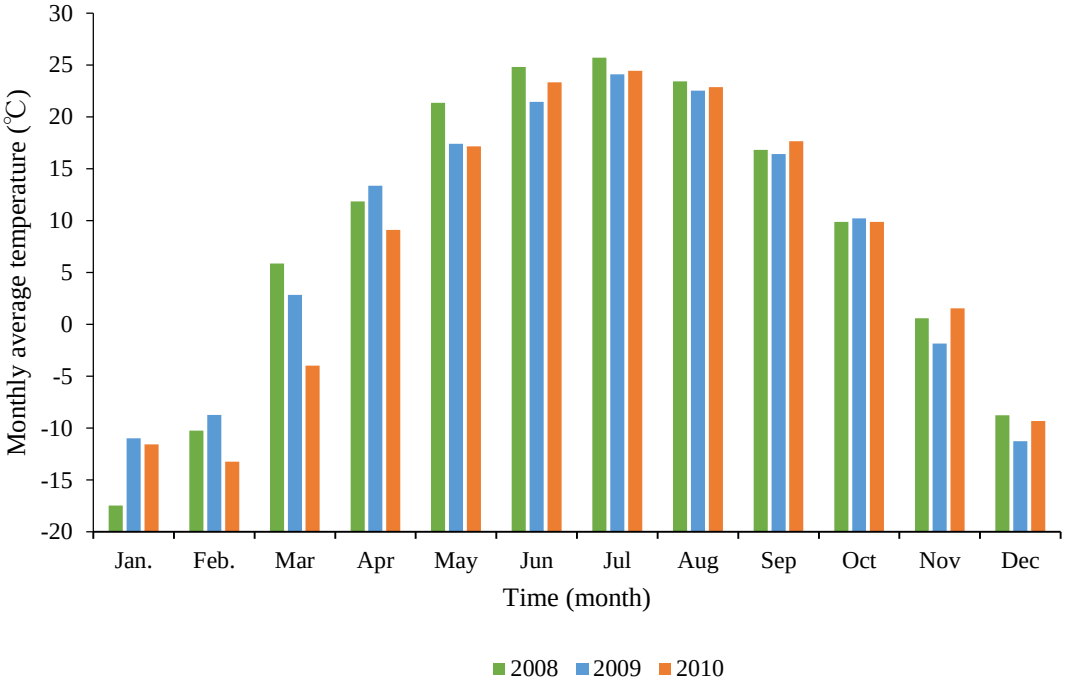

Fig.4.10 the monthly average temperature variation in north Xinjiang from 2008 to 2010

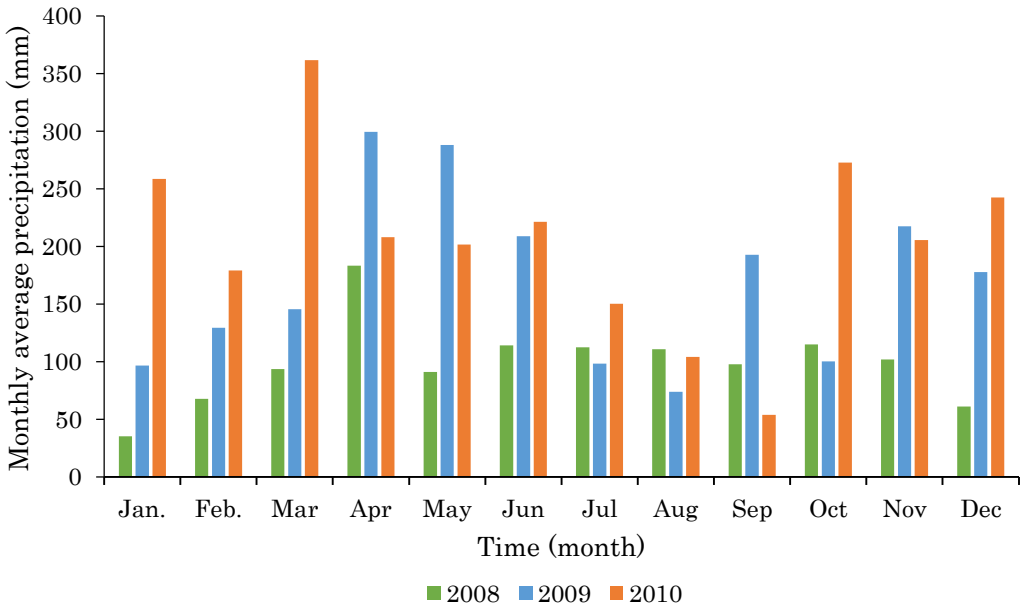

Fig.4.11 the monthly average precipitation variation in north Xinjiang from 2008 to 2010

To analysis the vulnerability to avalanche hazard, highway network system was selected as hazard-affected groups. The definition of "vulnerability" consider the intrinsic vulnerability of natural system, as well as it is indicates the responsiveness of social group. Vulnerability describes the extent of damage in environmental conditions that experience potential threats of disaster. Traffic and communication facility are easily affected by snow disaster. Therefore, usually, they are selected to describe socioeconomic vulnerability.

When looking for previous studies, Liang et al. (2004) used animal mortality as evaluation factor for snow hazard of grassland in winter to evaluated snow disaster risk for Altay region in north Xinjiang. Liu et al. (2004) used grassland area, soil and pasture property, livestock death rate and population of big animals and small animals, forage store, and economy (including communication, herdsman life, and house property) as evaluation indexes of snow disaster effect on grassland animal husbandry in Altay, north Xinjiang. Liang et al. (2007) used grassland capability index, grassland buried index as evaluation index for snow disaster in pastoral areas of north Xinjiang. Risk assessment of snow disaster in other regions of China, for example in Inner Mongolia, which is one of the snow centers in China, population numbers or livestock numbers used as evaluation index of snow disaster risk. Wu et al. (2008) used amount of livestock numbers and ration of cow to sheep as indicators of disaster bearing bodies, average income of herders, forage per stock, and shelter per stock as indicator of environmental possibilities with hazard to evaluate the risks of heavy snow disaster in Xilingol, Inner Mongolia. Tachiiri et al. (2008) used livestock number mortality to assessing the risks of Mongolian snow disaster. Liu et al. (2011) used population and livestock numbers as life factor in exposure index to assessment snow disaster risk in Xilingol, Inner Mongolia.

In the case of snow disaster in north Xinjiang area, environmental condition (for example, road provision) is of responding to snow disaster. Snow avalanches also blocks the highway. A heavy

snowfall leads accumulated snow on the road surface, and soaked embankments, which cause slope landslides, collapse, road froth, and swelling, affecting normal highway traffic. Because of these reasons, therefore, in this paper highway network system were considered as a more vulnerable for snow avalanche hazard in hazard-affected entities and selected as vulnerability index in risk assessment. Fig.4.12 shows the state of highway network system in north Xinjiang.

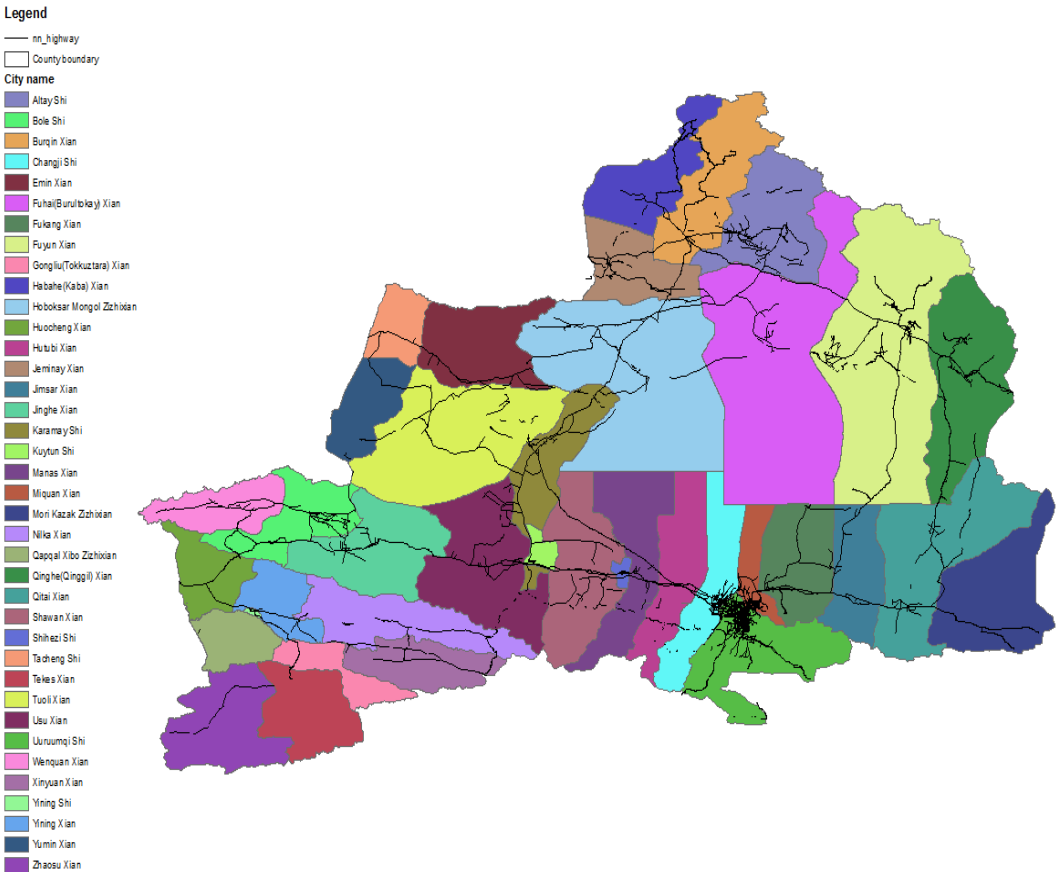

Fig.4.12. The situation of highway network system in north Xinjiang.

Chapter.5 Methodology of estimation of snow mass and creation of potential hazard map

The recognition of potential hazard area is a not easy work. In many mountain regions, nearly no information on avalanche release areas exists, mainly due to the very rough and poorly accessible terrain, the vast size of the region and the lack of avalanche records. By far the most reliable way to identify avalanche hazard areas is using historic avalanche records, such as the frequency and intensity of historical disaster and field investigations accomplished by avalanche experts. However, both methods are not feasible for this study area, because of the difficulty in accessing historical data associated with avalanches, and due to the rough terrain, its vast extent and lack of time, therefore, present study used solely existing snow products and topographic features of the terrain to estimate potential hazard area for avalanche prevention.

As mentioned in Chapter.2, avalanches are a falling mass of snow. It is a sudden flow of a large mass of snow down a slope or cliff. Snow mass is the indicator of accumulation of snowfall. It is the most important factor in the formation of an avalanche, while the duration of snow cover is the second most important factor. However, snow accumulation does not only parameter of constitute an avalanches; because an avalanche is the result of natural process, its occurrence also needed some other geomorphologic factors. Topography largely controls where avalanches start and how far they run. According to the theory of avalanches, prerequisites of avalanche are snow accumulation and steep topography. Slope inclination is most import factor that controls avalanche occurrences. In other words (technically), any amount of snow sliding down a mountainside is an avalanche. Technically, an avalanche is any amount of snow sliding down a mountain side. Under the pull of gravity, accumulated heavy snow downs a slope, due to structural weakness in the snow cover on that slope. “snow-slide” is another common name for

avalanche (Eckerstorfer, M., 2012). As an avalanche becomes nearer to the lowest position of the slope, it gets speed and power, this can induce even the smallest of snow-slides to be a major disaster.

Since a large mass of snow is necessary for an avalanche to occur, and slope angle is most import parameter that controls avalanche occurrences, therefore, is in this study, snow mass and slope were considered as parameters to attribute to avalanche trigger, and selected as the evaluation factor of estimating potential hazard area.

Although meteorological factors are favorable for avalanche release, such as wind velocity and direction, air temperature, as well as direct solar radiation over various time scales, all dynamically interacting with the terrain, however, other factors like wind speed, temperature or topographic features of a snow-covered area complicate the determination of snow cover risk on a macro scale (Liu et al., 2014), and are therefore not considered in this macro-scale regional study, but must be considered when conducting a relatively small-scale assessment or snowdrift risk assessment. Whilst being aware of the fact that the avalanche is a combination of many factors, the attention is here focused only on topographical factors, because the underlying hypothesis is that, the topography is the primary factor influencing avalanche formation.

Accordingly, methodology of this study consists of two parts estimation of snow mass and estimation of potential hazard area. The flowchart of estimating potential hazard area was shown in Fig.5.1

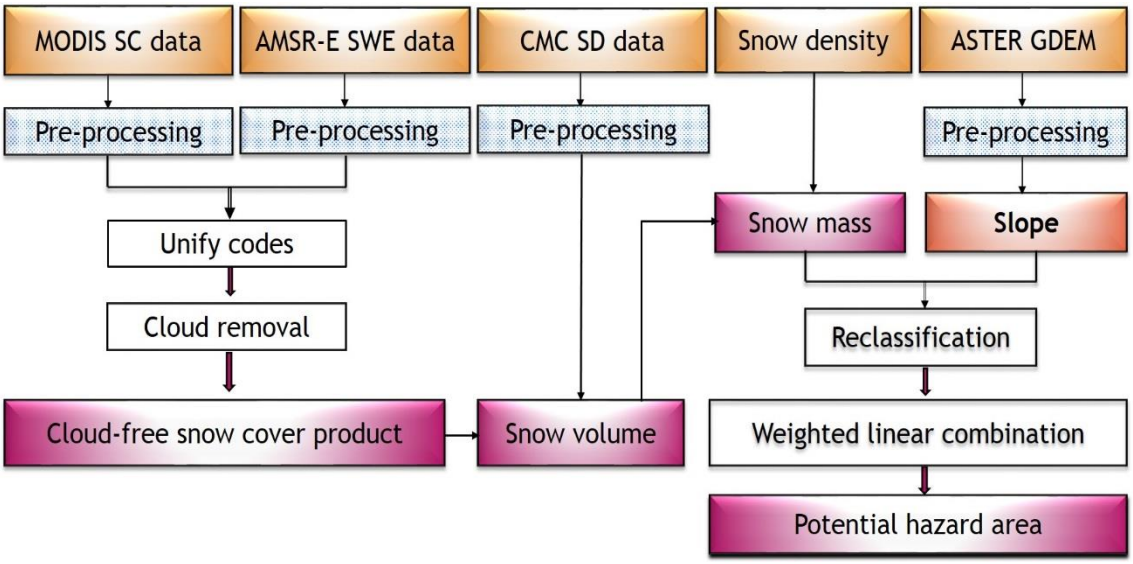

Fig.5.1 Flowchart of estimating potential hazard area.

Prior to the procedure, image pre-processing to the data are needed. It is including mosaicking, resampling, and subset, etc. Using the MODIS Re-projection Tool, total184 eight-day MODIS snow cover products were mosaicked and geo-referenced from sinusoidal map projection to Geographical latitude/longitude projection with the WGS84 ellipsoid, respectively. The nearest neighbor resampling approach was employed. The mosaicked images were saved as a Geo-tiff file format, and transformed into ESRI grid data, as well as subset according to study area vector file. Total 48 AMSR-E SWE images were re-projected from North Pole azimuthally equidistant projection to Geographical latitude/longitude projection, and were transformed into ESRI grid format files. The grid size of 25 km was resampled to 500m, using nearest neighbor approach, in order to combine with the MODIS snow cover product. And, also, subset data based on vector file of study area, it is same as MODIS snow cover product. Due to CMC snow depth data are provided in tab-delaminated ASCII text files, so, snow depth data, firstly, converted to raster data through ArcGIS Python language. Then the grid size of 24 km was resampled to 500m using nearest neighbor approach, in order to make same spatial resolution as the MODIS snow cover

product and AMSR-E SWE product. Subset the data based on vector file of study area, as the same way with MODIS and AMSR-E data.

5.1 Estimation of snow mass

Estimation of snow mass requires a reliable snow volume data with a high spatial resolution and covering a sufficient length of time and snow density data. The microwave snow estimates have been recognized as an efficient means of the large-scale mapping of snow depth and snow-water equivalent (SWE) with a high spatial density. Actually, the existing AMSR-E SWE data was enough to use as snow mass data to estimate hazard area, however, it is low resolution of 25km is not efficient for this study area to see more detail information about the area effected by hazard.

As mentioned in Chapter.4, existing MODIS snow covered data included cloud coverage. So, cloud-remove became the prerequisite of estimating accurate snow volume. An attractive alternative of cloud-remove is to merge multiple remote sensing products with complementary characteristics. Utilizing MODIS snow cover data and AMSR-E SWE data with complementary spatiotemporal resolution characteristics is taken to generate cloud-free snow cover products.

5.1.1 Generation of cloud-free snow cover product

Detail explanation of cloud remove process as followings:

(1) Unifying codes:

In order to combine (merge) MODIS and AMSR-E data, the step of unify codes were needed, because MODIS and AMSR-E snow products have different code devising system. For example, code number of snow only represent 200 in MODIS data, but it repents 1 to 240 in AMSR-E data, while same integer number 254 meaning no meaning data in MODIS, but

it meaning water body in AMSR-E data. So, it cannot be simply add these two products, in combining products process. Unify codes, which mean is the original integer numbers of MODIS and AMSR-E transformation into same unit new codes. The rules of unification are included in Table 5.1.

Table 5.1. Rules for unify codes

MODIS		AMSR-E	
original integer number	new code	original integer number	new code
200, snow	4	1--240, SWE	4
37, water	3	254, water	3
25, land	2	0/252, land/ snow impossible	2
50, cloud	1		
others	0	others	0

The new codes include five integer numbers: 0 to 4, here, 4 shows snow covered area, 3 shows water body, 2 shows land area, 1 shows cloud covered area, and 0 shows no meaning data. The rules for transforming MODIS integers to new codes are: 200 (snow) converted to 4, 37 (inland water) converted to 3, 25 (land) converted to 2, 50 (cloud) converted to 1, and 0, 1, 254, 255 (no meaning) converted to 0. The rules for converting AMSRE integers to new codes are: 1–240 (snow-covered) converted to 4, 254 (water) to converted 3, 0 (snow-free land) converted to 2, and 248, 252, 255 (no meaning) converted to 0. The program of unifying codes of MODIS and AMSR-E products are:

DOC ---- code----------

Model on "K:\TestAnalyz\MODIS_SCA\ucode/2009_1.tif"

```
Local int i, fa, fout
For i =23 to 46
fa = DBOpen("K:\TestAnalyz\MODIS_SCA\8day/2009_"+F$STRING(i)+".tif","r")
fout = DBOpen("K:\TestAnalyz\MODIS_SCA\ucode/2009_"+F$STRING(i)+".tif","r+")
%{ fout, 1} = 0
IF (%{ fa, 1} = 200) %{ fout, 1} = 4
IF (%{ fa, 1} = 37) %{ fout, 1} = 3
IF (%{ fa, 1} = 25) %{ fout, 1} = 2
IF (%{ fa, 1} = 50) %{ fout, 1} = 1
endfor
endmodel
DOC ---- code----------
Model on "F:\Analyze data\AM_ucode/09_1.tif"
Local int i, fa, fout
For i =23 to 46
fa = DBOpen("F:\Analyze data\AM09_8daytiff/09_"+F$STRING(i)+".tif","r")
fout = DBOpen("F:\Analyze data\AM_ucode/09_"+F$STRING(i)+".tif","r+")
DOC ---- code----------
%{ fout, 1} = 0
IF (%{ fa, 1} >0 AND %{ fa, 1} <240) %{ fout, 1} = 4
IF (%{ fa, 1} = 254) %{ fout, 1} = 3
IF (%{ fa, 1} =0 AND %{ fa, 1} =252) %{ fout, 1} = 2
End for
End model
```

(2) Combination processes:

In this step, the cloud covered pixels of the MODIS were replaced using the value of AMSR-E data. Similar to Xie et al. (2009) and Wang et al. (2009) methods, two products were combined, as following rules:

If $Value_{MODIS}$ <= 1, $Value_{MA}$ = $Value_{AMSR-E}$; Else $Value_{MA}$ = $Value_{MODIS}$

The program of combining MODIS and AMSR-E data are:

```
DOC ---- code----------------------------------------------------------------------------------------
Model on "M:¥1TestAnalyz¥testcom/com_1.tif"
Local int i, fa, fb, fout
For i =1 to 22
fa = DBOpen("M:¥1TestAnalyz¥09MOD_SCA¥resizetif/re_"+F$STRING(i)+".tif","r")
fb=DBOpen("M:¥1TestAnalyz¥09AMSRE¥ucodAM/ucodAM_"+F$STRING(i)+".tif","r")
fout = DBOpen("M:¥1TestAnalyz¥testcom/com_"+F$STRING(i)+".tif","r+")
IF %{ fa, 1} =1 then %{ fout, 1} = %{ fb, 1}
else %{ fout, 1} = %{ fa, 1}
End for
End model
```

5.1.2 Estimation of snow volume

Snow volume is sum of all non-zero snow depth pixels multiplied by the snow covered area pixel (Biancamaria, S. et. al., 2011). Equation 5.1 shows simple formula of calculate snow volume product.

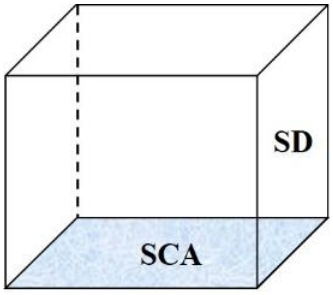

$$SV = \sum_{k=1}^{n} SD * SCA \qquad \text{(Eq.5.1)}$$

Where, SV represents snow volume, SD represents snow depth, SCA represents snow covered area, k is pixel value. Therefore, estimation of snow volume requires the depth of snow and the area covered by snow.

CMC snow depth data was applied as snow depth data in this study. Actually, the volume of snow is possible to calculate directly from CMC snow depth data. Which mean is CMC snow depth multiply to its surface area (CMC snow depth *24km*24km). However, the result of snow volume product will be at very low resolution of 24km. In order to get more detail information about hazardous area, the high spatial resolution snow covered product was used.

5.1.3 Generation of snow mass

In mathematically, snow mass is multiplication of snow volume with snow density. Accordingly, snow mass in this study calculated from snow volume and snow density data. Formula of estimating snow mass was:

$$SM = \sum_{k=1}^{n} SV * SD \qquad \text{(Eq.5.2)}$$

Where, SM represents snow mass, SV represents snow volume, and, SD represents snow depth, k is pixel value. Based on Eq.5.2 estimation of snow volume requires the depth of snow and the area covered by snow. Snow density token the average value of snow density of 0.2g/cm^3, based on Dai, et.al. (2012) field work research in north Xinjiang area.

5.2 Creation of potential hazard map

In hazard mapping procedure, a very important step is to determine dangerous areas. Aiming at estimating the potential avalanche hazard area, the two selected evaluation parameters, which are snow mass and slope, must be combined. To be able to satisfy this new requirement, the model were integrated into a GIS-based user environment. Map overlaying analysis in GIS were used for combination of snow mass and slope data, since map overlaying is regarded as the major operation in analyzing the environmental features for regional planning (Peng, S. et al., 2012). In order to use GIS for estimate potential hazard area, data were stored in the GIS system. Each data used in this operation considered as a layer.

With the help of Weighted Linear Combination (WLC) method in GIS, the estimation of potential hazard area was preceded for the values of grids. This method can provide the decision makers several options for selecting appropriate strategies, because using this method, the final output map will range from the "high dangerous" to "no dangerous".

5.2.1 Weighted linear combination

Weighted linear combination (WLC) is one of the widely used MCE methods. A multi-criteria evaluation (MCE) method is mainly involved with how to combine the information from several criteria to form a single index of evaluation (Al-Hanbali, et al., 2011). It is used to deal with difficulties that decision makers encounter in handling large amounts of complicated information. WLC is a concept which combines maps by applying a standardized score to each class of a certain parameter and a factor weight to the parameters themselves. It has been used in many studies, which are related to many various subjects including ecological sciences, urban-regional planning, waste management, hydrology, agriculture, forestry, natural hazards, recreation/tourism, housing/real estate, geological sciences, manufacturing and cartography.

A GIS based WLC analysis, examines a number of possible choices for a siting problem, taking

into consideration multiple criteria. WLC is an analytical method that can be used when dealing with multi-attribute decision making (MADM) or when more than one attribute must be taken into consideration. Every attribute that is considered is called a criterion. Each criterion is assigned a weight based on its importance. The results are multi-attribute spatial features with final scores. The higher score shows the more suitable area, which mean is more dangerous area for likelihood of snow avalanches.

The explanations about how to perform weighted linear combination analysis in GIS are as following:

(a) all input attribute were given scores to reclassify. Since these input layers are in different numbering systems and with different ranges, raster's of these data could not be simply added. For each layer, reclassification system is required;

(b) Identify weights for input attributes. Evaluation factors in the model may have different importance. Before the factors are combined, the factors can be weighted, based on their importance. As a general rule, it was decided to give higher weights to the factor that affect directly on the community. Because of the meaningfulness and consistent of output map, the total weight must be added up to 1 and based on the scheme that was the same for each layer, the attribute score should be chosen;

(c) Then, a final composite map was produced using WLC. The cell values of each input raster are multiplied by the raster's weight. The resulting cell values are added to produce the final output raster.

5.2.2 Data processing operation

(1) Extraction of slope

Input data of slope is derived from ASTER GDEM data. Before obtain slope map, pre-

processing, such as mosaicking, sub-set study area, were needed.

(2) Reclassification

Since these two input layers are in different numbering systems and with different ranges and raster's of these data could not be simply added. So, for each layer, reclassification system is required. The score assess their importance on avalanche occurrence on study area that range from 0 to 10. The higher score was obtained, the more importance it would present. A score of 0 indicates no potential danger, and a score of 10 indicates an extremely serious dangers. The total values with the higher scores will represent the events most in need of organization planning for emergency preparedness. Reclassify tools of spatial analyst function in ArcGIS software were used to reclassify the input data.

Based on the effects of slope on the trigger of avalanches, slope α were given scores to reclassify. A score of 10 were given to slope degree from 30 to 35. A score of 8 were given to slope degree from 35 to 45. The result of reclassified slope was shown in Fig.5.2 in one pixel size, where it is compared to original slope data.

For the reclassification of snow mass, there is no research related to explain relationship of mass of snow and avalanche occurrence. Liu. et al. (2009) studies shows the snow depth reclassification and dangerous score in North Xinjiang area. Based on the reclassification system of his studies, snow mass in current study were reclassified.

(3) Weighted linear combination of layers.

In order to apply the WLC analysis, Weighted Sum tool of spatial analyst function in ArcGIS were used, because it is act as a WLC analysis. The weighted sum tool provides the ability to weight and combine multiple inputs to create an integrated analysis. It is similar to the Weighted Overlay tool in that multiple raster inputs, representing multiple factors, can be easily combined incorporating weights or relative importance. One major difference between

the weighted overlay tool and the Weighted Sum tool is the Weighted Sum tool allows for floating point values whereas the Weighted Overlay tool only accepts integer raster as inputs. In other words, WLC combines multiple raster inputs, representing multiple factors, of different weights or relativ611e importance. It is one of common methodologies used for snow disaster monitoring in general, and for defining potential hazard area in particular. The WLC analysis was applied using the following equation:

$$H = \sum Wi * Xi \quad \text{(Eq. 5.3)}$$

Where H is the potential hazard degree, W*i* is a weighting of factor i, and X_i is the criteria score of factor i. The cell values of each input raster are multiplied by their weights. The resulting cell value is added to produce the final output raster.

Weights were generally assigned to these two layers to express the relative importance. In this study, the input data were given equal importance, because snow volume and slope considered as same importance on avalanche occurrence. The category of layers, the criteria of reclassification, the scores of given, and weights of each layer were summarized in Table 5.2.

Table. 5.2 The reclassification system of snow mass and slope to estimating potential hazard area.

Category	Criteria	Score	Weights
Snow mass (g/cm2)	0< 140	0	0.5
	140<= V< 200	6	
	200<= V< 400	7	
	400<= V< 600	9	
	600<= V	10	
Slope (°)	α< 25	1	0.5
	25< α< 30	2	
	30< α<35	10	
	35< α<45	8	
	45< α<60	4	
	60< α	2	

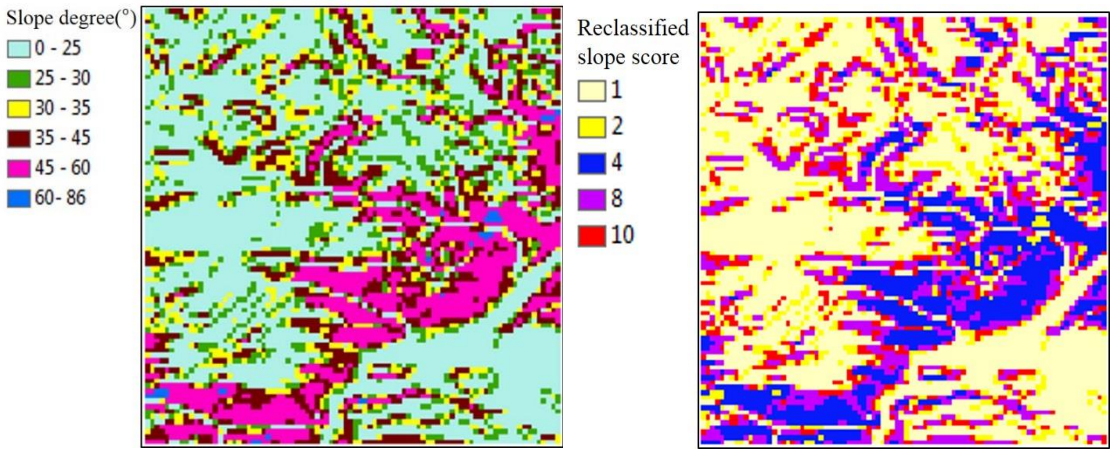

Fig.5.2 Comparison of original and reclassified slope data. (Left: original slope data, Right: reclassified slope data (sample pixel: UL: 87.173E, 48.855N, LR: 87.533E, 48.496N)).

Chapter.6 Results and discussions

6.1 Snow volume outputs and discussions

Fig.6.1 shows the MODIS snow products and new cloud-free snow cover products in monthly time scales over 2008 to 2010 of north Xinjiang area. X- axis shows time (month) and Y-axis shows percentage of snow, no-snow, and cloud area. By taking advantage of both MODIS and AMSR-E data, the positive combination of them removed all the cloud area in MODIS data. This method makes greatly complete the deficiency of MODIS product. This process demonstrated that combining existing MODIS and AMSRE snow products to generate cloud-free snow cover product is practicable. The results indicated that the new cloud-free snow cover product at 500m spatial resolution could effectively capture information of snow cover, during the period of January 2008 to December 2010.

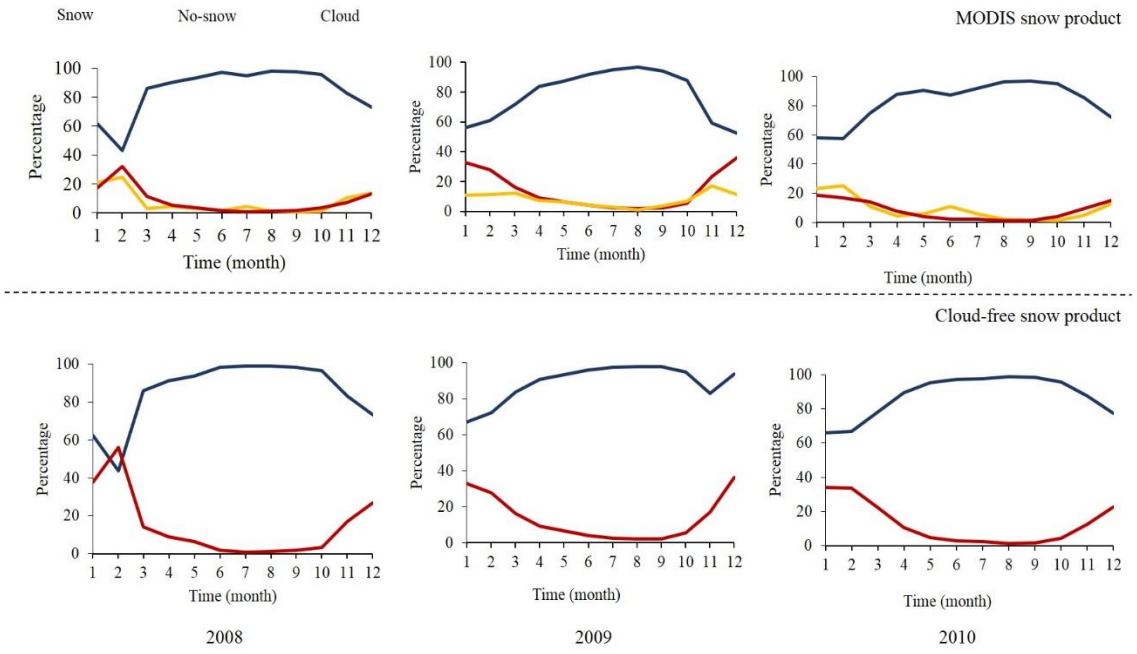

Fig.6.1 The situation of the existing MODIS snow cover data (upper part) and cloud-free snow cover products (lower part) in monthly time scales over 2008 to 2010 in north Xinjiang area.

Based on the definition of snow volume, snow volume was estimated from cloud-free snow-covered area and snow depth. Due to source data of snow volume product, which are MODIS snow cover data, AMSR-E SWE data, and CMC snow depth data were published with the quality assessment, and, in previous section 4.3, CMC snow depth data were validated with field work data. Therefore, the validation of snow volume product was shortened, because of lack of in situ data of snow volume for this study region. From Fig.6.2 to Fig.6.4 shows the monthly snow volume map over the study area, during January 2008 and December 2010. Serious snow volume change mainly concentrated on Altay, Tacheng, and Ili regions.

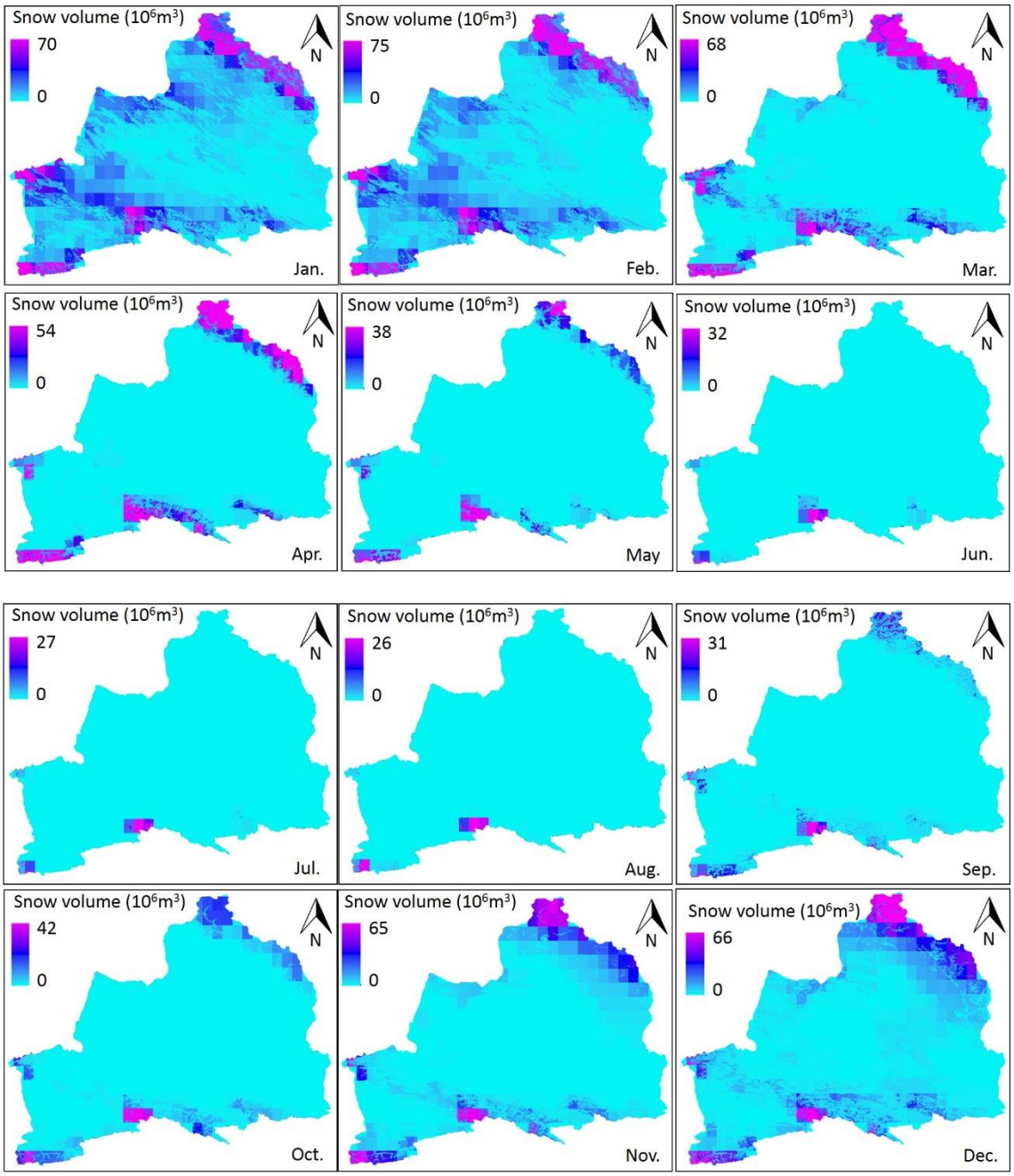

Fig.6.2. Monthly snow volume map of north Xinjiang in 2008.

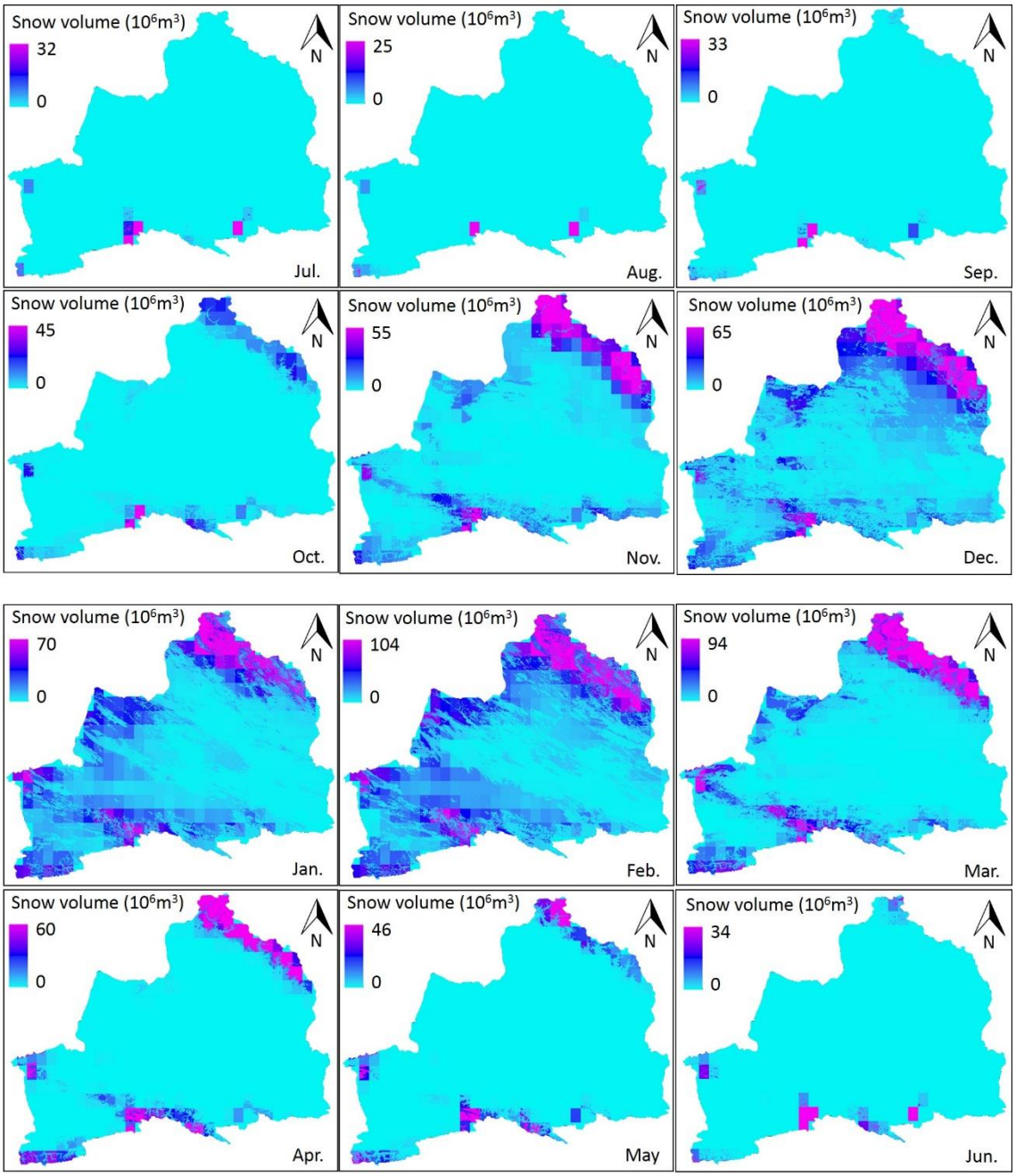

Fig.6.3. Monthly snow volume map of north Xinjiang in 2009.

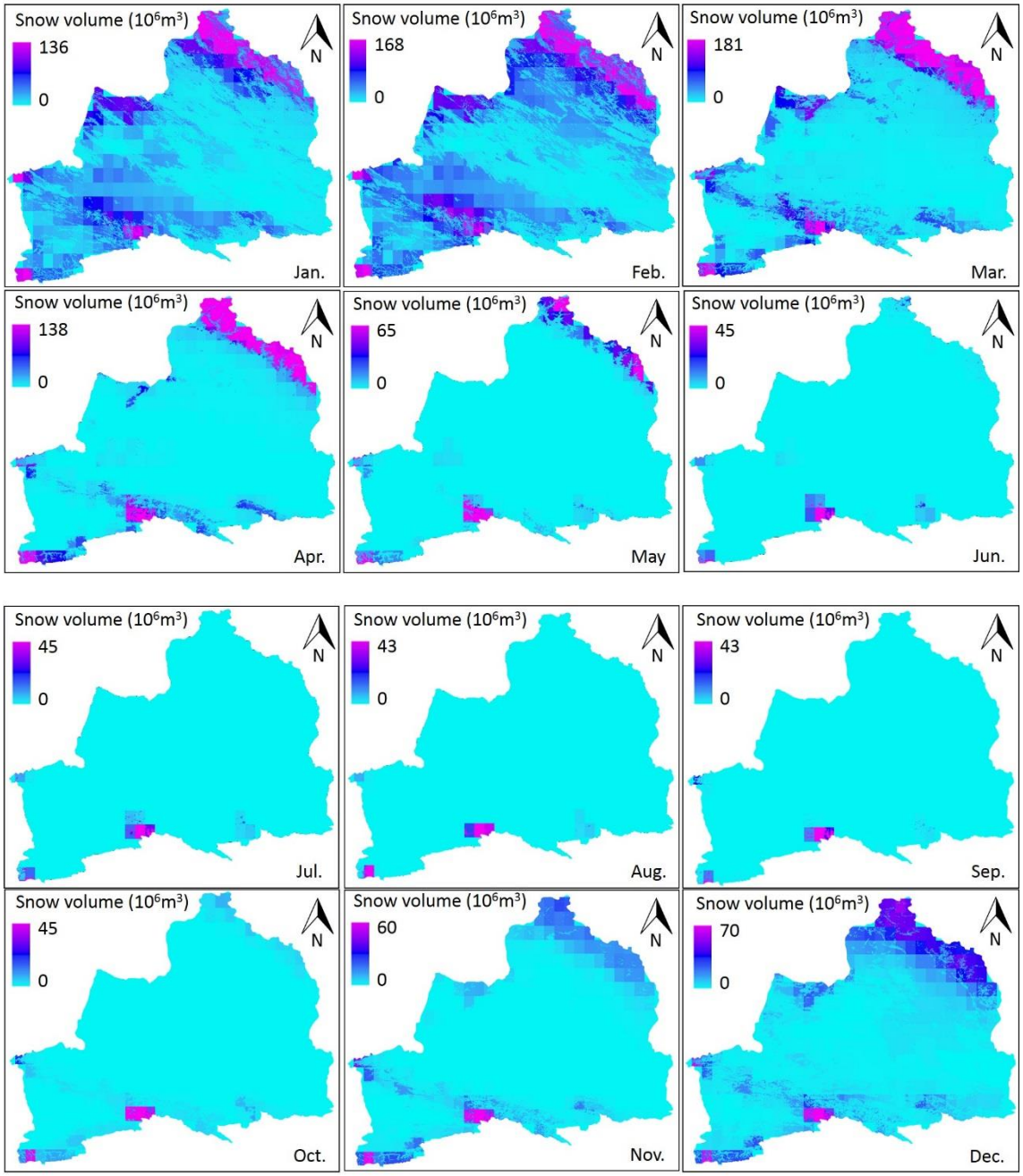

Fig.6.4. Monthly snow volume map of north Xinjiang in 2010.

Here, in order to see the meaning of snow volume product at 500m spatial resolution, snow volume product at 500m spatial resolution and 24km resolution were compared. Snow volume product at 24km resolution is directly derived from CMC snow depth data. Snow volume product

at 500m resolution is derived from MODIS, AMSR-E and CMC snow depth data. Fig.6.5 shows the comparison of these two snow volume products. The comparison was carried on within one sample pixel (Upper left: 87.173E, 48.855N, Lower right: 87.833E, 48.496N). This comparison shows that the volume of snow was $6.58*10^6m^3$ at the product of 24km spatial resolution, and it is equal to $6.11*10^6m^3$ at the product of 500m spatial resolution. The difference of snow volume in the same pixel was very clear. In addition, it suggest that new snow volume product at 500m resolution gives more detail and correct information.

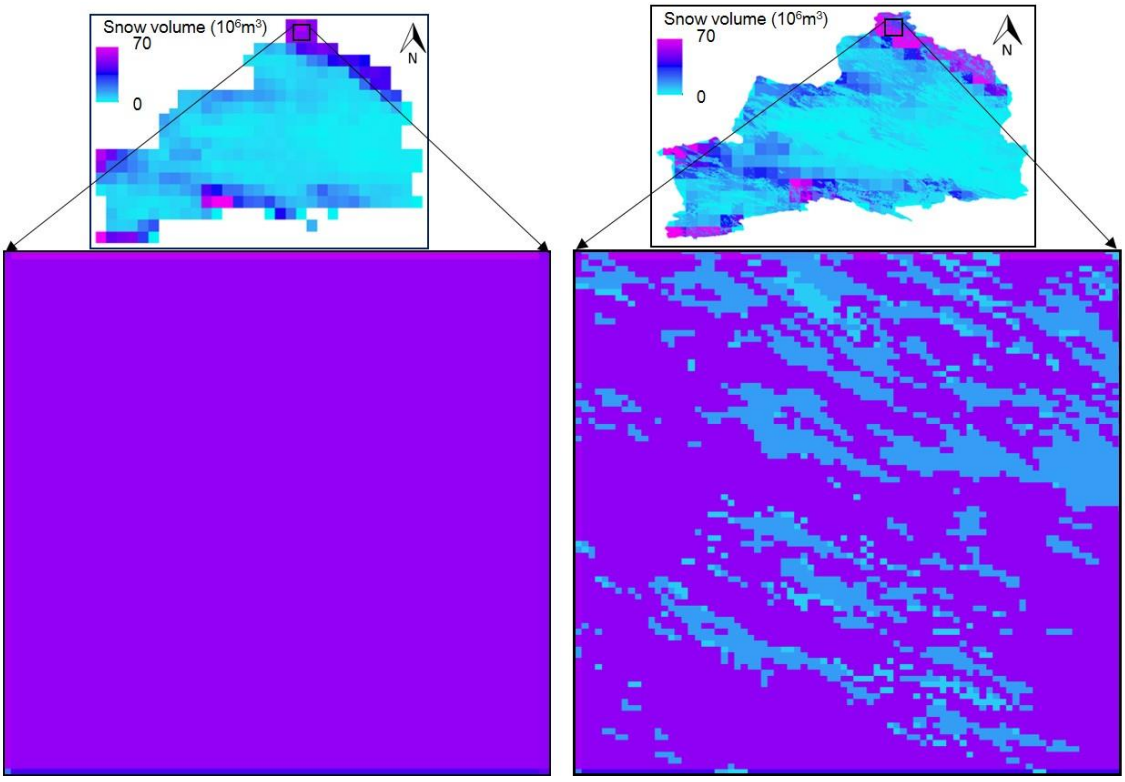

Fig.6.5 comparison of two snow volume products. The comparison was carried on within one pixel (UL: 87.173E, 48.855N, LR: 87.833E, 48.496N). Left side shows snow volume product at 24km resolution, which is directly derived from CMC snow depth data. It shows snow volume of $6.58*10^6m^3$. Right side shows snow volume product at 500m resolution, which is derived from MODIS, AMSR-E and CMC snow depth data. It shows snow volume of $4.53*10^6m^3$.

Fig.6.6 shows the statement of monthly total snow volume variation over the period of January, 2008 to December 2010. Results presented that the total snow volume of 2010 was higher than 2008 and 2009. The total snow volume over the whole study area equals to 310.54 $*10^9 m^3$, 345.48 $*10^9 m^3$, and 682.91 $*10^9 m^3$ over this three year time period, respectively. In addition, the time variations of the snow volume are almost dominated by the seasonal cycle.

The snow volume of snow season in 2008 was $231.67*10^9\ m^3$; it is equal to 75% of total snow volume of this year. The snow volume of snow season in 2009 was $281.51*10^9\ m^3$; it is equal to 81% of total snow volume of this year. The difference of snow volume of snow season between these two years was $49.84*10^9\ m^3$. The snow volume of snow season in 2010 was $552.09*10^9\ m^3$; it is equal to 81% of total snow volume of this year. The difference of snow volume of snow season between the year of 2009 and 2010 was $270.58*10^9\ m^3$. This difference approximately equals to the volume of snow in snow season in 2009.

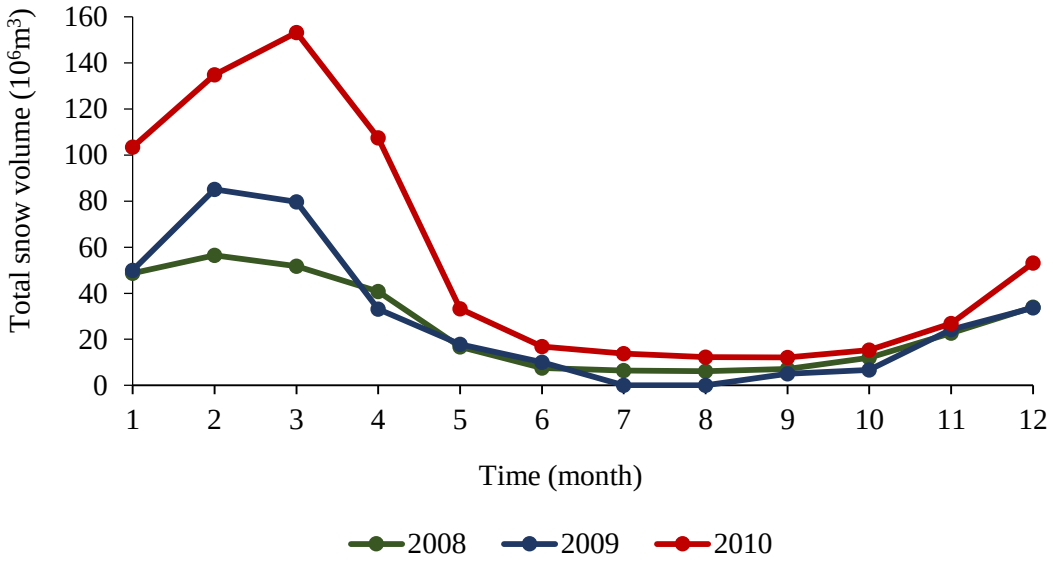

Fig.6.6 Monthly snow volume variation over the 2008- 2010 in north Xinjiang

Fig.6.7 and Fig.6.8 shows the difference of monthly snow volume between the year of 2008 and 2009 and the difference of monthly snow volume between the year of 2009and 2010. The biggest difference of snow volume between 2008 and 2009 appeared as $28.56*10^9m^3$ in February and $27.87*10^9m^3$ in March. The big difference of snow volume between 2009 and 2010 was $53.47*10^9m^3$ in January, $49.8*10^9m^3$ in February, $73.53*10^9m^3$ in March, and, $74.3*10^9m^3$ in April.

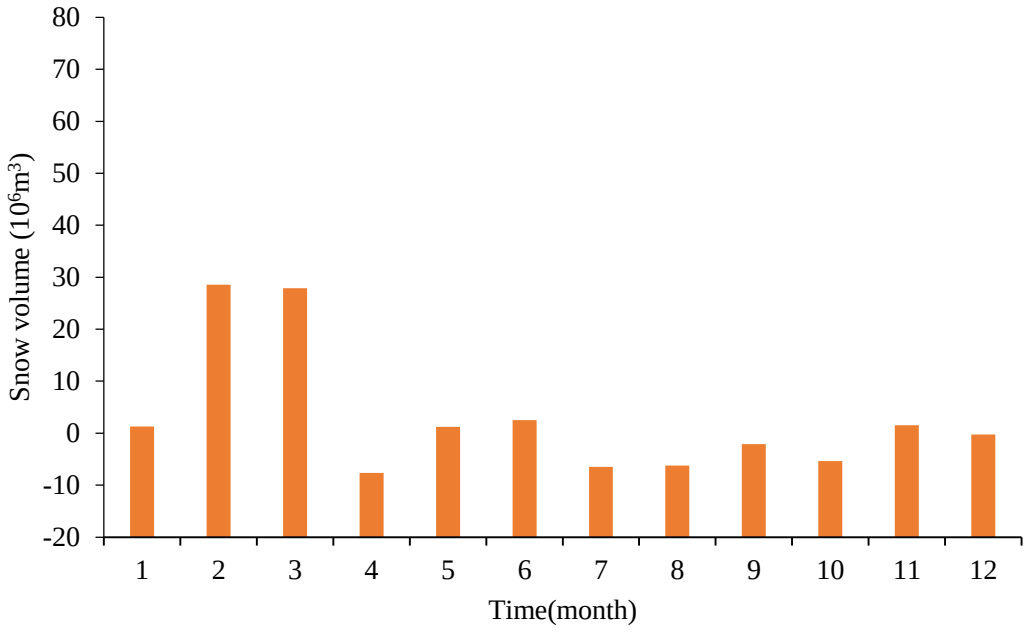

Fig.6.7 the difference of monthly snow volume between the year of 2008 and 2009.

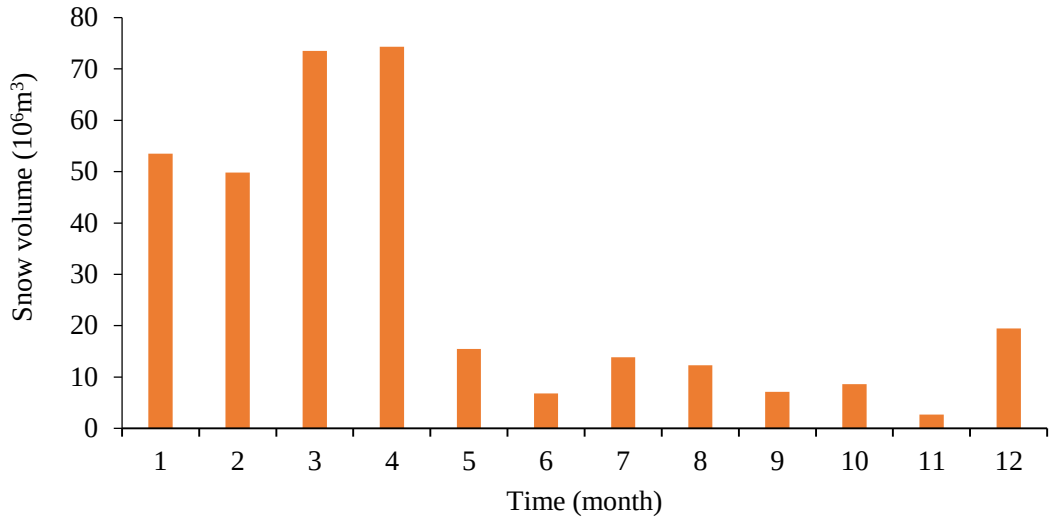

Fig.6.8 The difference of monthly snow volume between the year of 2009 and 2010.

Based on the records of historical avalanche accidents, snow volume was analyzed, in the five main cities, where avalanches were happen. From Fig.6.9 to Fig.6.13 shows monthly snow volume variation over the 2008- 2010 in this five cities and red circles snow the time of avalanche was happen. Snow volume change of these five cities also analyzed with climate parameters, such as temperature, precipitation. Fig.6.14 to Fig.6.18 shows the correlation between snow volume variation and temperature change over the 2008- 2010 in the five cities, north Xinjiang. Fig.6.19 to Fig.6.23 shows the correlation between snow volume variation and precipitation change over the 2008- 2010 in the five cities, north Xinjiang.

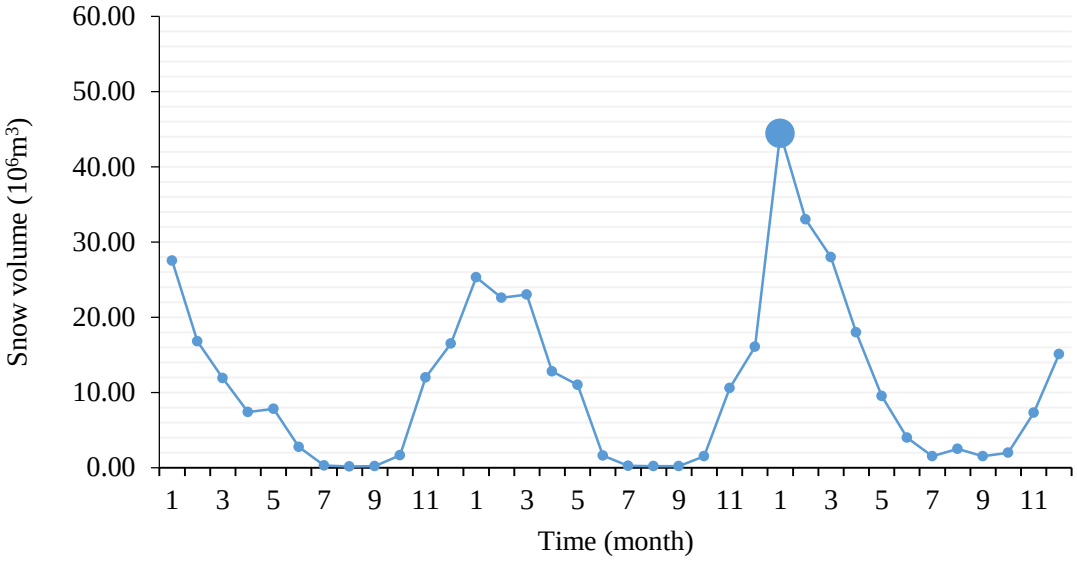

Fig. 6.9 Monthly snow volume variation over the 2008- 2010 in Altay region, north Xinjiang (the big blue point shows the time of avalanche accident happened).

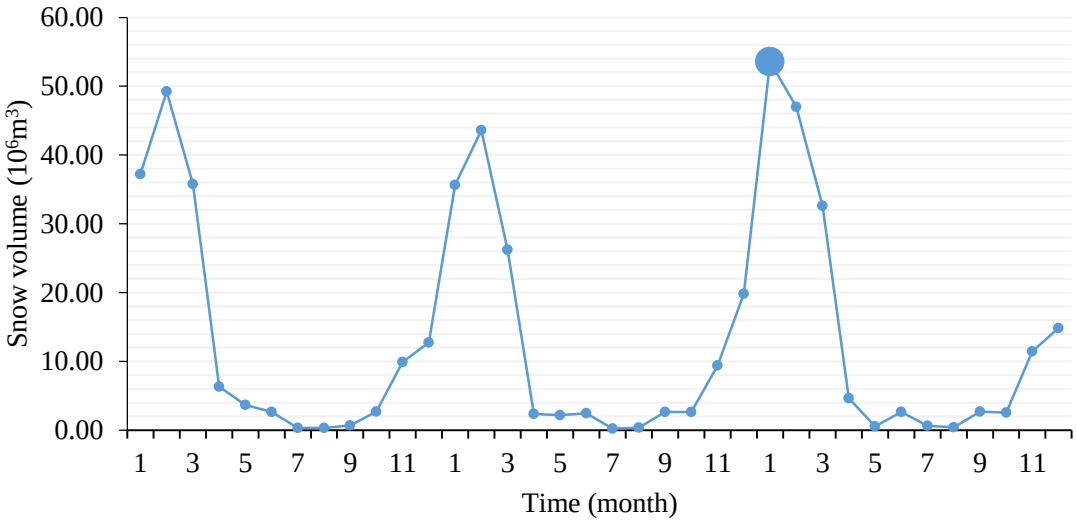

Fig.6.10 Monthly snow volume variation over the 2008- 2010 in Tacheng region, north Xinjiang (the big blue point shows the time of avalanche accident happened)

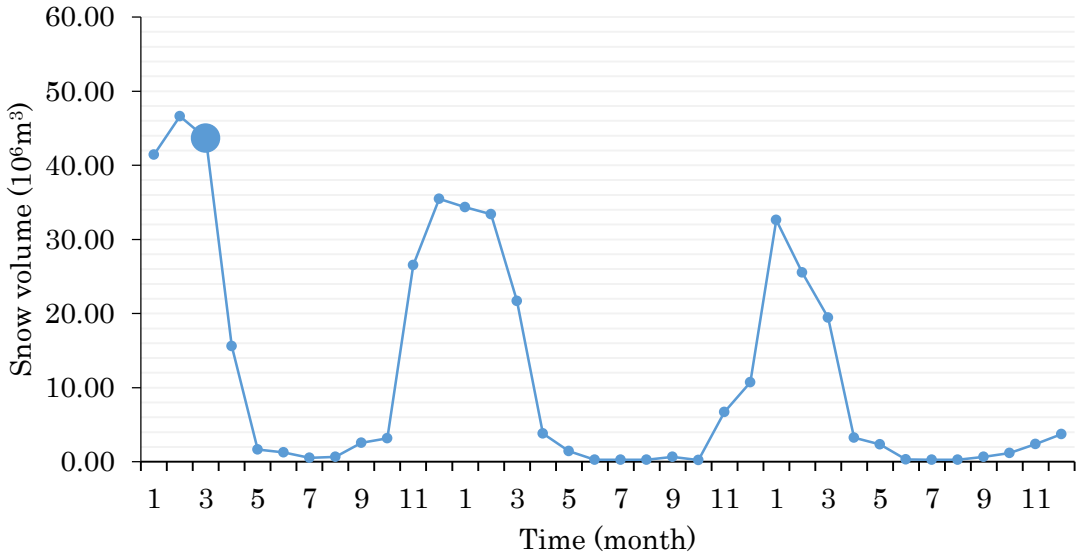

Fig. 6.11 Monthly snow volume variation over the 2008- 2010 in Ili region, north Xinjiang (the big blue point shows the time of avalanche accident happened).

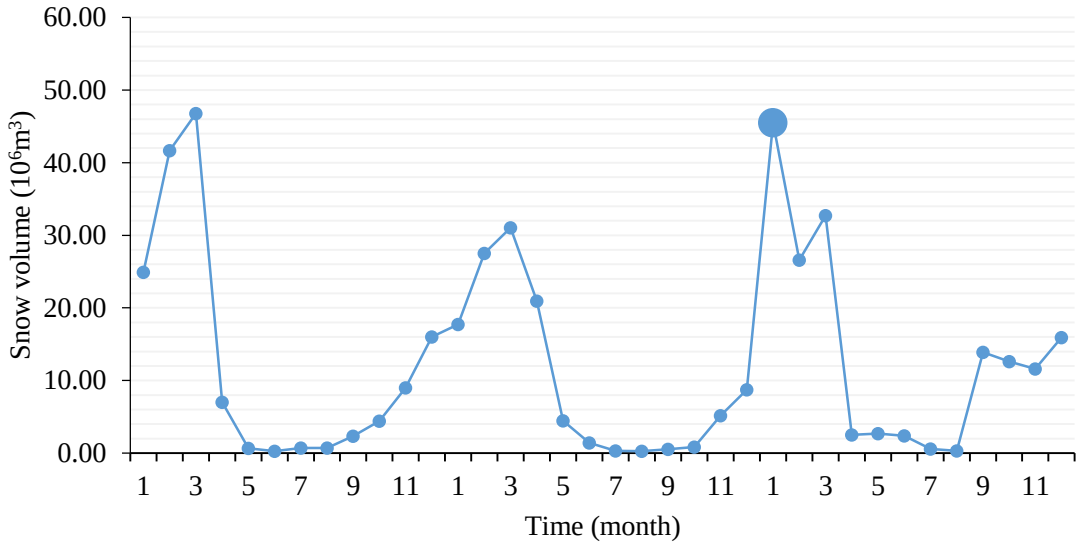

Fig.6.12 Monthly snow volume variation over the 2008- 2010 in Tekas region, north Xinjiang (the big blue point shows the time of avalanche accident happened).

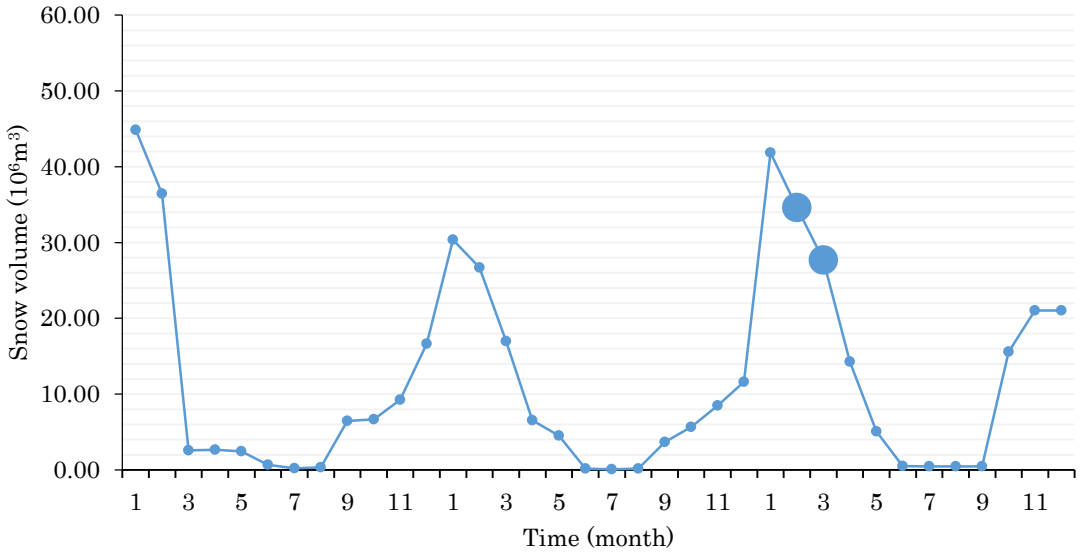

Fig. 6.13 Monthly snow volume variation over the 2008- 2010 in Nilka region, north Xinjiang (the big blue point shows the time of avalanche accident happened).

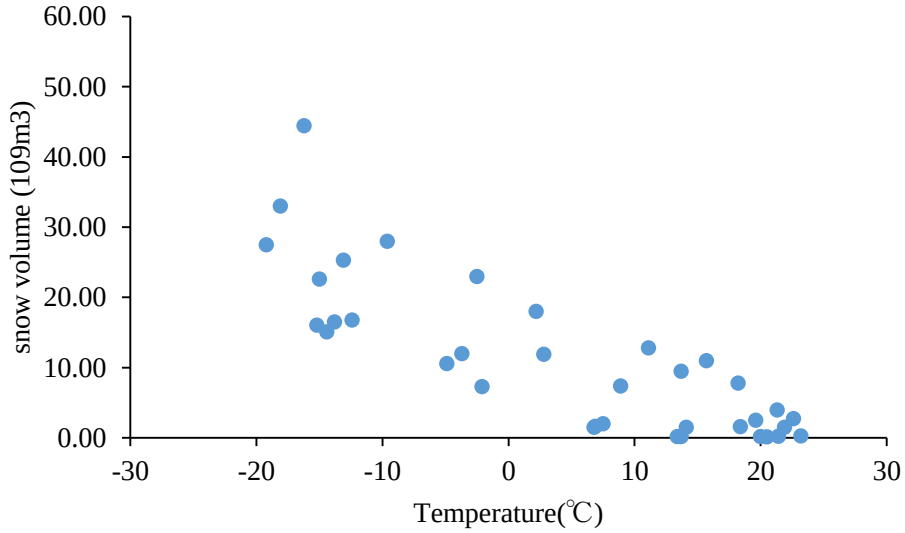

Fig.6.14 The correlation between snow volume variation and temperature change over the 2008-2010 in Altay region, north Xinjiang.

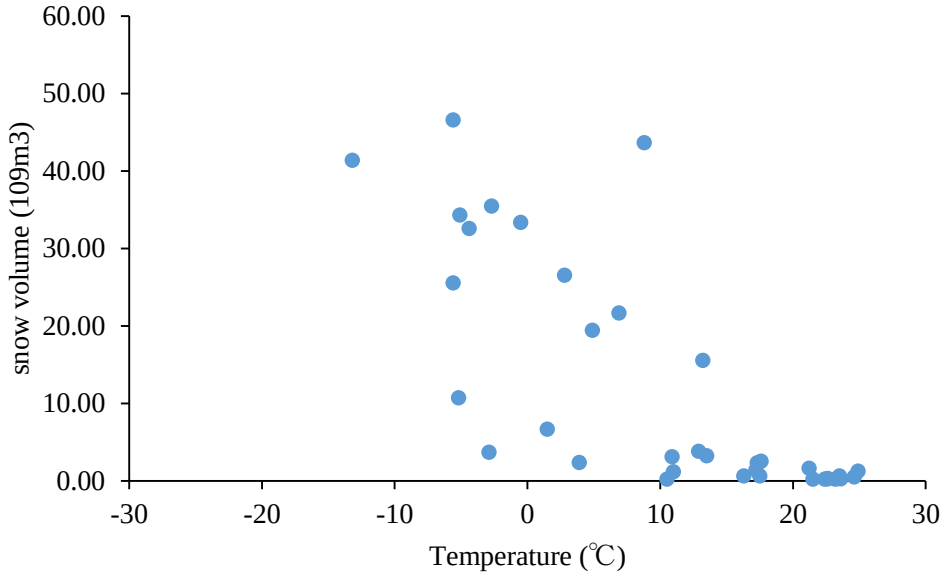

Fig.6.15 The correlation between snow volume variation and temperature change over the 2008-2010 in Ili region, north Xinjiang.

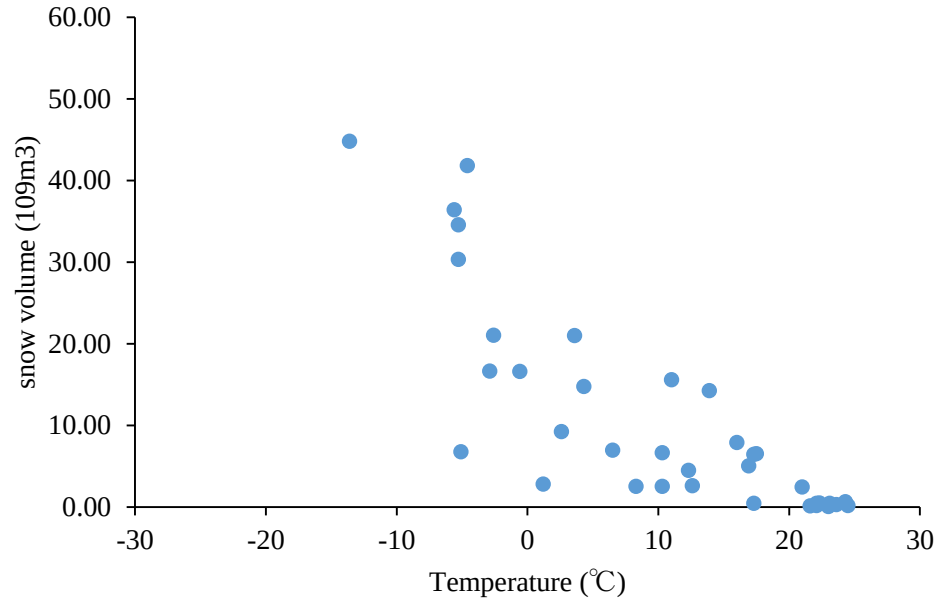

Fig.6.16 The correlation between snow volume variation and temperature change over the 2008-2010 in Nilka region, north Xinjiang.

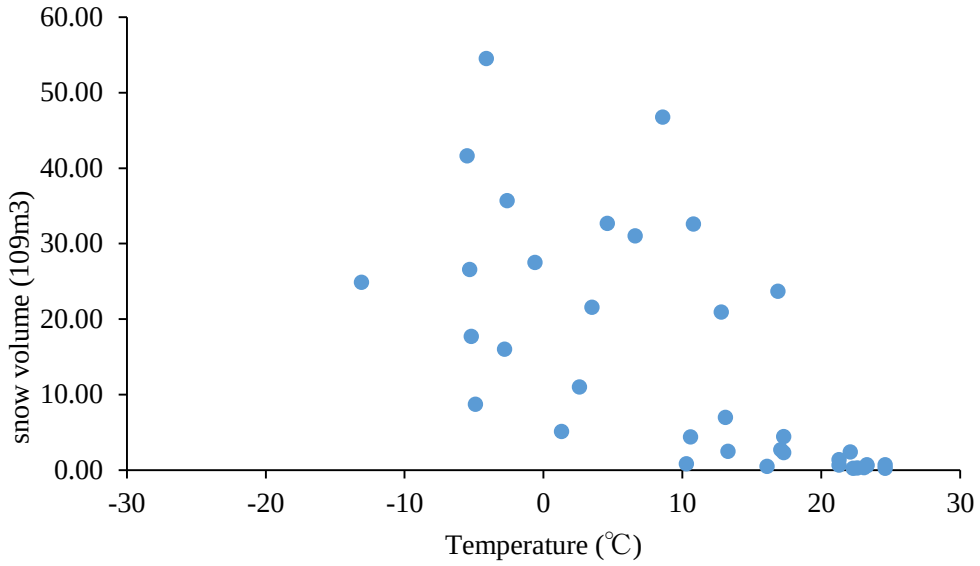

Fig.6.17 The correlation between snow volume variation and temperature change over the 2008-2010 in Tekas region, north Xinjiang.

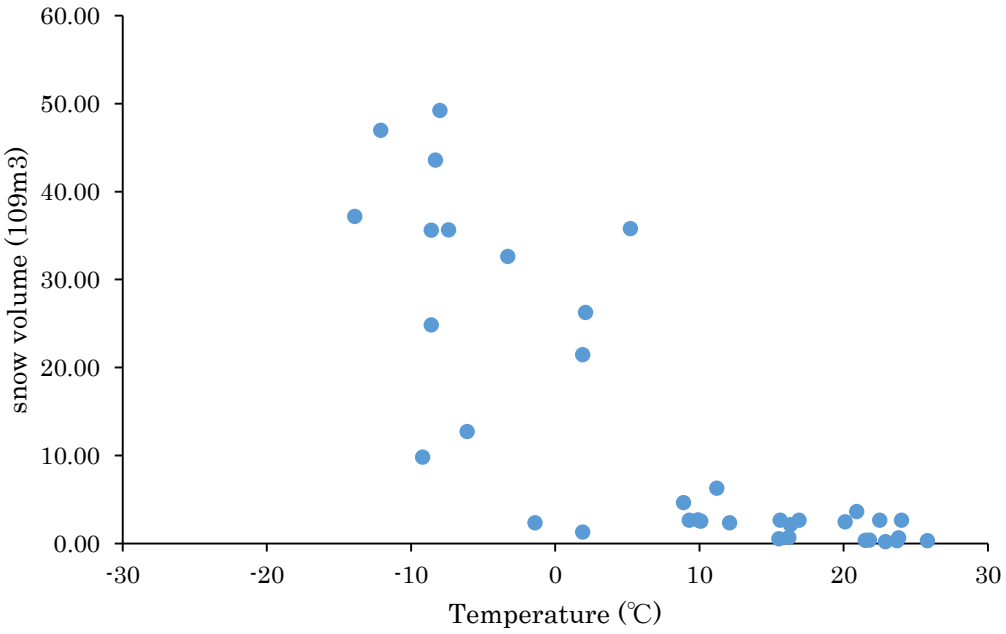

Fig.6.18 The correlation between snow volume variation and temperature change over the 2008-2010 in Tacheng region, north Xinjiang.

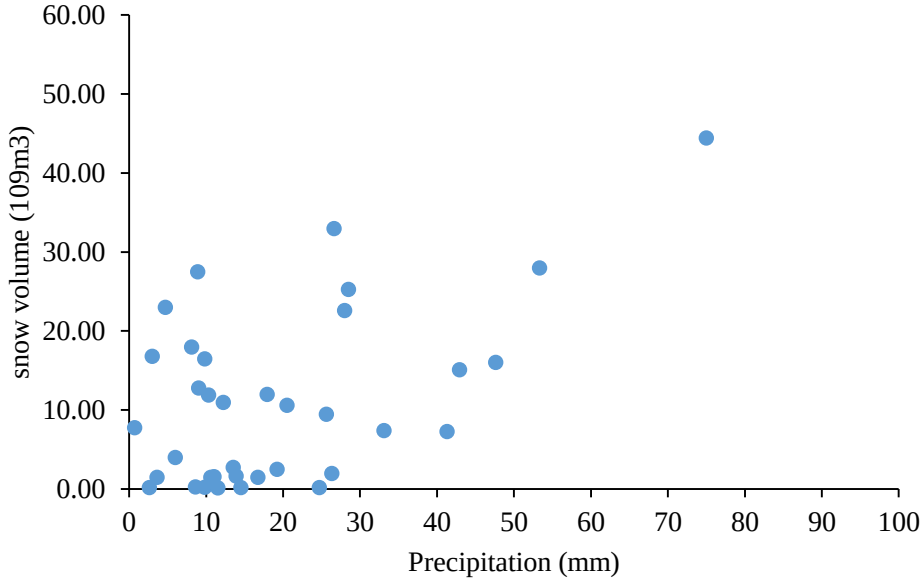

Fig.6.19 The correlation between snow volume variation and precipitation change over the 2008- 2010 in Altay region, north Xinjiang.

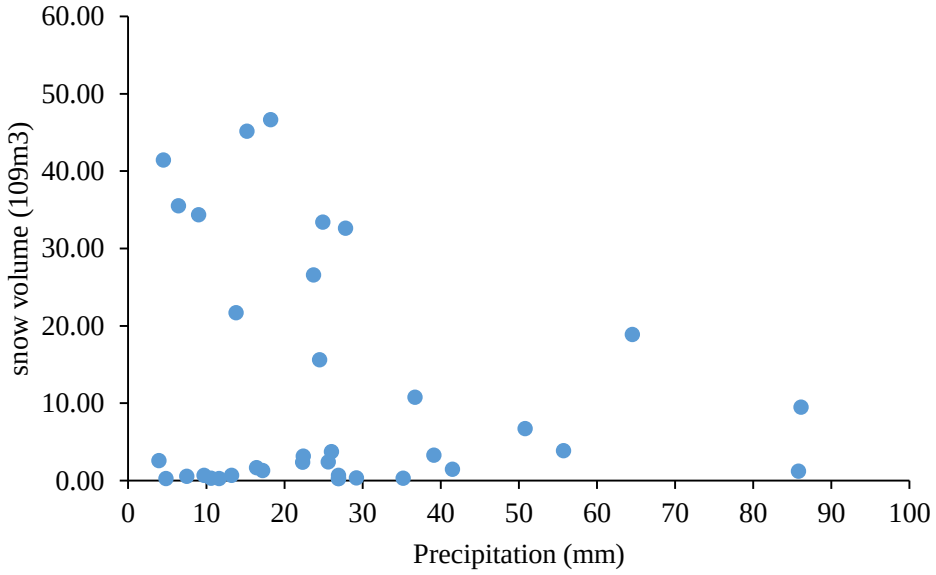

Fig. 6.20 The correlation between snow volume variation and precipitation change over the 2008- 2010 in Ili region, north Xinjiang.

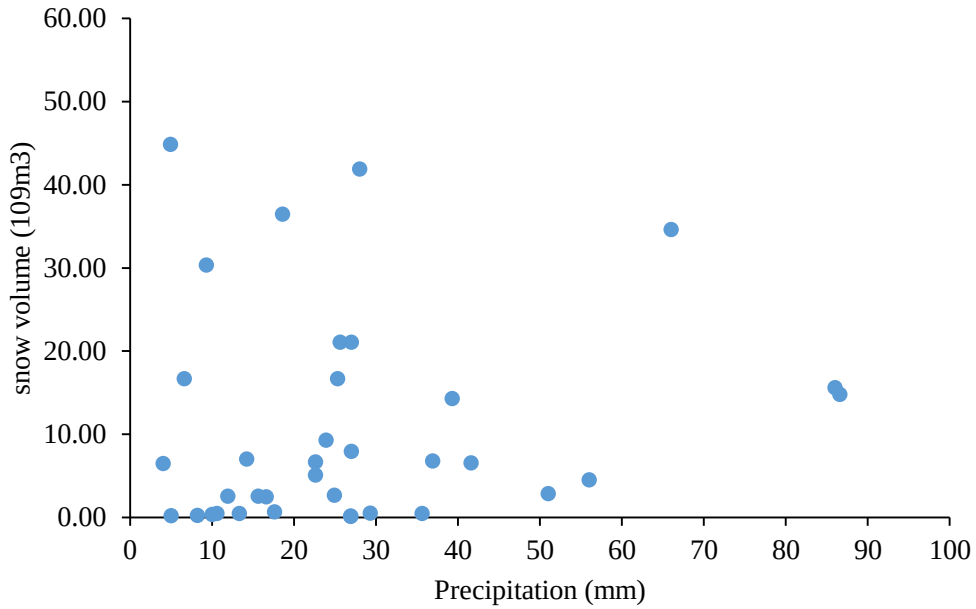

Fig.6.21 The correlation between snow volume variation and precipitation change over the 2008- 2010 in Nilka region, north Xinjiang.

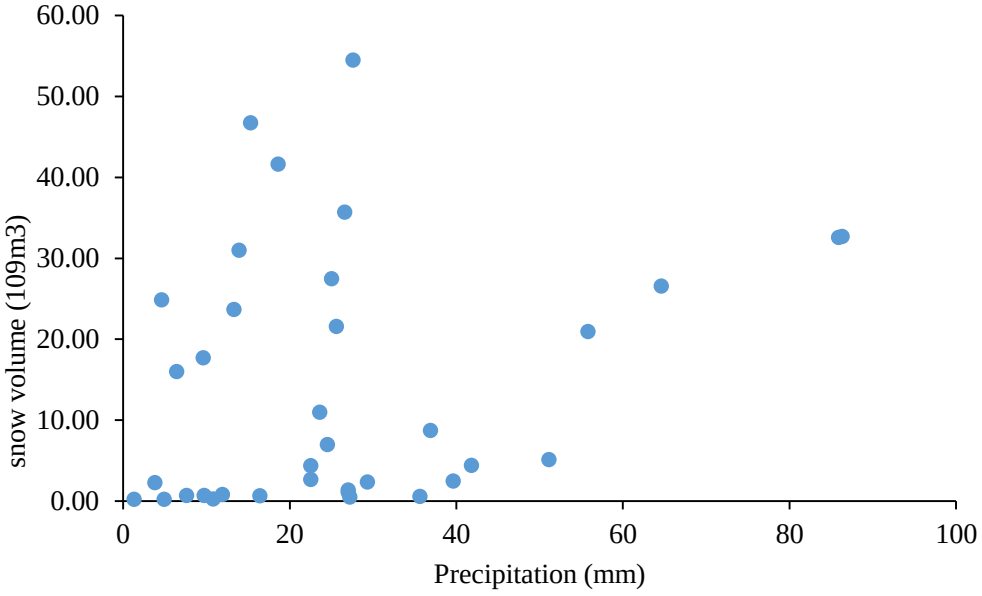

Fig.6.22 The correlation between snow volume variation and precipitation change over the 2008- 2010 in Tekas region, north Xinjiang.

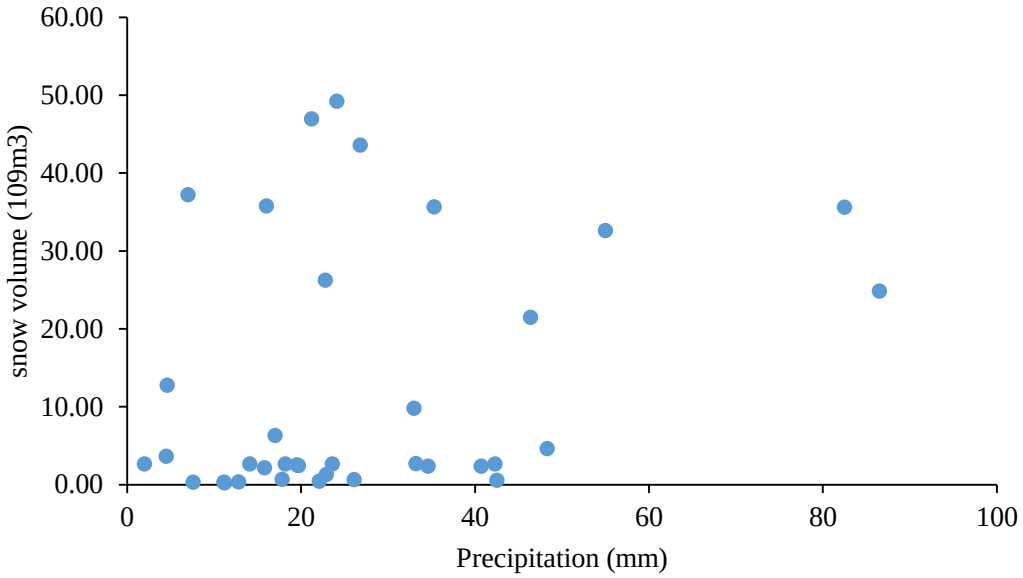

Fig.6.23 The correlation between snow volume variation and precipitation change over the 2008- 2010 in Tacheng region, north Xinjiang.

6.2 Snow mass outputs and discussion

Based on the definition of snow mass, snow mass were estimated from snow volume and average snow density. From Fig.6.24 to Fig.6.26 shows snow mass outputs over the period January, 2008 to December, 2010. As it shows, the temporal change of snow mass, also, dominated by the seasonal cycle. It was increasing from end of autumn season to winter season, and decreasing from beginning of spring season. Highest snow mass were appeared in January and February.

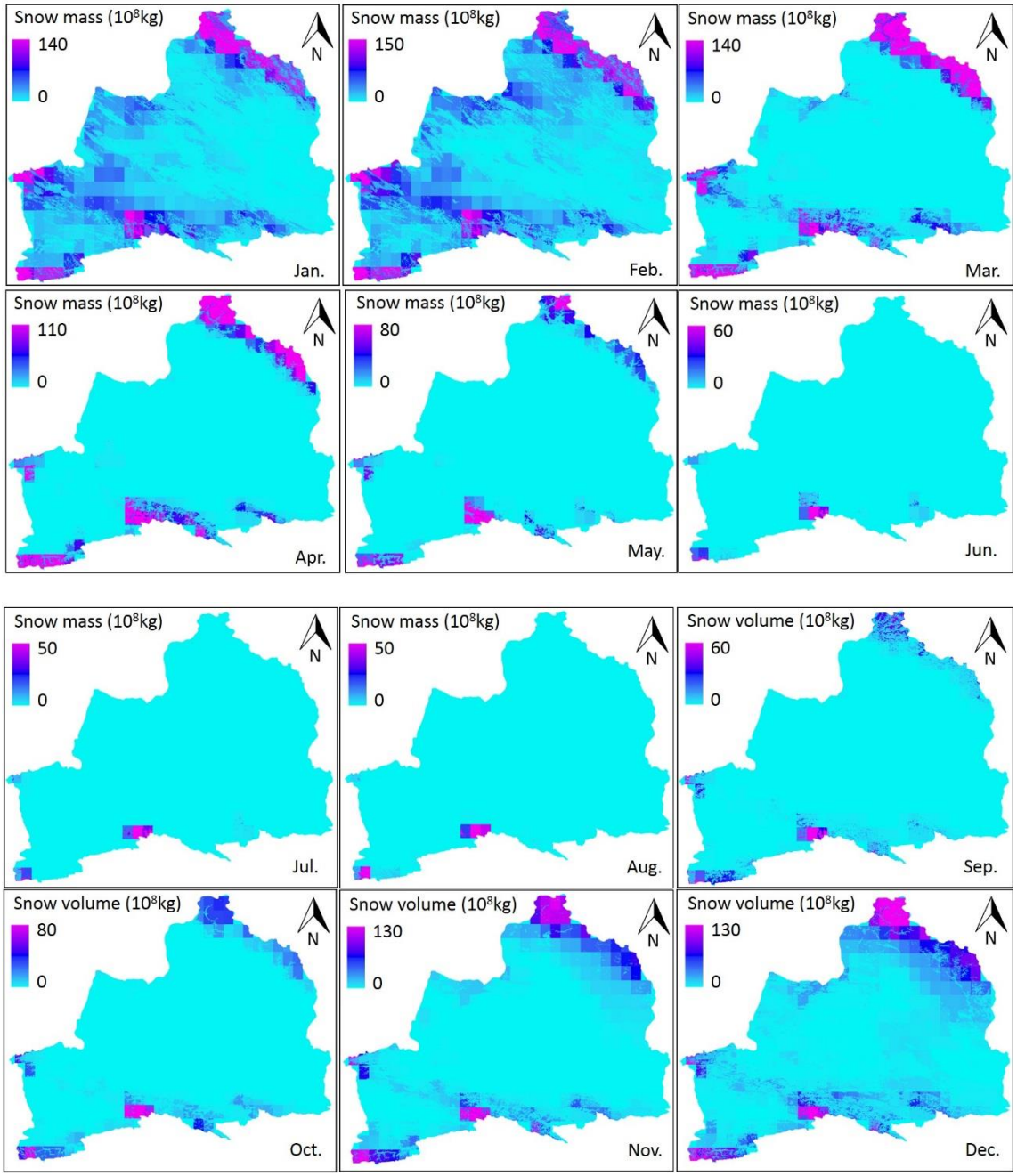

Fig.6.24 Snow mass outputs of the period of 2008

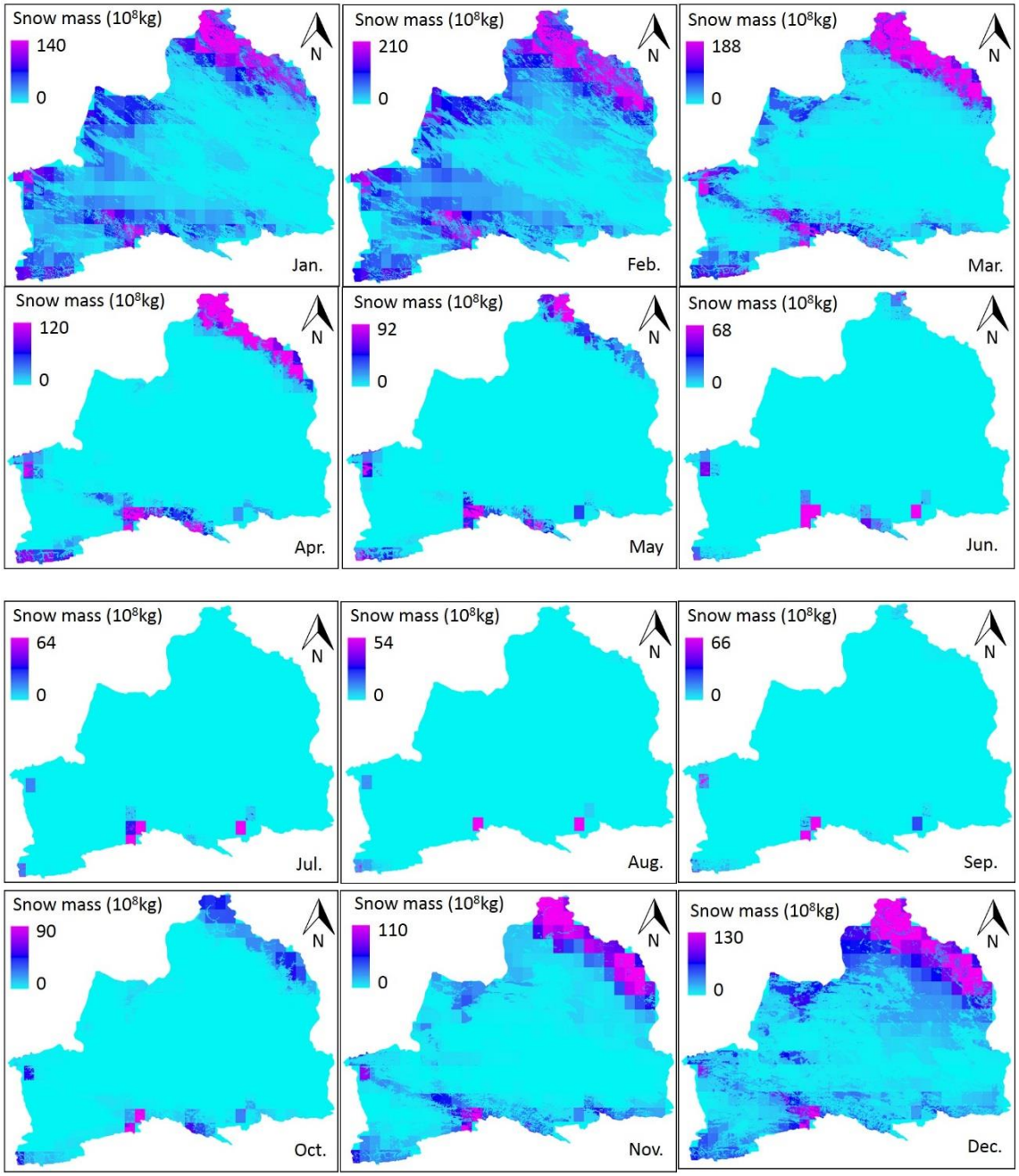

Fig.6.25 Snow mass outputs of the period of 2009

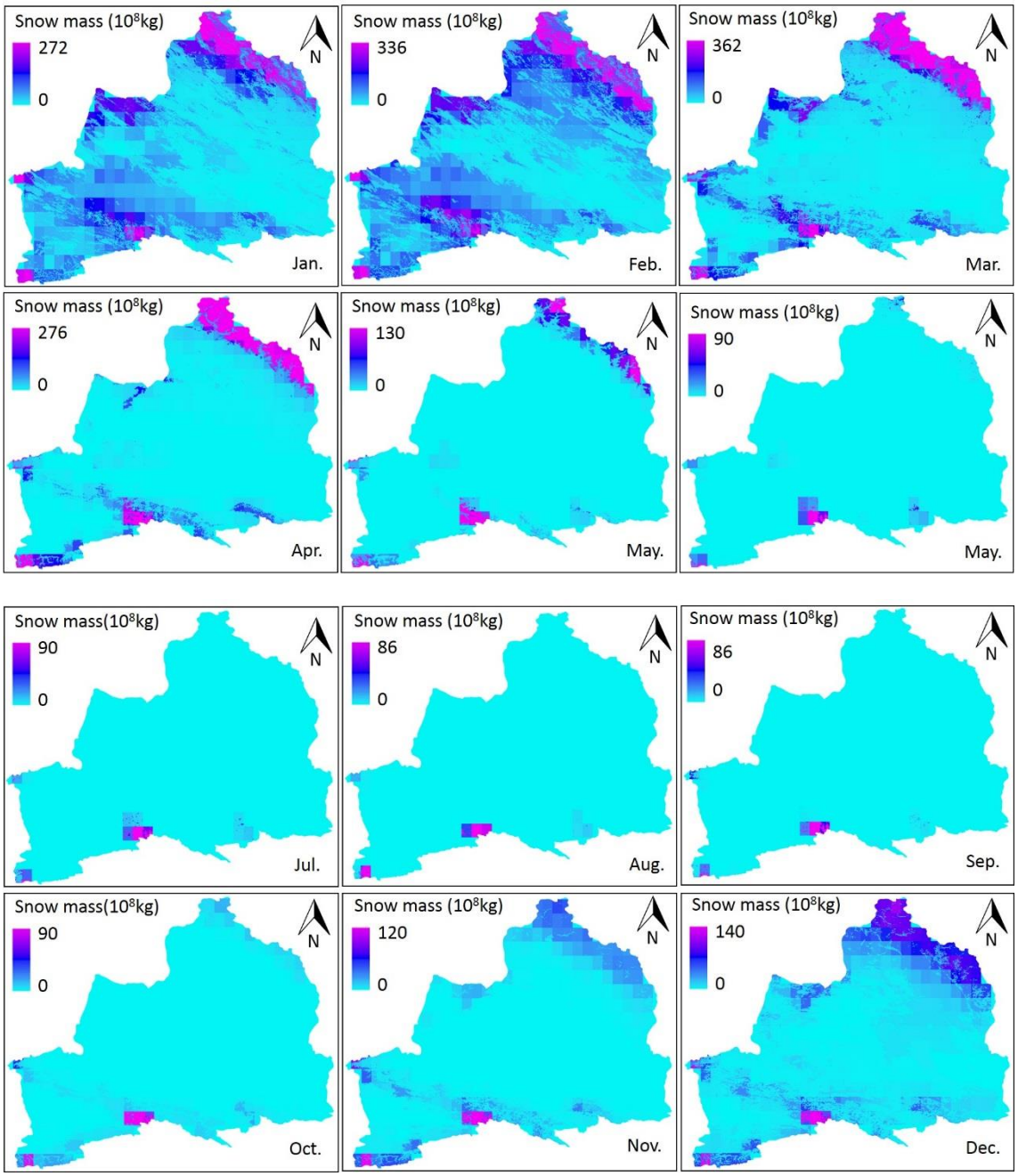

Fig.6.26 Snow mass outputs of the period of 2010

To see the situation of snow mass changes in spatially and temporally, the five cities were pick up and analyze their snow mass changes, in statistically. From Fig.6.27 to Fig.6.36 shows snow mass situation and snow mass temporal changes of five cities over the period January, 2008 to

December, 2010.

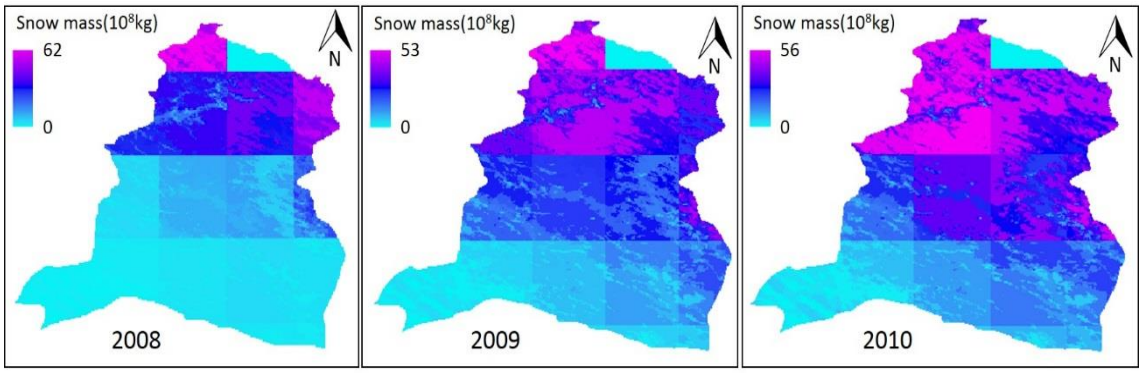

Fig.6.27 Snow mass situation of Altay region.

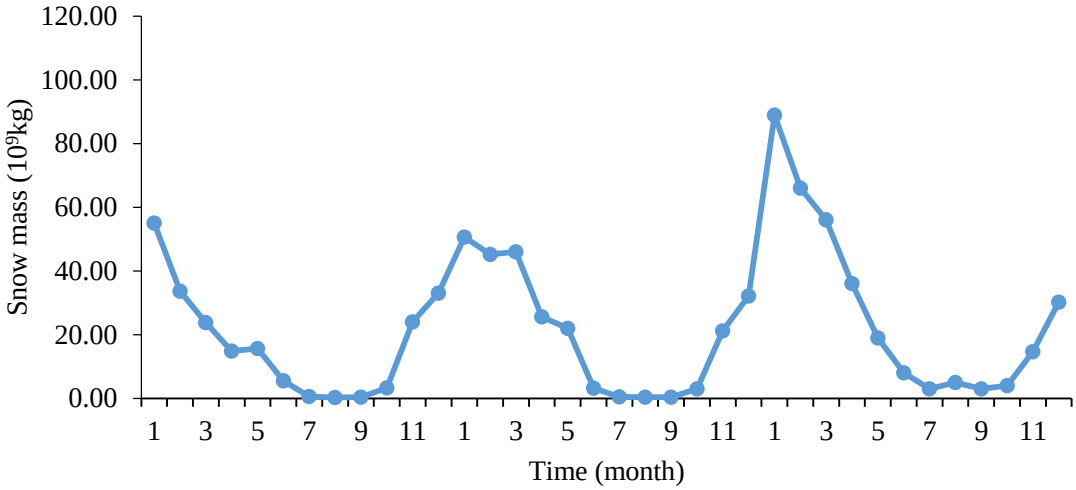

Fig.6.28 Snow mass changes of Altay region over the period January, 2008 to December, 2010.

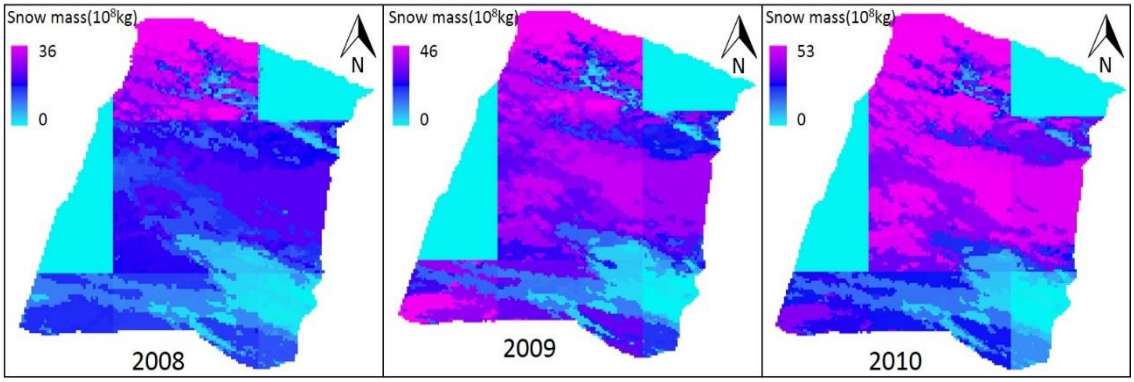

Fig.6.29 Snow mass situation of Tacheng region.

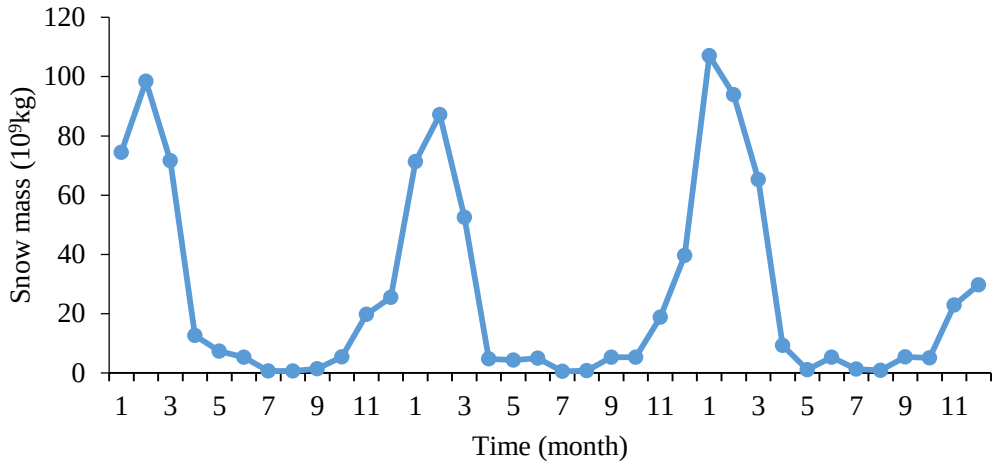

Fig.6.30 Snow mass changes of Tacheng region over the period January, 2008 to December, 2010.

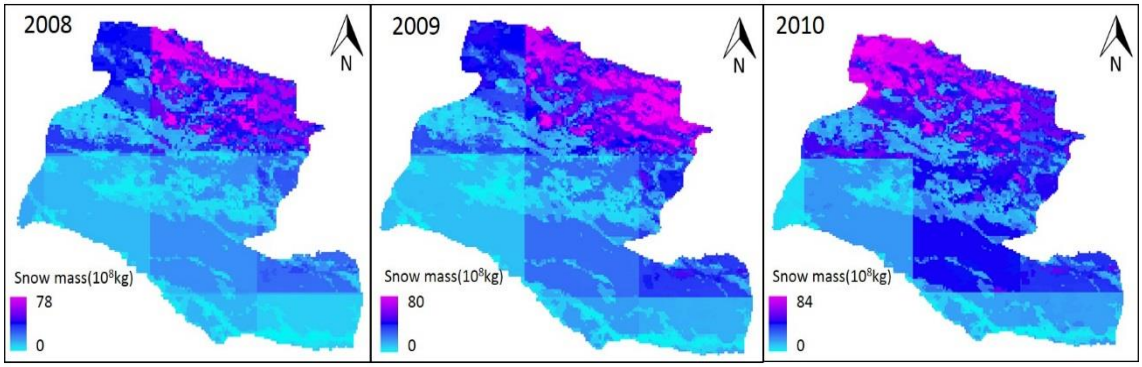

Fig.6.31 Snow mass situation of Ili region

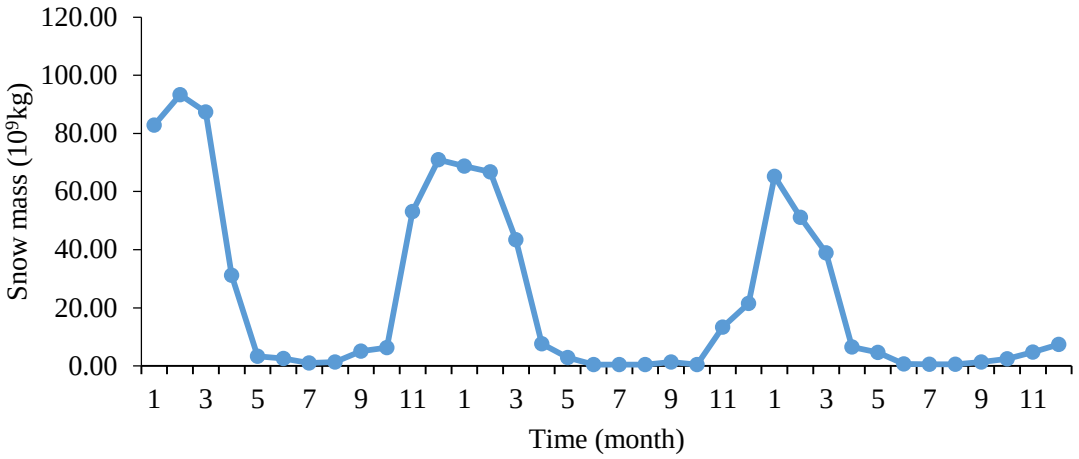

Fig.6.32 Snow mass changes of Ili region over the period January, 2008 to December, 2010.

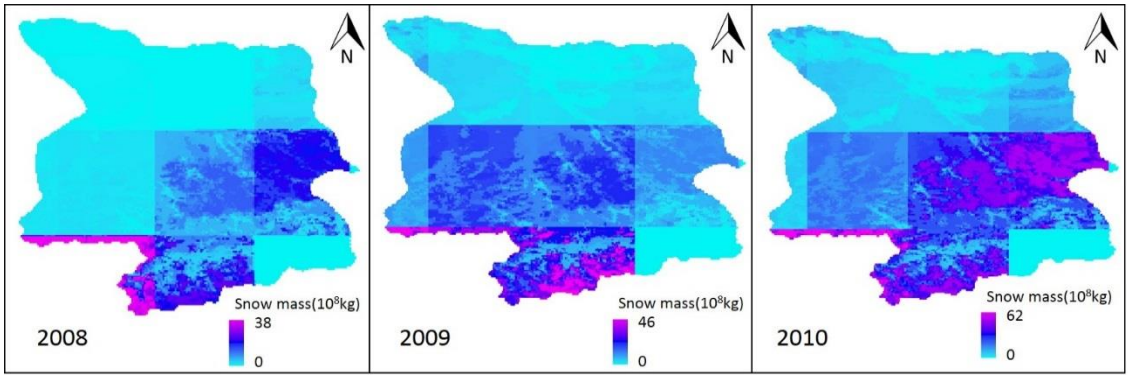

Fig.6.33 Snow mass situation of Tekas region

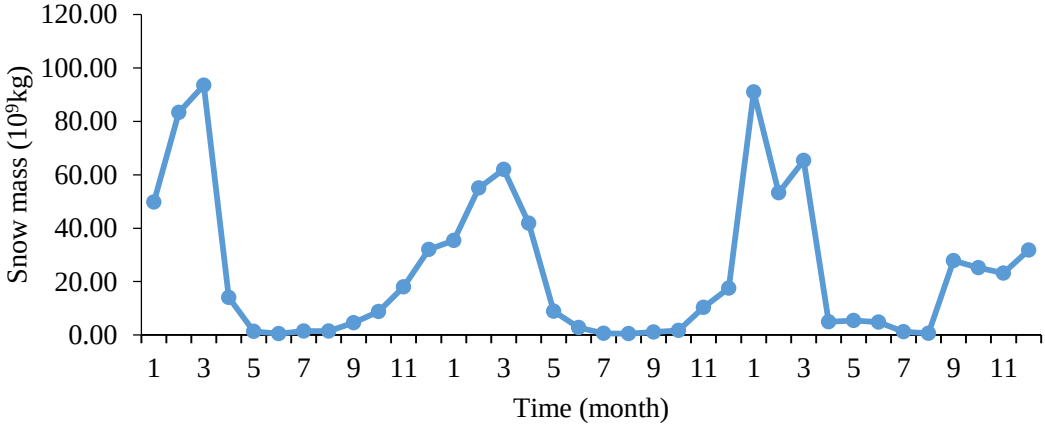

Fig. 6.34 Snow mass changes of Tekas region from January, 2008 to December, 2010.

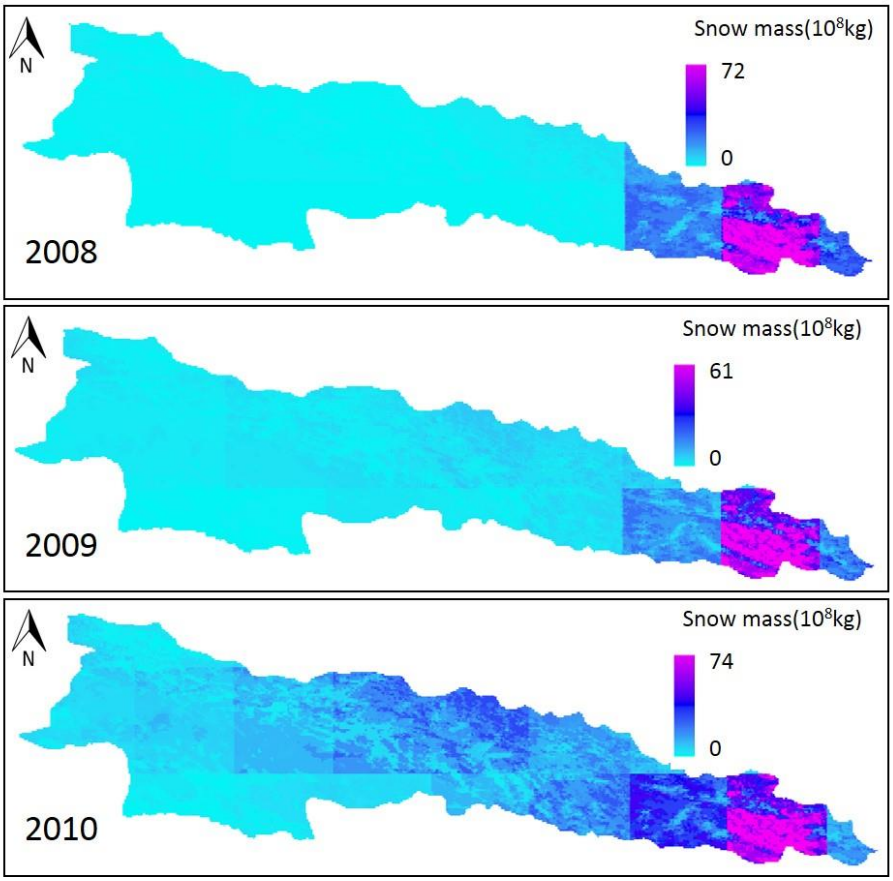

Fig. 6.35 Snow mass situation of Nilka region

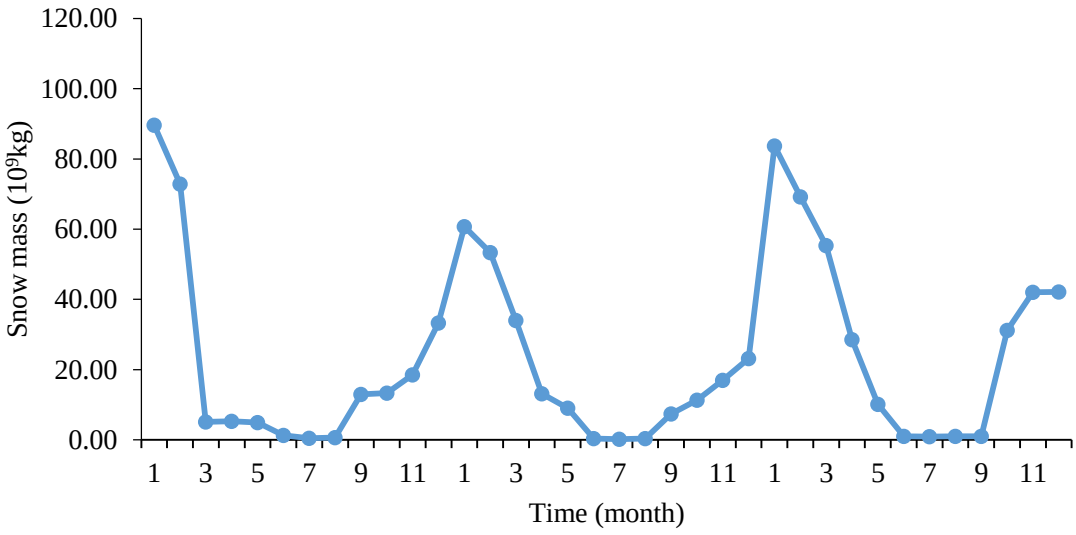

Fig. 6.36 Snow mass changes of Nilka region over the period January, 2008 to December, 2010.

6.3 Potential hazard map outputs and discussion

In the help of GIS-based WLC method, avalanche hazard map at 500m spatial resolution were created from snow mass and slope, which are prerequisite of an avalanche trigger. From Fig. 6.37 to Fig.6.39 show three avalanche hazard map of north Xinjiang area from 2008 to 2010, respectively. Dangerous degree of avalanche hazard map ranges from 0.5 to 10.

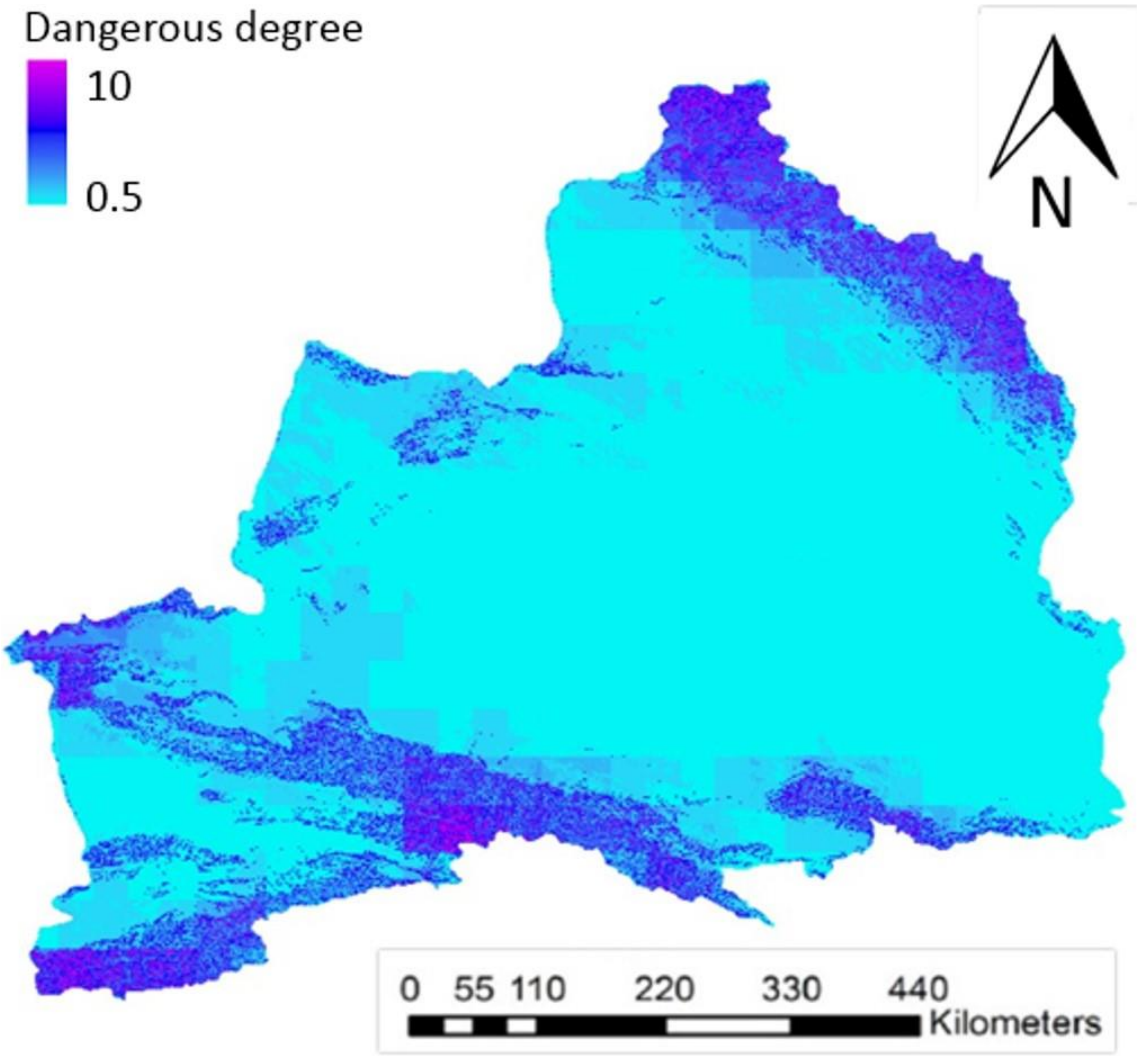

Fig.6.37 The output of avalanche hazard map of 2008 of north Xinjiang.

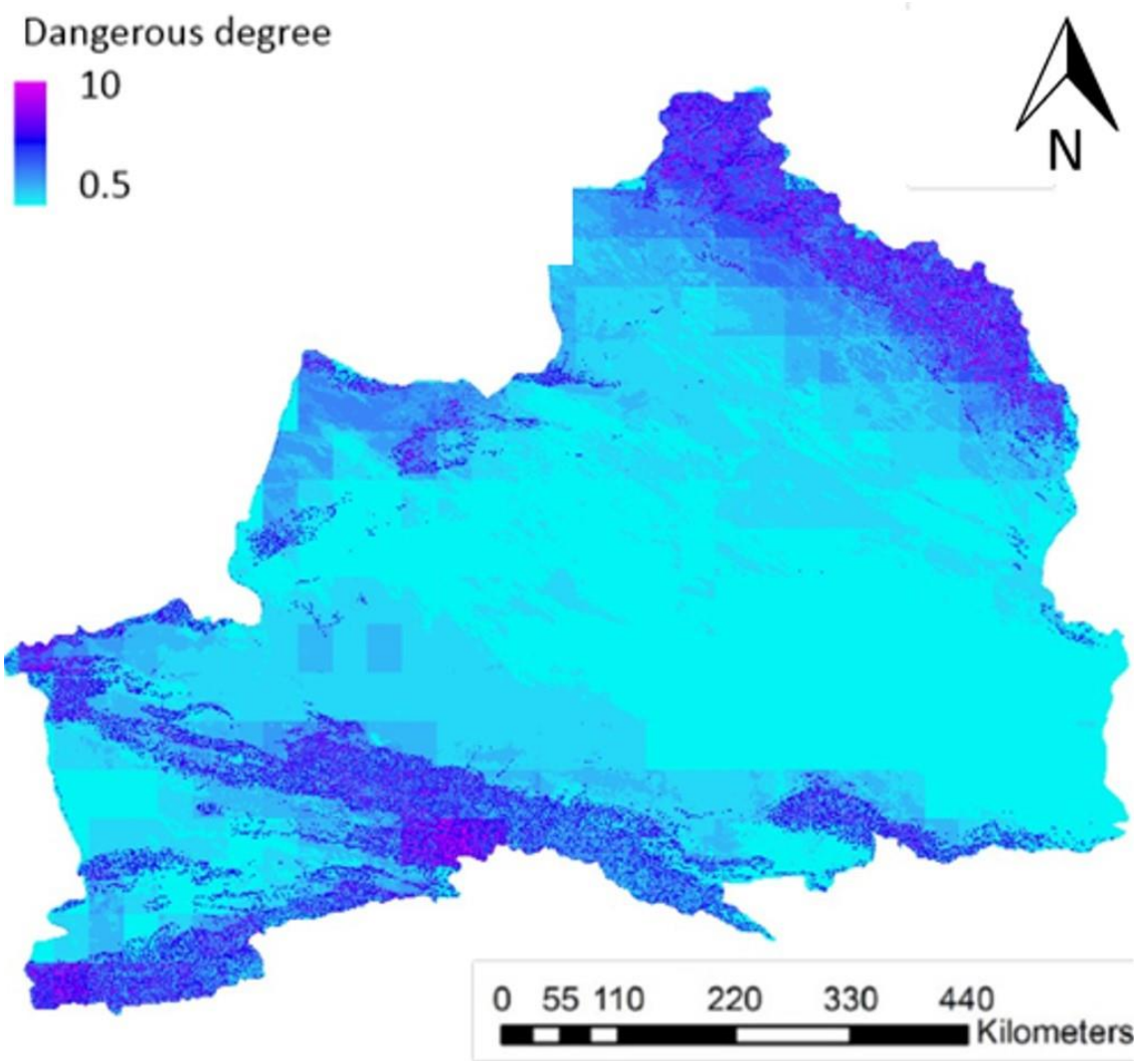

Fig.6.38 The output of avalanche hazard map of 2009 of north Xinjiang.

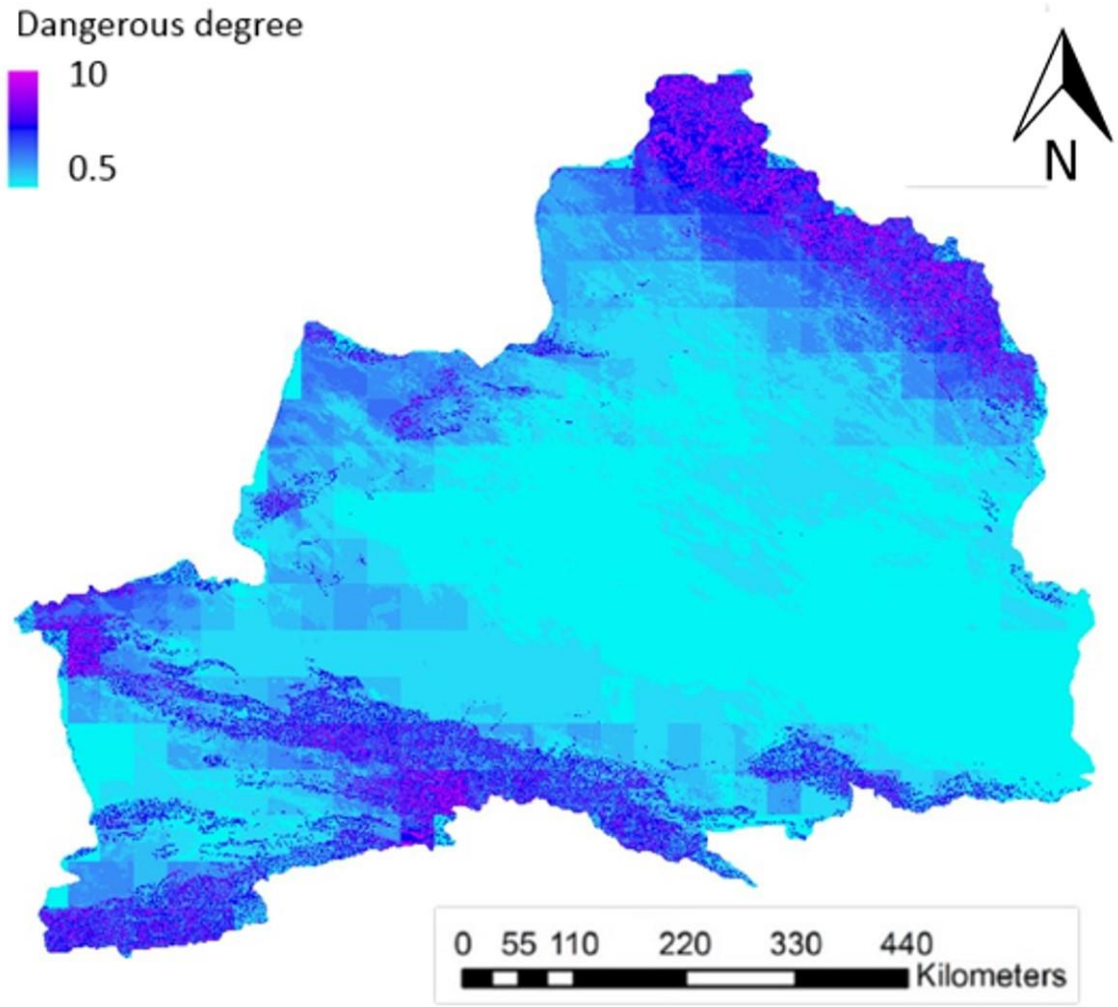

Fig.6.39 The output of avalanche hazard map of 2010 of north Xinjiang.

In order to see the meaning of avalanche hazard map at 500m spatial resolution, two avalanche hazard map, which are at 24km spatial resolution (derived from existing data set) and 500m spatial resolution (created in this study) were compared. The comparison shows that the new avalanche hazard map at 500m spatial resolution gives more detail information about dangerous degree in the regions. For example, in sample pixel (UL: 87.173E, 48.855N, LR: 87.533E, 48.496N), avalanche hazard map at 24km spatial resolution shows dangerous degree of 8.5, while avalanche hazard map at 500m spatial resolution shows dangerous degree from 2.5 to 8.5 (Fig.40).

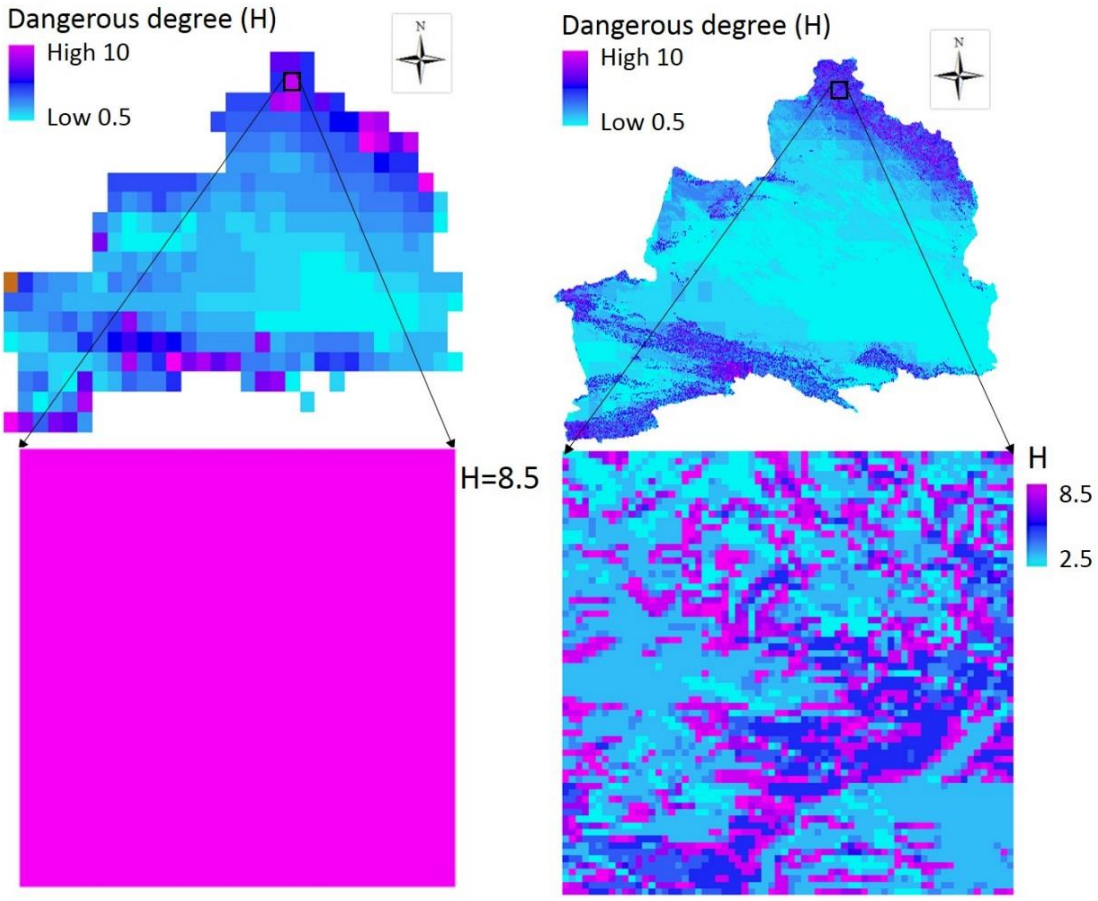

Fig.40 The comparison of two avalanche hazard maps of 24km spatial resolution (left) and 500m spatial resolution (right) within sample pixel (UL: 87.173E, 48.855N, LR: 87.533E, 48.496N). Avalanche hazard map at 24km spatial resolution shows dangerous degree of 8.5, while avalanche hazard map at 500m spatial resolution shows dangerous degree from 2.5 to 8.5.

Fig.6.41 shows dangerous degree change of 37 counties in north Xinjiang from 2008 to 2010, in order to see the situation of dangerous degree of 37 counties. It shows that the areas of Altay, Wenquan, and Xinyuan almost had high dangerous degree in these three years. The areas of Qing he, Jimunai, Tachneg, and Yumin had lower dangerous degree in the year of 2008, but they gets moderate dangerous degree in the year of 2009 and 2010. The areas of Kuytun, Shihezi, Hutubi, Wujiaqu, and Qitai always in low dangerous area, and it is doesn't change these three years.

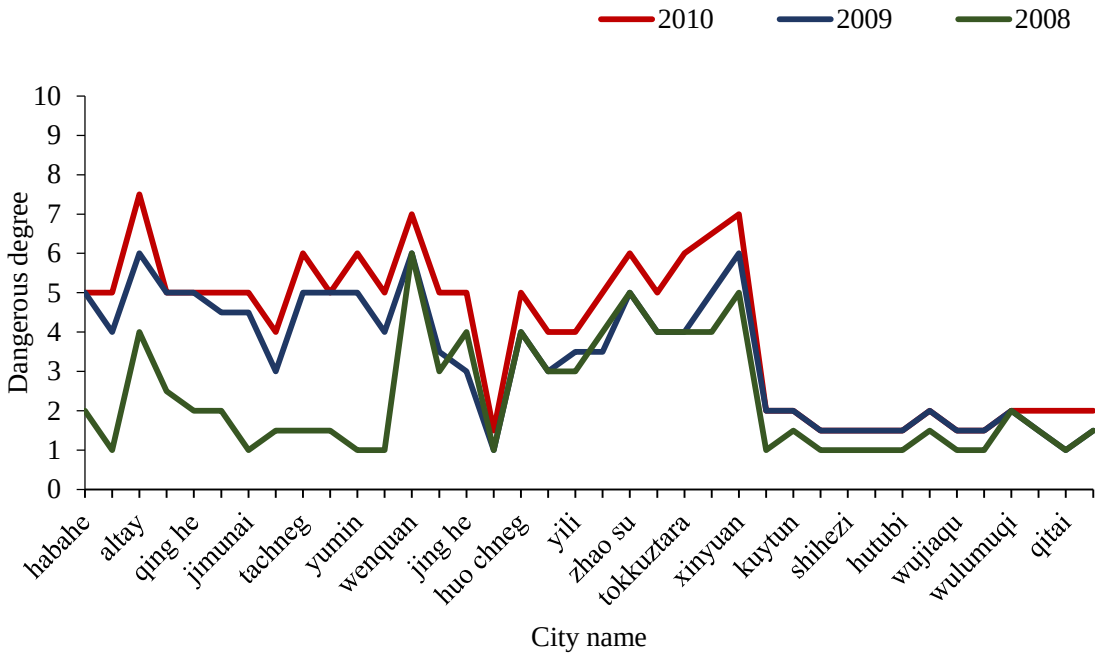

Fig. 6.41 the situation of dangerous degree change of 37 cities or counties in north Xinjiang from 2008 to 2010.

Based on the records of historical avalanche accidents, the dangerous degree of historical avalanche accident sites was calculated. And base the dangerous degree of historical avalanche accident site, the areas of dangerous degree more than 5.0 deiced as high dangerous area that may endangers to villages and human activities. High dangerous areas were shown from Fig.42 to Fig.6.44. The high dangerous areas equal to 9%, 10%, and 12% of total land area, from 2008, 2009, and 2010, respectively.

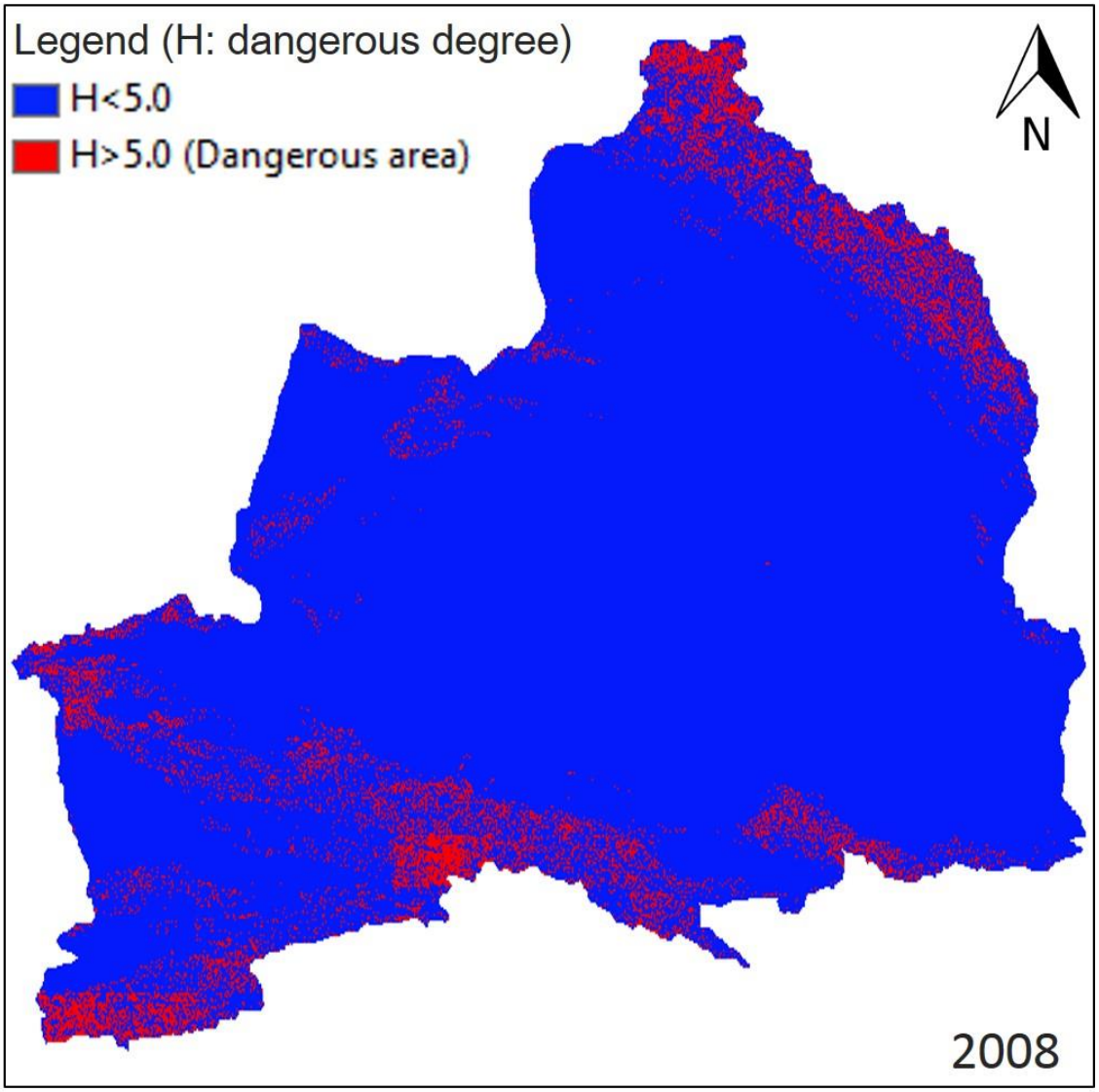

Fig.6.42. High dangerous area in 2008.

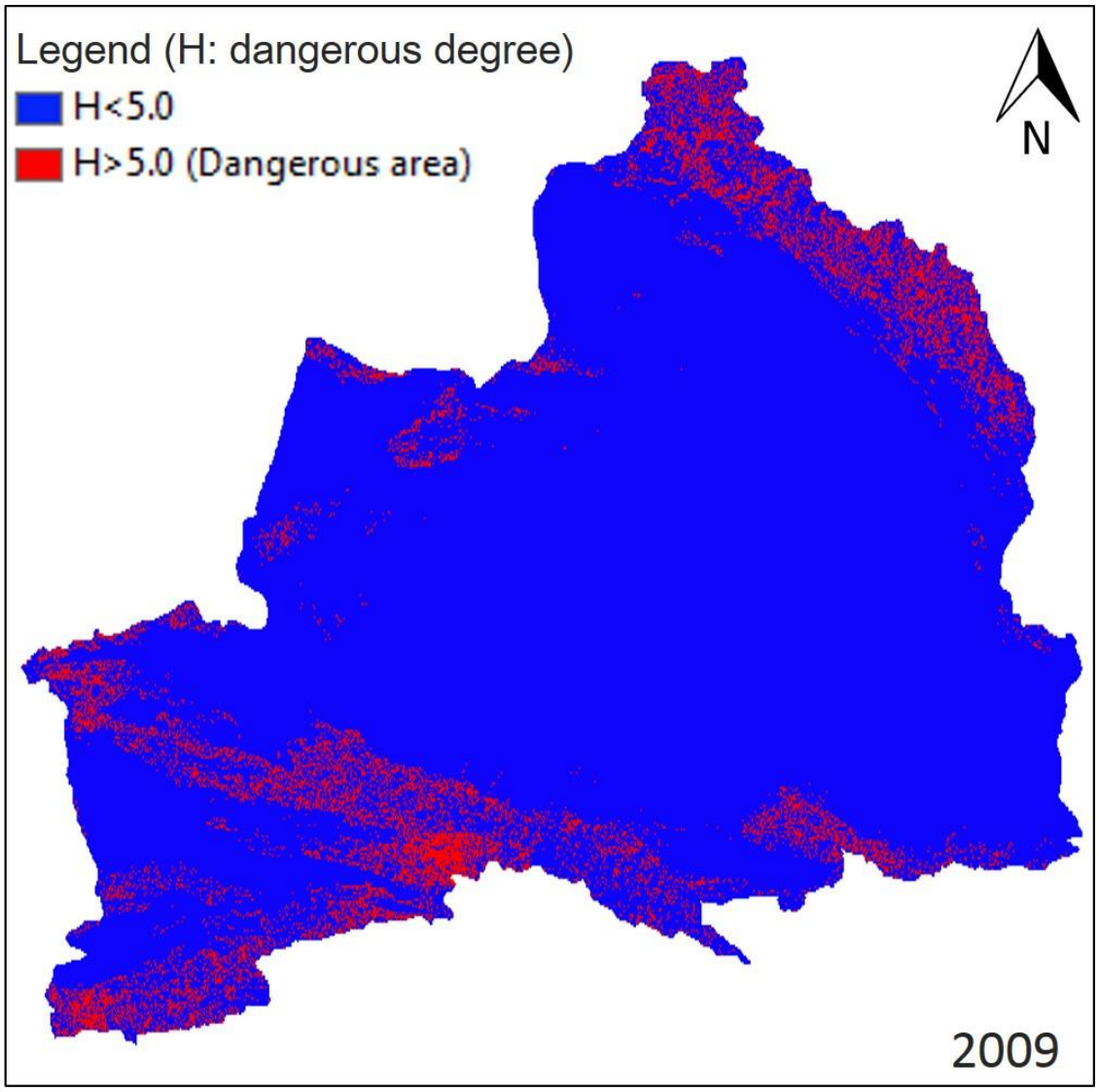

Fig.6.43. High dangerous area in 2009.

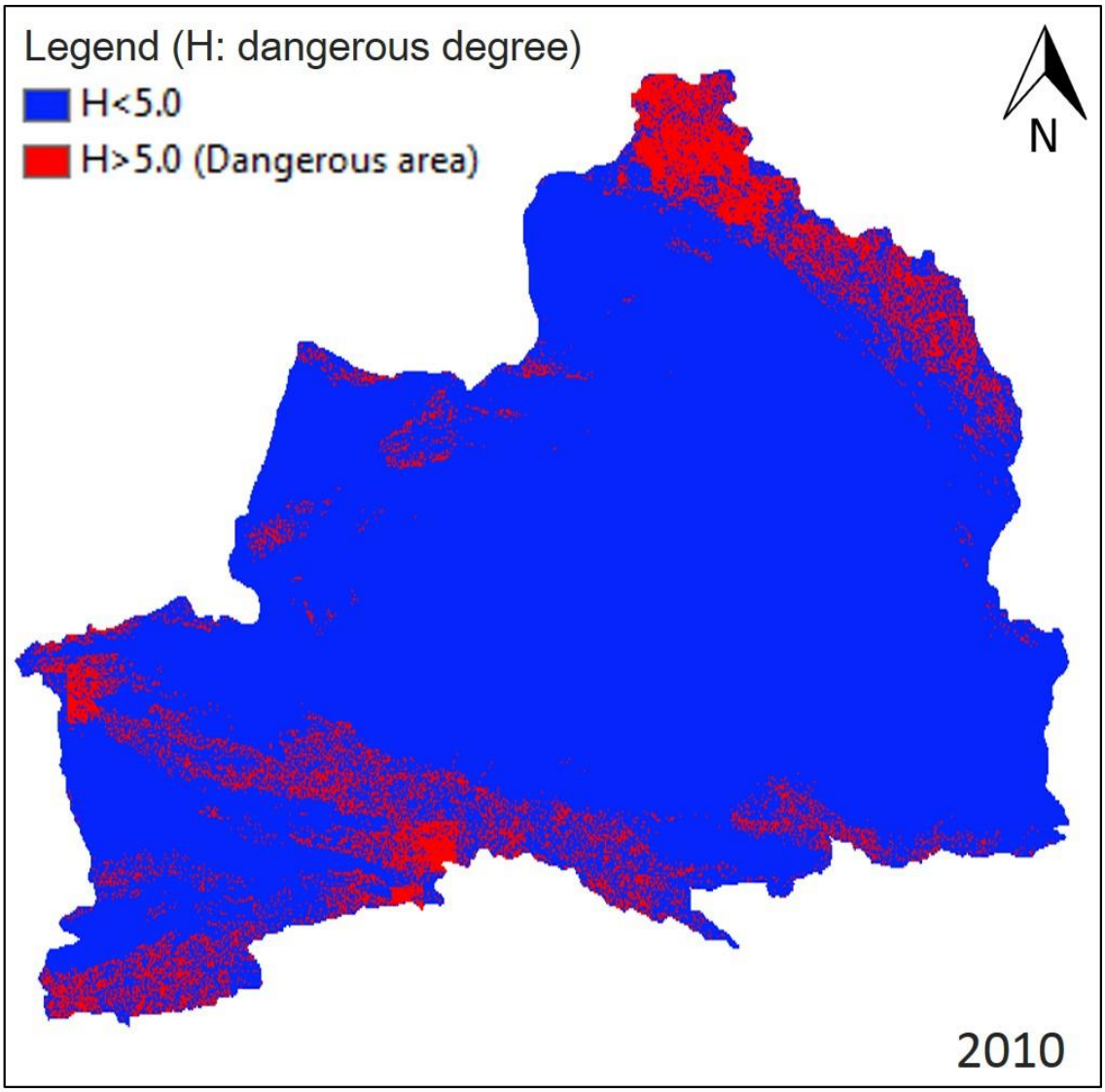

Fig.6.44. High dangerous area in 2010.

To prevent for a future avalanche hazard, potential hazard map was generated from the average of three annual avalanche hazard map, by taking their averages. Fig.6.45 shows the potential hazard map of north Xinjiang at 500m spatial resolution. The highly potential dangerous areas (dangerous degree more than 5.0) are mainly located in the north eastern part and south western part of the study area (Fig.46), and it is equal to 10.33% of total land area. It suggested that those areas should be prepared for the future potential avalanches.

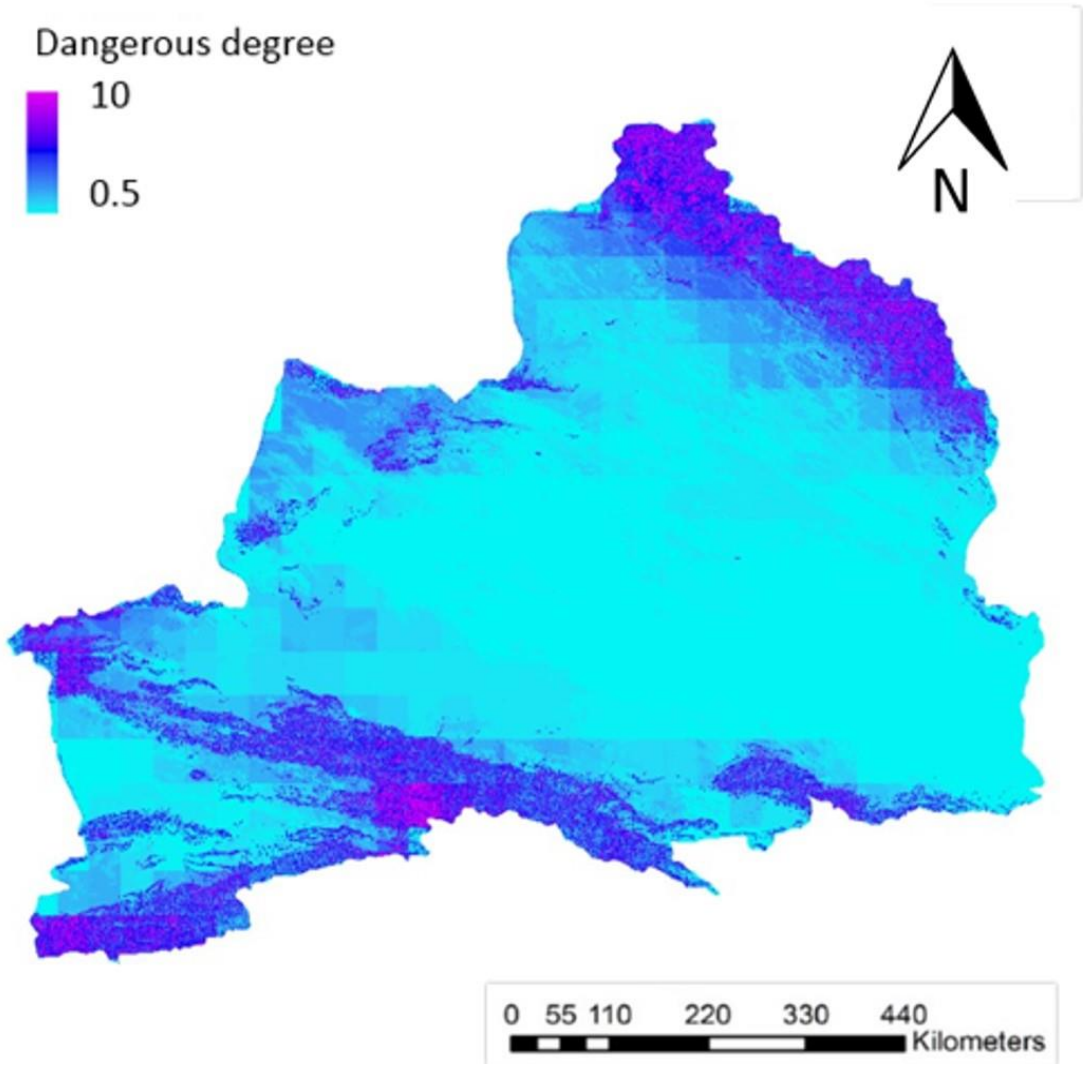

Fig.6.45 The final potential hazard map of north Xinjiang.

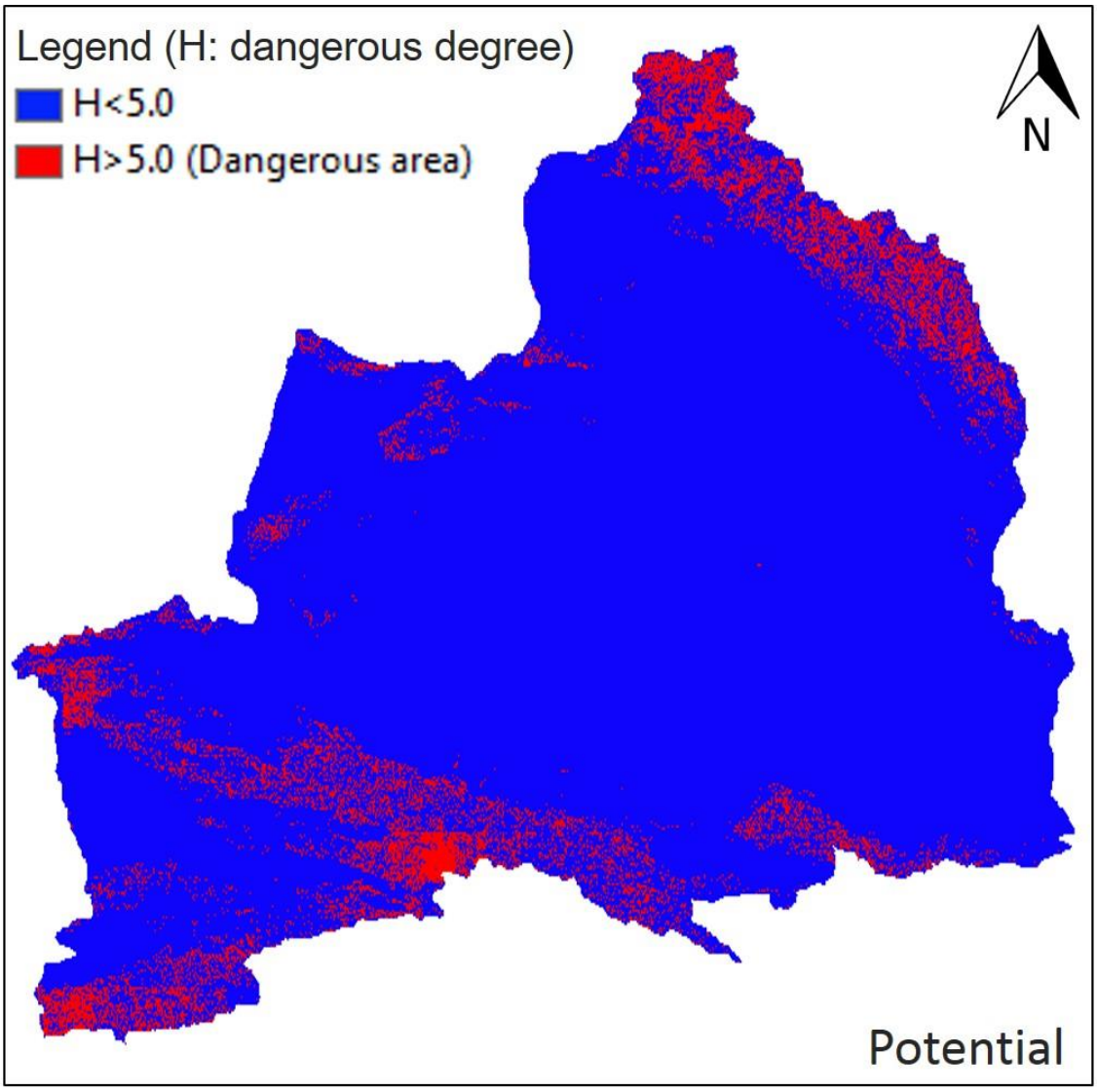

Fig.46. High potential dangerous area in north Xinjiang.

In order to see the difference between potential hazard map and topographic map, this two products were compared each other and with snow mass and Google earth image within sample pixel (UL: 87.173E, 48.855N, LR: 87.533E, 48.496N). The comparison presented that steepest high mountain area does not equal to potential hazard area. We cannot simply use the topographic map as potential hazard map (Fig.6.47).

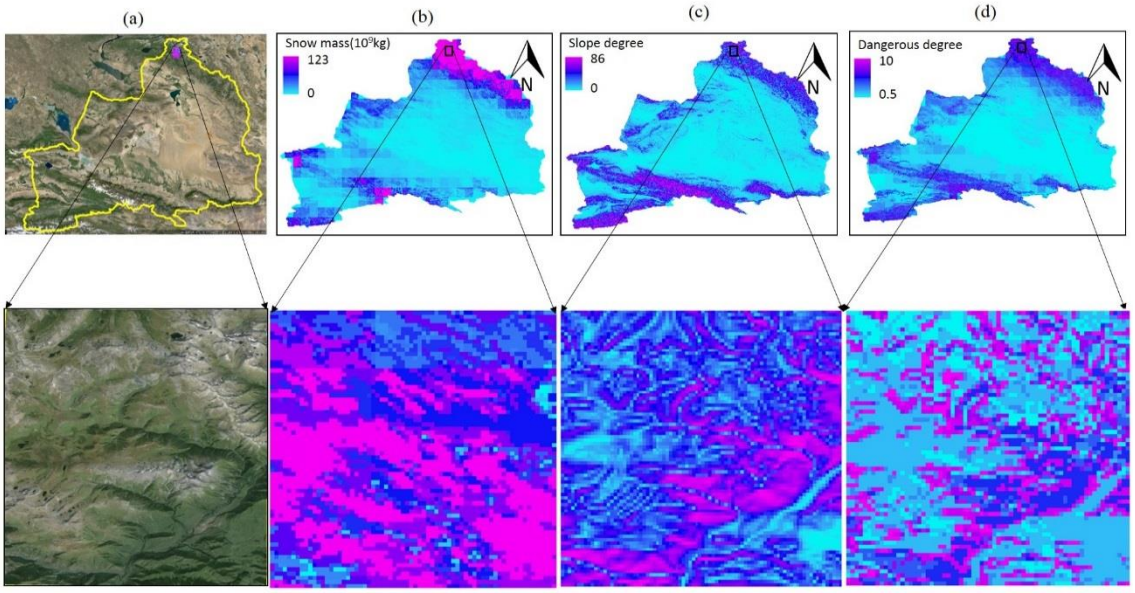

Fig.6.47 the comparison of potential hazard map, slope, and snow mass snow season output with one pixel size (UL: 87.173E, 48.855N, LR: 87.533E, 48.496N). (a) Google image of this sample pixel; (b) snow mass snow season output; (c) slope output; and (d) avalanche hazard map output.

Chapter 7 Road accessibility and highway sections dangerous situation

Road accessibility is strategically important for the maintenance of economic activities, but also for the emergency services. In mountains area, avalanches are a strong threat because, in addition to the victims and direct damage, they cause a loss of accessibility in roads. To see the risk of traffic roads, dangerous degree of highway sections were analyzed. Highway sections was classified by dangerous degree. From Fig.6.48 to Fig.6.50 shows the situation of dangers level of highway network system in three avalanche hazard maps from 2008 to 2010.

The length of highway sections in each dangerous degree was calculated, for each year. Table 6.1 shows the lengths of highway section in each dangerous degree from 2008 to 2010. They were 1857.4 km, 1995.3km, and 2295.2 km, from 2008, 2009, and 2010, respectively, and they are approximately equal to 10.9%, 11.8%, and 13.0% of the total land area. From this report we can see that dangerous degree of highway sections were changed temporally and spatially.

The highway sections in the highly dangerous area (H> 5.0) were shown in Fig.6.51. It shows that the highway section in the high potential dangerous area equals to 3246km, which is 19% of the total highway length, 16929km.

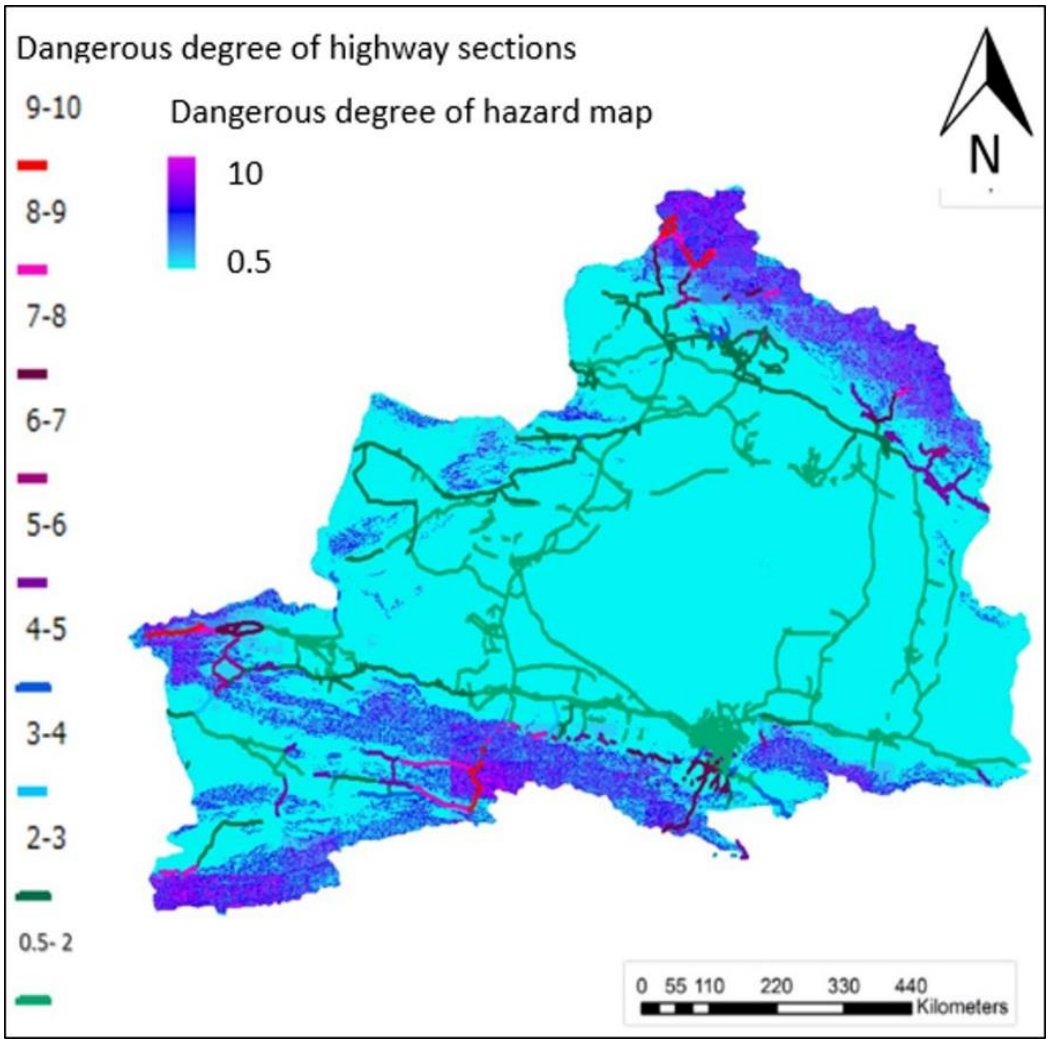

Fig. 6.48 The situation of dangerous level of highway network system in avalanche hazard map of 2008.

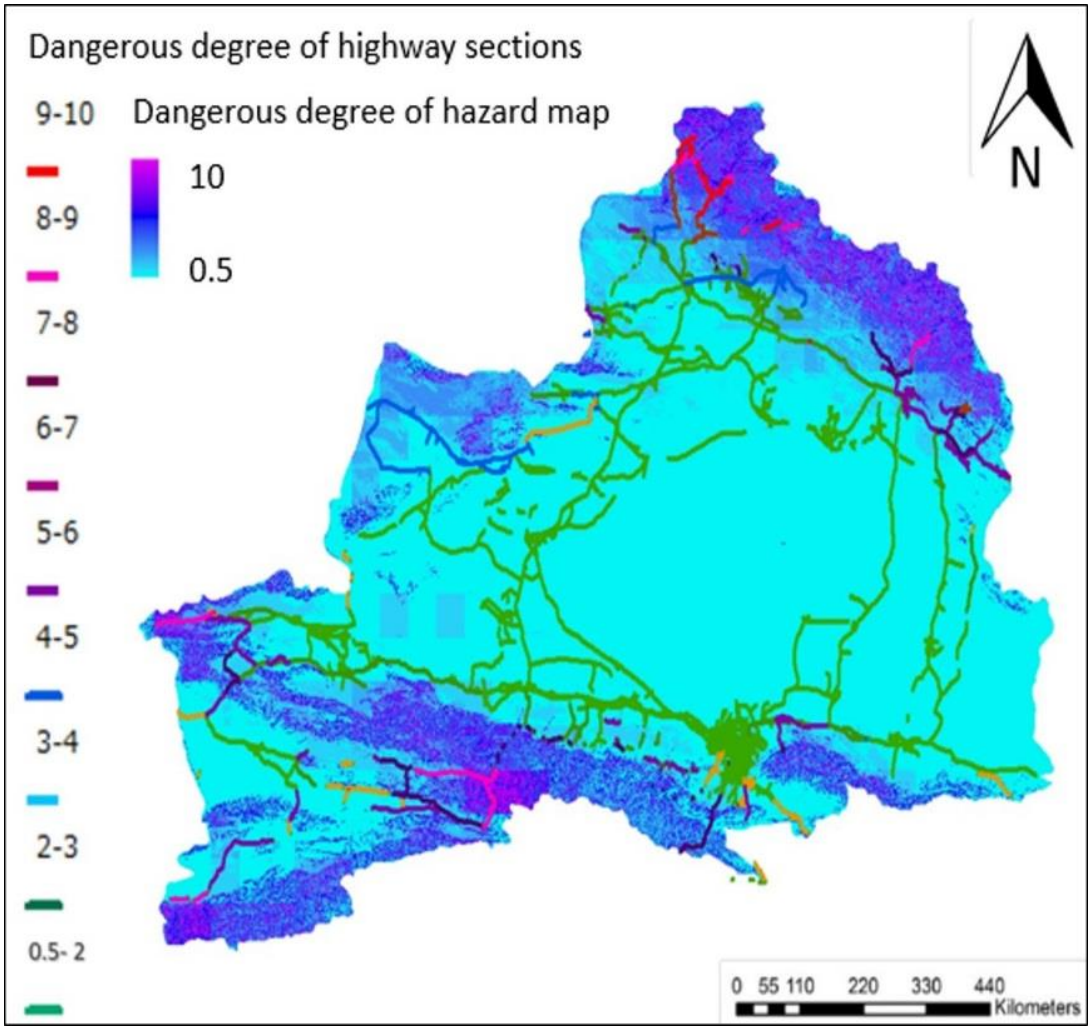

Fig. 6.49 The situation of dangerous level of highway network system in avalanche hazard map of 2009.

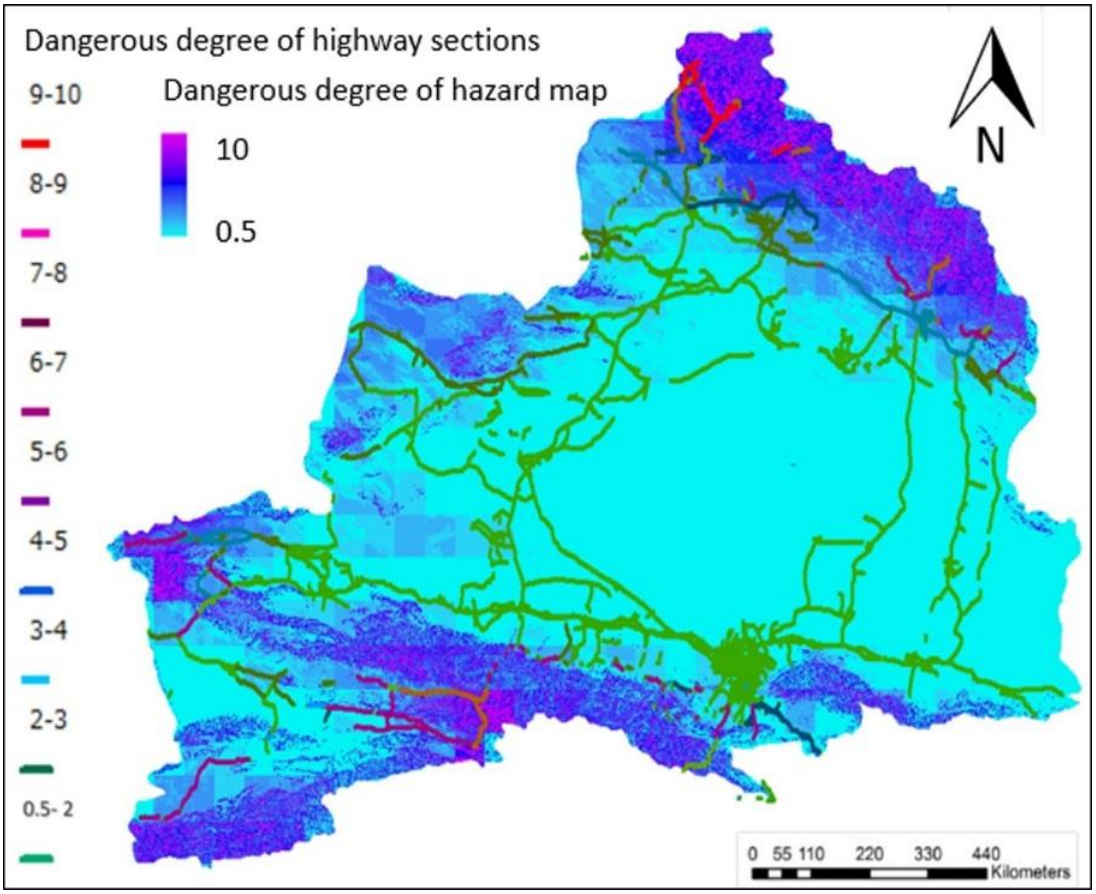

Fig. 6.50 The situation of dangerous level of highway network system in avalanche hazard map of 2010.

Table.6.1 The lengths of highway sections in each dangerous degree from 2008 to 2010.

Dangerous degree	Length of highway section (km)		
	2008	**2009**	**2010**
9—10	187.76	191.49	202.76
8—9	300.20	324.52	316.65
7—8	339.58	502.28	409.41
6—7	414.17	513.35	514.98
5—6	615.64	763.61	608.34
4—5	831.72	818.84	800.38
3—4	1162.46	1036.64	1055.64
2—3	2581.29	2634.63	3348.80
0.5—2	10561.73	10144.19	9672.58

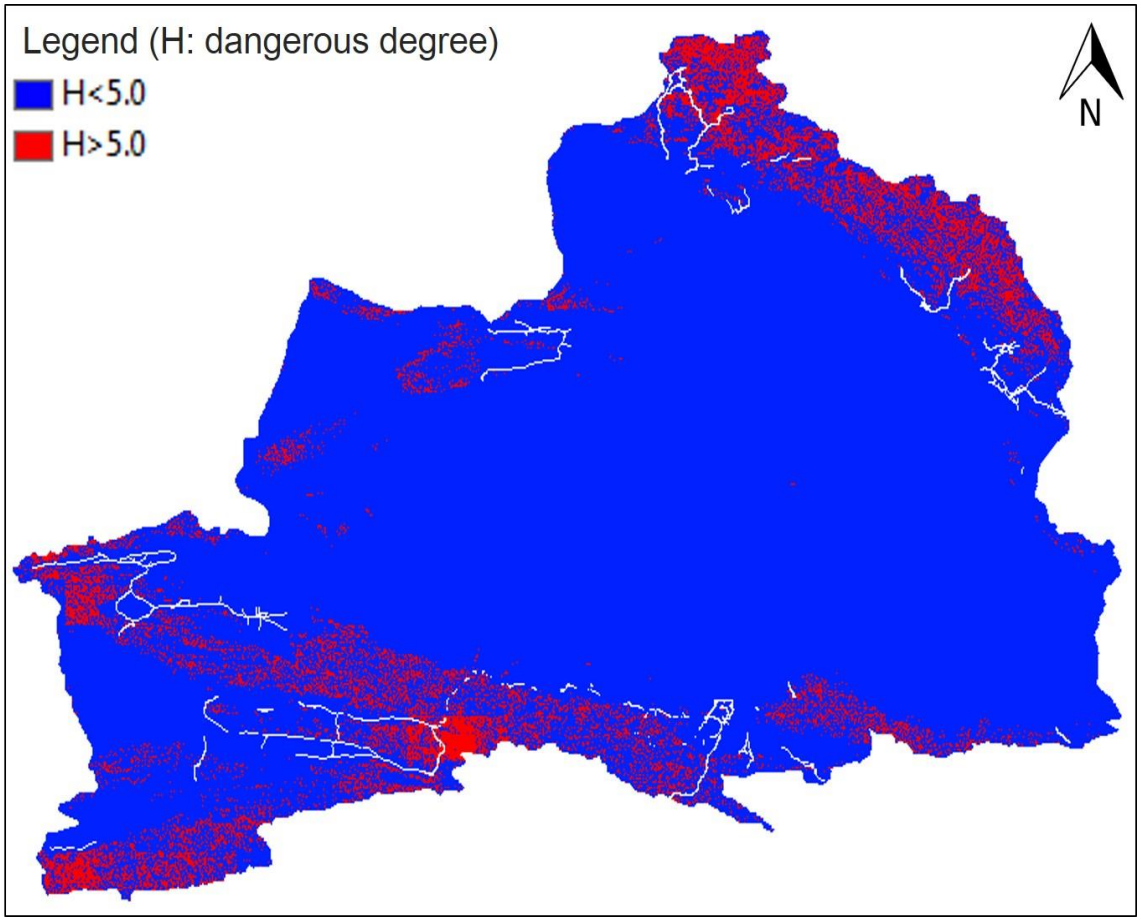

Fig. 6.51 The highway sections in the high dangerous area (H>5.0).

Three avalanche hazard maps are examined with available historical avalanche accident records. Table 8.1 summarized the location name of avalanche accidents in the past, the time of avalanche accidents happen, the human and livestock's losses from avalanche accidents, snow mass of avalanche accident sites at that time, average hazard score of avalanche accident site, and hazard score of avalanche accident sites in that avalanche happen year. Fig.6.52 and Fig.6.53 show historical avalanche accidents sites and their hazard scores in avalanche hazard map. Where, H represented hazard score of historical avalanche accident site.

Table 6.2 Hazard degree and snow mass of each avalanche accident locations.

	Location name	year	Human loss	Livestock's loss	Avg. HS	HS 2008	HS 2010	SM
1	Nilka	2010.02.25	Killed 9, Trapped >400		6.3	6.1	**6.7**	69.18
2	Nilka	2010.03.02	Killed 2, Missed 2, Trapped 27		6.1	5.8	**6.3**	29.54
3	Ili	2008.03.14	12 missing, 5 died		3.5	**5.7**	3.1	90.34
4	Nilka	2010.02.28	130 trapped		6.3	6.1	**6.7**	69.18
5	Tekas	2010.01.27	14 died	1000 died	7.2	6.8	**7.5**	109.00
6	Tacheng	2010.01.10	97,000 evacuated		5.8	5.6	**6.5**	71.26
7	Altay	2010.01.07	620,000 affected	9,234 died	6.3	5.8	**6.7**	18.42

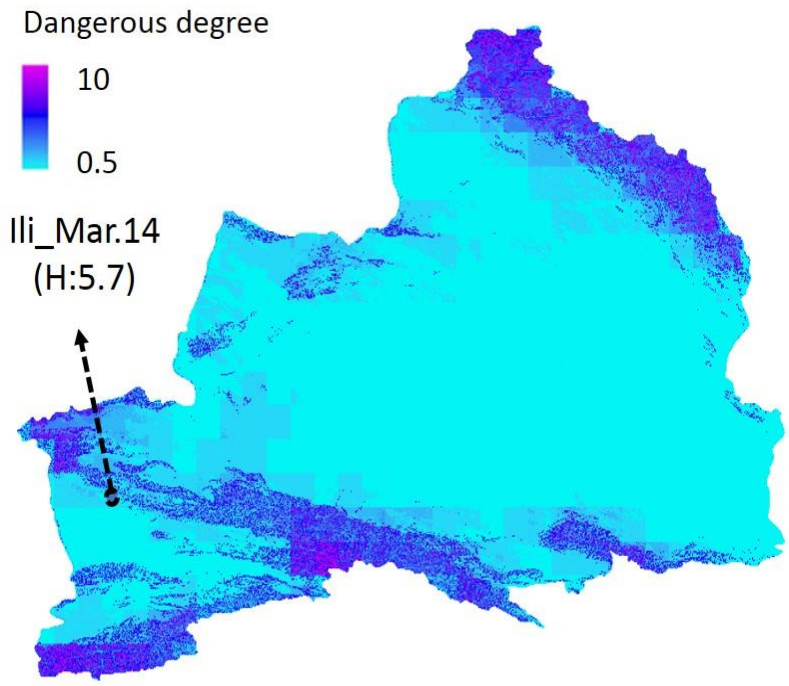

Fig.6.52 Ili avalanche accident site (Mar.14, 2008) in avalanche hazard map of 2008.

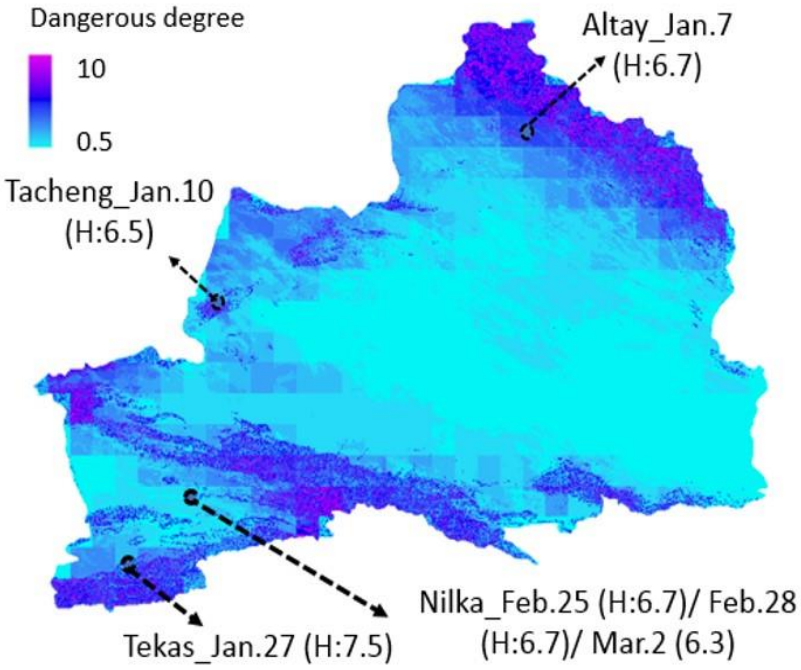

Fig.6.53 Four avalanche accident sites in avalanche hazard map of 2010.

Chapter 8 Conclusion

Due to frequent experience of avalanche disaster in north Xinjiang, almost every year avalanches affect people's lives and productivity, causing serious damage to towns and farms. Therefore, the problem of living with this natural hazard is seriously recognized known and its scientific measures. Accordingly, monitoring potential hazard area to prevent for a future avalanche hazard is significantly important for this region. With the help of RS and GIS techniques, and modern mathematical analysis methods, the final target of this study to produce potential hazard map has been achieved.

Conclusions of this study listed as following:

1. Using MODIS and AMSR-E snow data, cloud-free snow cover data with 500m spatial resolution was generated. Cloud coverage in existing MODIS snow cover products at 500m spatial resolution was removed by microwave (AMSR-E) snow product with cloud penetration capability. The output shows that in northern Xinjiang area, the percentage of mean monthly snow-covered area ranges from about 2% in summer to over 30 % in winter.
2. Using cloud-free snow cover data and Canadian meteorological center (CMC) snow depth data, snow volume product with 500m spatial resolution was generated.

   The outputs of snow volume show that the temporal change of monthly snow volume over the period of January 2008 to December 2010 are almost dominated by the seasonal cycle. The total snow volume over the whole study area equals to 310.54 $*10^6$ m^3, 345.48 $*10^6$ m^3, and 682.91 $*10^6$ m^3 over these three years, respectively. The total snow volume of 2010 was higher than 2008 and 2009. The temporal change of snow volume was analyzed with air temperature and precipitation. It shows that the changes of air temperature is the main reason of snow volume change (r= 0.65), and precipitation change is not much related to snow

volume change (r= -0.38).

Snow mass were calculated from snow volume with an assumed average snow density, because of unavailability of snow density data. Snow mass product at 500m spatial resolution and 24km resolution were compared, this comparison shows the difference between two products, e.g. in a sample pixel (Upper left: 87.173E, 48.855N, Lower right: 87.533E, 48.496N) snow mass was $9.06*10^9$ kg at 500m resolution product, while it equals to $13.16*10^9$ kg at 24km resolution product.

3. GIS-based weighted linear combination (WLC) method were applied to create avalanche hazard maps using snow mass and slope data, which are prerequisite of avalanches trigger. Snow mass and slope were transformed to a score between zero (least possibility of avalanche occurrence) and 10 (most possibility of avalanche occurrence) by level slicing. Threshold values for level slicing were decided by previous research.

   The output of the dangerous degree of avalanche hazard map was expressed by the score from 0.5 to 10. The areas of dangerous degree more than 5.0 were decided as the highly dangerous area that may endanger villages or human activities, based on the dangerous degree of historical avalanche accidents. The highly dangerous areas were 9%, 10%, and 12% of total land area, from 2008 to 2010, respectively.

4. To prevent a future avalanche hazard, potential hazard map was produced from the average of three annual avalanche hazard maps from 2008 to 2010. The highly potential dangerous areas (dangerous degree more than 5.0) are mainly located in the north eastern part and south western part of the study area, and it was 10.33% of total land area; those areas should be prepared for the future potential avalanches.

5. Because of the importance of road accessibility, highway network system was analyzed. Highway network system was classified by dangerous degree. The length of highway in each

dangerous degree was calculated for each year. They were 1857.4 km, 1995.3km, and 2295.2 km, from 2008, 2009, and 2010, respectively, and they were approximately 10.9%, 11.8%, and 13.0% of the total highway length.

Highway sections in the highly potential dangerous area equals to 3246km, which is 19% of the total highway length, 16929km.

In summary, potential hazard map at 500m spatial resolution gives more detail and accurate information about dangerous degree of potential avalanche hazard in this region. The need has been filled for better analysis, communication, and visualization of avalanche hazard to aid decision makers to mitigate avalanche hazards.

Potential hazard map by this study would be useful for mitigation of future avalanche hazards and play a significant role in sustainable development in north Xinjiang areas. It was specifically intended to support the local government and native people in the future.

In future work, more advanced data acquisition techniques should be introduced into potential hazard monitoring model, and new avalanche hazard map will be created based on the trigger condition of each avalanche types.

Reference

Al-Hanbali, A.., Alsaaideh, B. and Kondoh, A. (2011) Using GIS-Based Weighted Linear Combination Analysis and Remote Sensing Techniques to Select Optimum Solid Waste Disposal Sites within Mafraq City, Jordan. Journal of Geographic Information System, Vol. 3, pp 1-12

Biancamaria, S., Cazenave, A., Mognard, N.M. Llovel,W. and Frappart, F. (2011) Satellite-based high latitude snow volume trend, variability and contribution to sea level over 1989/2006. Global and Planetary Change. Global and Planetary Change. Vol. 75, pp 99-107

Brasnett, B. (1999) A Global Analysis of Snow Depth for Numerical Weather Prediction. Journal of applied meteorology. Vol.38, pp726-740

Brown, R.D. (2000) Northern Hemisphere Snow Cover Variability and Change, 1915–97. Journal of climate. Vol.13, pp 2339-2355

Brown, R.D., Brasnett, B., and Robinson, D. (2003) Gridded North American monthly snow depth and snow water equivalent for GCM evaluation. Atmosphere Ocean. Vol.41 No.1, pp 1-14

Brown, R., and Brasnett, B. (2011) The Canadian Meteorological Centre Global Daily Snow Depth Analysis, 1998-2011: Overview, Experience and Applications. 68th Eastern snow conference, McGill University, Montreal, Quebec, Canada. Pp 197-200

Brown, R.D., Derksen, C., and Wang, L. (2010). A multi-data set analysis of variability and change in Arctic spring snow cover extent, 1967–2008. Journal of. Geophysical Research Vol.**115**. Doi: 10.1029/2010JD013975.

Brown,R.D and Mote, P.W (2009) The Response of Northern Hemisphere Snow Cover to a Changing Climate. Journal of climate. Vol.22, pp 2124-2145

Brown, R. D. and Robinson, D. A. (2011). Northern Hemisphere spring snow cover variability and change over 1922–2010 including an assessment of uncertainty. The Cryosphere. Vol. **5,** pp 219−229, doi: 10.5194/tc-5-219-2011.

Chang, A. T. C., Foster, J. L., and Hall, D. K. (1987). Nimbus-7 Derived Global Snow Cover Parameters. Annals of Glaciology. Vol. 9, pp 39-44.

Chang, A. T. C., Foster, J. L., and Hall, D. K., Goodison, B. E., Walker, A. E., and Metcalfe, J. R. (1997) Snow parameters derived from microwave measurements during the Boreas winter field experiment. Journal of Geophysical Research. DOI: 102: 29663-29671.

Chrustek, P., Swierk, M., and Biskupic, M. (2013) Snow avalanche hazard mapping for different frequency scenarios, the case of the Tatra Mts., Western Carpathians. International snow Science Workshop Grenoble- Chamonix Mont-Blanc. pp745-749

Covăsnianu, A., Grigoraş, I.R., State, L.E., Balin, D., Hogaş, S., Balin, I. (2011) Mapping snow avalanche risk using GIS technique and 3d modeling, case study- Ceahlau national park. Romanian Journal of Physics, Vol.56, No.3-4, pp476-483.

Dai,L., Che, T., wang,J., and Zhang, P. (2012) Snow depth and snow water equivalent estimation from AMSR-E data based on a priori snow characteristics in Xinjiang, China. Remote Sensing of Environment. Vo. 127, pp 14-29

Delpare, D.M. (2008). Avalanche Terrain Modeling in Glacier National Park, Canada. PhD thesis. Department of geography, University of Calgary, Alberta

Dietz, A.J., Kuenzer, C., and Conrad, C. (2013) Snow-cover variability in central Asia between 2000 and 2011 derived from improved MODIS daily snow-cover products. International

journal of remote sensing. Vol.34, No.11, pp 3879-3902. Doi:10.1080/01431161.2013.767480

Eckerstorfer, M. (2012). Snow avalanches in central Svalbard: A field study of meteorological and topographical triggering factors and geomorphological significance. PhD thesis. The University Centre in Svalbard, Norway

Gao, Y., Xie, H., Lu, N., Yao, T., Liang, T. (2010) Toward advanced daily cloud-free snow cover and snow water equivalent products from Terra–Aqua MODIS and Aqua AMSR-E measurements. Journal of Hydrology. Vo.385, pp 23–35

Grant, S. (2008) Avalanche hazard, danger and risk – a practical explanation. International Snow Science Workshop. Canada. pp 224-227

Li, C., Huang, L., Li, J. (1997). Preventing avalanche at Guozigou in Xinjiang autonomous Uyghur Region of China. Snow engineering: Recent advances, Izumi, Nakamura and Sack (eds). Balkema Rotterdam. pp 361-370

Liang, T., Gao, X., Liu, X. (2004) snow disaster in Aletai region- its remote sensing monitoring and evaluation method. Chinese journal of applied ecology. Vol.15, No.12, pp2272-2276

Liang, T., Liu,X. wu, C., Guo, Z. and Huang, X. an evaluation approach for snow disaster in the pastoral areas of northern Xinjiang, PR China. New Zealand of agricultural research. Vol.50, pp 369-380

Liang, T., Zhang, X., Xie, H Wu, C., Feng, Q., Huang, X., Chen, Q. (2008) Toward improved daily snow cover mapping with advanced combination of MODIS and AMSR-E measurements. Remote Sensing of Environment Vo.112 pp3750–3761

Liang, S., Huo, Z., and Niu, Y. (2009) Assessment of Snow Drifting Hazard along Railway A Case Study of JYH Railway in Xinjiang, China. International Conference on Environmental Science and Information Application Technology pp44-47 DOI 10.1109/ESIAT.2009.107

Liu, F., Mao, X., Zhang, Y., Chen, Q., Liu, P., Zhao, Z. (2014) Risk analysis of snow disaster in the pastoral areas of the Qinghai-Tibet Plateau. Journal of geographical science, Vo.24, no.3, pp411-426. DOI: 10.1007/s11442-014-1097-z

Liu, X., Liang, T. and Guo, Z. (2004) evaluating model and approach of snow disaster effect on grassland animal husbandry. Acta Botanica Boreali-Occidentalia Sinica. Vol.24, No.1, pp 94-99.

Liu, X., Liu, Y.,Li, L., and Ren, Y. (2009) Disaster monitoring and early-warning system for snow avalanche along tianshan highway. IGRARSS. pp II-634-637

Liu, X., Zhang, J., Tong,Z., Bao, Y., Zhang, D. (2011) Grid-Based Multi-Attribute Risk Assessment of Snow Disasters in the Grasslands of Xilingol, Inner Mongolia. Human and Ecological Risk Assessment, No.17, pp 712-731 (DOI: 10.1080/10807039.2011.571123)

Luojus, K., Pulliainen, J., Takala, M., Lemmetyinen, J., Derksen, C., and Wang, L. (2010) Snow Water Equivalent (SWE) product guide. GLOBSNOW: Global Snow Monitoring for Climate Research. V.1.0, Rev.01.

Ma, W. and Hu, R. (1990) relationship between the development of depth hoar and avalanche release in the Tian Shan mountains, china. Journal of glaciology. Vol.36, No.122, pp 37-40

Maggioni, M. (2004) Avalanche release areas and their influence on uncertainty in avalanche hazard mapping. PhD thesis. University of Z¨urich, Italy

Peng, S., Shieh, M., Fan, S. (2012) Potential Hazard Map for Disaster Prevention Using GIS-Based Linear Combination Approach and Analytic Hierarchy Method. Journal of Geographic Information System, Vo.4, pp 403-411

Qiu, J., Xu, J., Jiang, F. (1997) Study of avalanche in the Tien Shan Mountains, Xinjiang, China. Snow engineering: Recent advances, Izumi, Nakamura and Sack (eds). Balkema Rotterdam. Pp 85-90

Salzmann, N., Ka¨a¨ b, A., Huggel, C., Allgo¨wer, B., Haeberli, W. (2004) Assessment of the hazard potential of ice avalanches using remote sensing and GIS-modelling. Norwegian Journal of Geography, Vol. 58, pp 74–84.

Semakova1, E., Myagkov, S., and Armstrong, R.L. (2009) The current state of avalanche risk analysis and hazard mapping in Uzbekistan. International Snow science Workshop, Davos 2009, Proceedings, pp 509-513

Sun, G., Chen, Y., Li, W., Pan, C., Li, J. and Yang, Y. (2013) Spatial Distribution of the Extreme Hydrological Events in Xinjiang, North-West China. Natural Hazards, 67, 483-495. Doi: 10.1007/s11069-013-0574-5

Tachiiri, K., Shinoda, M., Klinkenberg, B., and Morinaga, Y. (2008) Assessing Mongolian snow disaster risk using livestock and satellite data. Journal of Arid Environment. Vol. 72, pp 2251-2263

Tao, J. (2007). Snow hazard potential evaluation along G217 highway in Tian Shan Mountains by using GIS and RS. Proceeding of remote sensing and GIS data processing and applications; and Innovative multispectral technology and applications. Vo. 6790. doi:10.1117/12.748696

Wang, S., Ren, J., (2012). A Review of the Progresses of Avalanche Hazards Research. Progress in geography. CNKI

Wang, W., Liang, T., Huang, X., Feng, Q., Xie, H., Liu, X, Chen, X., Wang, X. (2013). Early warning of snow-caused disasters in pastoral areas on the Tibetan Plateau. Natural Hazards and Earth System Sciences. Vo.13, pp 1411–1425

Wang, X., Xie, H., and Liang, T. (2007). Evaluation of MODIS snow cover and cloud mask and its application in Northern Xinjiang, China. Remote sensing of Environment. Vo. XX, pp1-17. doi:10.1016/j.rse.2007.05.016

Wei, S., Zhang, Z., Wang, Z., Su, X., Huang, J., Yang, Y., and Liu, S. (2011). Analyzing disaster-

forming environments and the spatial distribution of flood disasters and snow disasters that occurred in China from 1949 to 2000. Mathematical and computer modelling. No.54, pp 1069-1078. doi:10.1016/j.mcm.2010.11.037

Xiong, H., Liu, G., Cui, Z. (1999). The characteristics and vertical zone spectrum of natural disasters in the Tian Shan Mountains, Xinjiang. Chinese geographical science. vo.9, no. 2, pp 126-133.

Wu, J., Li, N. and Yang, H (2008) Risk evaluation of heavy snow disaster using BP artificial neural network: the case of Xilingol in Inner Mongolia. Stoch environ Res risk assess. Vol. 22, pp 719-725

Ye, H., Zhang, R., Shi, J., and Huang, J. (2012). Black carbon in seasonal snow across northern Xinjiang in northwestern China. Environmental research letter. Vo.7, pp 1-9.